CHONDROCYTE GENE EXPRESSION AND INTRACELLULAR SIGNALING PATHWAYS IN CARTILAGE MECHANOTRANSDUCTION

JONATHAN BASIL FITZGERALD

B.Eng(hons)., Electrical & Electronic Engineering, University of Western Australia, 1999

B.Sc., Physiology, University of Western Australia, 1998

Submitted to the Biological Engineering Division

in partial fulfillment of the requirements for the degree of

DOCTOR OF PHILOSOPHY IN BIOENGINEERING

at the

MASSACHUSETTS INSTITUTE OF TECHNOLOGY

July 2005 [September 2005]

Signature of Author_____

Biological Engineering Division

Certified by_____

Alan J. Grodzinsky, Thesis Supervisor
Professor of Biological, Electrical, and Mechanical Engineering

Accepted by_____

Ram Sasisekharan, Graduate Program Committee
Professor of Biological Engineering

Abstract

Chondrocytes respond to *in vivo* mechanical loads by regulating the composition of the cartilage extracellular matrix. This study utilized three loading protocols that span the range of forces and flows induced by *in vivo* loading. Constant (static) compression of cartilage explants induces a transient hydrostatic pressure buildup and fluid exudation from the compacted matrix until relaxation leads to a new equilibrium compressed state. Dynamic compression induces cyclic matrix deformation, hydrostatic pressures, fluid flows, and streaming currents. Dynamic tissue shear causes cyclic matrix deformation only. After applying these loading protocols to intact cartilage explants for 1 to 24 hours, we used real-time PCR to measure the temporal expression profiles of selected genes associated with cartilage homeostasis. In concurrent experiments, we assessed the involvement of intracellular signaling pathways using molecular inhibitors. In order to interpret the results we developed two techniques that reliably clustered intermediate-sized datasets using principal component analysis and *k*-means clustering. Mechanical loading regulated a variety of genes including matrix proteins, proteases, protease inhibitors, transcription factors, cytokines, and growth factors. Static compression transiently upregulated matrix proteins, however, mRNA levels were suppressed by 24 hours. Dynamic compression and dynamic shear increased matrix protein transcription particularly after 24 hours. In contrast, matrix proteases were upregulated by all 24 hour loading regimes, particularly static compression. Taken together these results demonstrate the functionally-coordinated regulation of chondrocyte gene transcription in response to mechanical forces, and support the hypothesis that dynamic loading is anabolic for cartilage and static loading is anti-anabolic. Intracellular calcium release, cAMP activation of protein-kinase-A, and the phosphorylation of MAP kinases (ERK1/2, p38), were all identified as signaling events necessary for mechanically-induced transcription. In addition, we measured the immediate, transient increase in mRNA levels of transcription factors downstream of the MAP kinase pathway (c-Fos and c-Jun), in response to all three loading types. The prevention of protein synthesis during static compression suppressed mechanically-induced transcription suggesting that signaling molecules are synthesized in response to mechanical forces. Comparison of this well characterized model of normal cartilage mechanotransduction to what occurs within diseased cartilage will hopefully provide insight into the mechanisms driving the progression of osteoarthritis.

Thesis Supervisor:

Alan J. Grodzinsky — Professor of Biological, Electrical, and Mechanical Engineering
Massachusetts Institute of Technology

Thesis Committee:

Roger Kamm — Professor of Biological and Mechanical Engineering
Massachusetts Institute of Technology

Richard Young — Professor of Biology
Whitehead Institute for Biomedical Research, Massachusetts Institute of Technology

Acknowledgements

Completing a PhD at MIT has been a challenging and rewarding experience. I couldn't have done it without the help and support of numerous people. Firstly I would like to acknowledge my terrific advisor, Al. Not only is he a hard working genius but he has managed to create a very friendly and supportive lab group. Thanks Al for all the enthusiasm and encouragement, and thanks for all the laughs!

I would like to thank the entire Grodzinsky lab, both past and present, for making my years here so enjoyable. Dr Moonsoo Jin helped me start my project and I am very thankful for his great ideas, motivation, and training. Laurel and Delphine have been great friends throughout the years and we successfully completed many subjects together. Thanks girls for all the chats and cakes! Thanks to Mike, Jenny, and Jon S for many fun lunchtimes and for keeping me on my toes regarding facts about Australia. Cameron, Bernd, Shuodan, Anna, Diana, Lin, Paul, Yi and Bo Bae have continued the friendly nature of our group and I wish them all the best with their research. Eliot, Han-Hwa, and Linda were always there when I needed them, as they have been for all of Al's students, and I thank them for their many contributions to the lab environment.

During my studies I spent one year back in Australia doing research while I was getting married (thanks again Al!). I would like to thank Professors David Wood and Ming-Hao Zheng for supporting my research and training during that year. The members of the Orthopaedic Research Laboratory made me very welcome and I would especially like to thank Nathan, Tony, Verity, and Cathy. I am indebted to Rachel Duff who allowed me exclusive use of a half million dollar real-time PCR machine for an entire year, which was very helpful!

My wife, Roslyn, has been a terrific, loving support through my PhD. I would like to thank her for sticking with me through thick and thin, especially when we were on opposite sides of the world. I am very grateful to my parents, David and Rachel, and my parents in law, David and Ruth for being so supportive of me from across the ocean.

This wonderful opportunity was made possible by a Hackett Scholarship from the University of Western Australia, and encouragement from the Biological Engineering Division, particularly Professor Lauffenburger.

Jonathan FitzGerald

July 5th 2005

Contents

List of Figures

List of Tables

Chapter 1

Background

1.1 Cartilage Biology

Articular cartilage lines the surface of synovial joints, and the mechanical properties of cartilage are directly responsible for smooth ambulation and shock absorption. Cartilage is primarily composed of an extracellular matrix (ECM), with chondrocytes, the lone cell type, comprising only 1% of the volume. The ECM consists of a dense interconnected network of proteins, particularly the brush-like proteoglycan aggrecan which has charged glycosaminoglycan side chains, and coiled superfibers of type II collagen (Figure 1.1). The densely packed, negatively charged aggrecan molecules generate a large interstitial swelling pressure that is counteracted by type II collagen fibers that resist tensile forces (reviewed in [1]). Therefore, cartilage is a highly charged poroelastic tissue, capable of resisting sudden deformations due to repulsive negative charges, but permitting slow compressive loads to force interstitial fluid out of the tissue.

Link protein is an additional structural proteins that connects aggrecan to long hyaluronic acid backbones creating super aggregates [2,3]. Fibronectin connects the pericellular matrix surrounding the chondrocyte to the cell membrane by attaching to $\alpha 5\beta 1$ integrin [4], directly linking the chondrocyte cytoskeleton and the ECM. The compressive modulus of cartilage and chondrocytes are ~ 0.6MPa [5] and 0.6kPa [6,7] respectively; thus chondrocyte deformation is dictated by the mechanical properties of the ECM. In turn, chondrocytes are capable of regulating the composition of the ECM through synthesis of matrix proteins and enzymes capable of cleaving aggrecan and type II collagen. Matrix metalloproteinases (MMP's) and a

disintegrin and metalloproteinase with thrombospondin motifs (ADAMTS's) are usually secreted in an inactive form [8], and contain aggrecanase and/or collagenase activity. There is a natural turnover of aggrecan mediated by the matrix proteases; however, collagenase activity is a marker for the cartilage disease state osteoarthritis (OA) [9,10]. Chondrocytes also regulate the balance between anabolic and catabolic processes by secreting tissue inhibitors of matrix proteases (TIMPs), which inactivate matrix proteases with 1:1 stoichiometry [8].

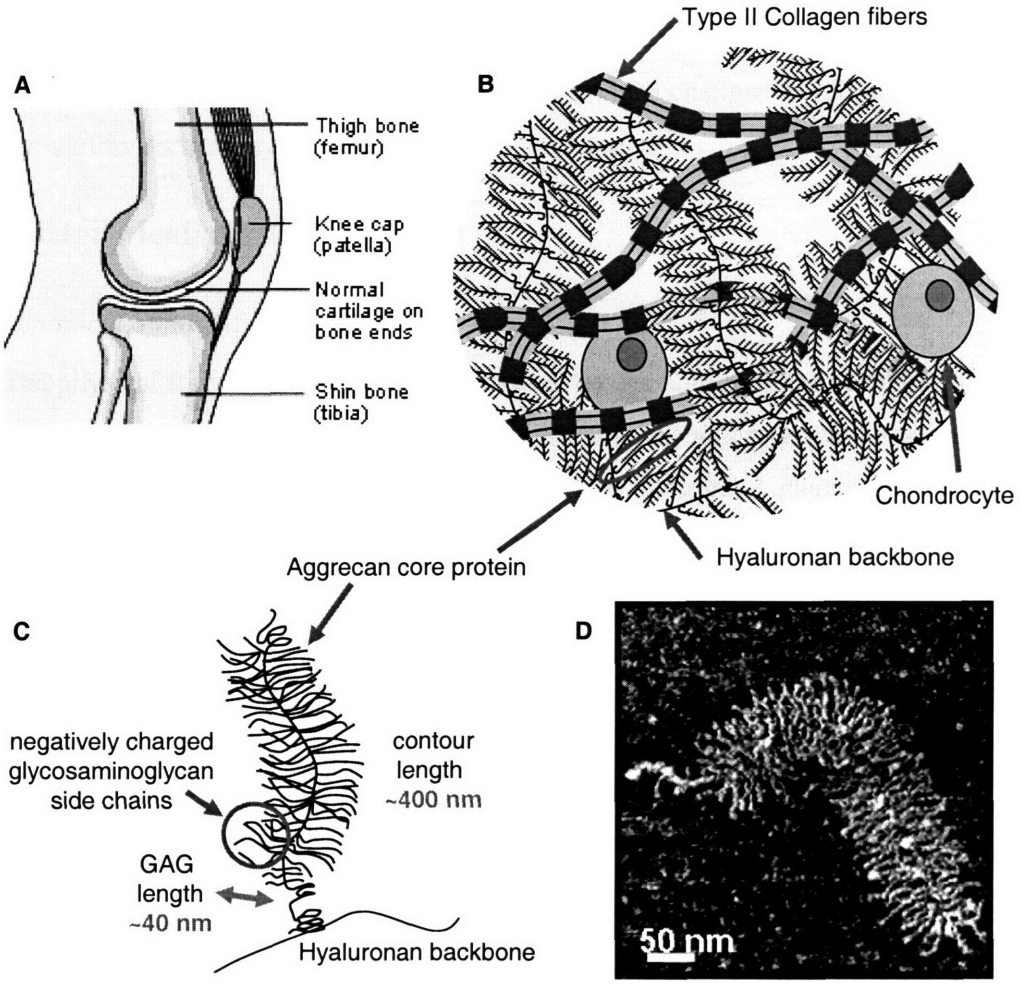

Figure 1.1: Composition of cartilage. A) Knee joint schematic (**www.arc.org.uk**). B) Schematics of the chondrocyte in the extracellular matrix and of the C) glycosalated aggrecan core protein (courtesy of Delphine Dean). D) Atomic force microscope image of the aggrecan macromolecule (courtesy of Laurel Ng, [11])

Adult cartilage contains no blood vessels or neural connections, but receives all nutrients and external stimuli from the synovial fluid. Growth factors, such as insulin like growth factor-1 (IGF1) and transforming growth factor beta (TGFβ), slowly diffuse into the dense ECM and regulate the production of matrix proteins [12-14]. In injured or osteoarthritic cartilage

inflammatory cytokines, tumor necrosis factor alpha (TNFα) and interleukin 1 beta (IL-1β), are secreted from the surrounding synovial tissue [15] and activate matrix proteases [16-18], intracellular signaling molecules (i.e. cyclooxygenase-2 (COX2) [19]), and transcription factors c-Fos and c-Jun [20].

Chondrocytes regulate the composition, and thus mechanical properties of the ECM, in response to physical and chemical cues. The mechanical properties of the ECM determine the fields, forces, and flows experienced by chondrocytes creating a feed-back cycle. Therefore it is of great interest to understand how mechanical forces induce changes in cell activity, such as the transcription of molecules involved in cartilage homeostasis.

1.2 Cartilage Mechanotransduction

1.2.1 Mechanical Stimuli & Cartilage

The physical forces experienced by chondrocytes are unique to the cartilage environment. There is great interest in understanding the exact biophysical and physicochemical phenomena induced by mechanical loading, along with associated biological changes. Compression of cartilage causes matrix compaction, which reduces the interstitial pH, and increases the tissue osmolarity, resulting in a buildup of hydrostatic pressure within the tissue. The hydrostatic pressure is relieved by interstitial fluid loss from high pressure regions. The interstitial fluid in cartilage is positively charged to counter-balance the negatively charged aggrecan molecules, therefore, fluid flows induce streaming ion currents and potentials (Figure 1.2A). The composition of cartilage resembles a porous, hydrated polymer network and cartilage exhibits poroelastic and viscoelastic behavior. For example, the rate at which a strain is applied to the tissue is important for determining the magnitude of the stress induced. Slow compression induces mild hydrostatic pressures (~0.5-2MPa, [21,22]) and results in fluid loss [23]. During fast compression (strain rate = 1mm/sec) cartilage appears incompressible and a large hydrostatic pressure buildups (~15-20MPa, [24]), with little fluid loss. Thus the biological response of chondrocytes to a mechanical force is expected to be dependent on the frequency of loading and the magnitude of the induced concomitant fields, forces, and flows.

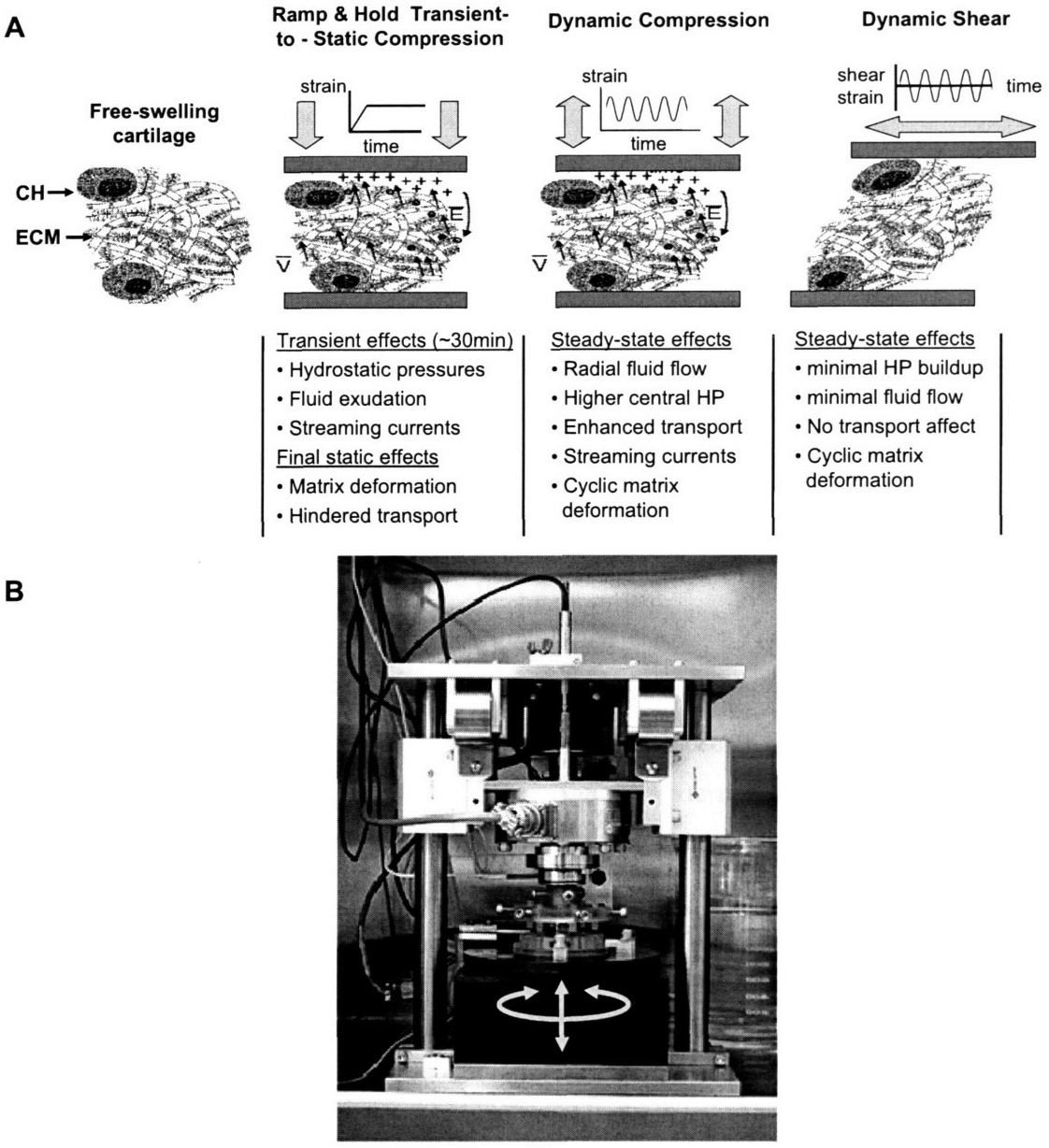

Figure 1.2: A) Physical stimuli induced by mechanically loading cartilage explants. CH = chondroyte, ECM = extracellular matrix. B) Incubator housed, feedback controlled loading apparatus [25].

Intact tissue explants preserve the native mechanical environment of cartilage and thus are useful for studying both the biophysical phenomena induced by mechanical loading and the biological outcomes. Researchers use a variety of mechanical loading regimes to decompose complex *in vivo* loading into well-defined physical components and to characterize chondrocyte activity [25-33] (an example device is in Figure 1.2B). Constant-strain static compression involves applying a ramp displacement to a cartilage explant of 10-50% strain. This can be

compared to compressive strains of up to 45% as measured by MRI using physiological static stresses applied to cadaver limbs [23]. In the explant the initial compression induces transient hydrostatic pressures, and radially-directed fluid flows that decay to an equilibrated compact matrix (Figure 1.2A). Constant-stress (creep) compression involves applying a constant load that slowly forces fluid out of the ECM causing continuous matrix compaction until a final static compression state is reached. Time varying compression involves applying a small strain (1-5%) dynamic compression at physiological frequencies (0.01-1Hz). Poroelastic theories predict that dynamic compression induces cyclic hydrostatic pressures within the center of the explant and cyclic radially-directed fluid flows which are greatest at the explant periphery (Figure 1.2A)[34,35]. In contrast, cyclic shear strains applied parallel to the explant surface induce minimal volume changes, fluid flows, or hydrostatic pressures. Therefore, dynamic shear is useful for studying the biological effects of isolated cyclic matrix deformation.

1.2.2 Chondrocyte Responses to Mechanical Stimulation

Mechanical forces are transduced to chondrocytes through the much stiffer ECM. In order to interpret mechanical stimuli chondrocytes must 1) detect the mechanical cues (most likely through cell-matrix interactions), 2) process the external signals using intracellular signaling pathways, 3) modulate the transcription and 4) synthesis of appropriate structural and signaling molecules (Figure 1.3). A variety of chemical assays are used to characterize the response of chondrocytes at each level of the mechanotransduction pathway.

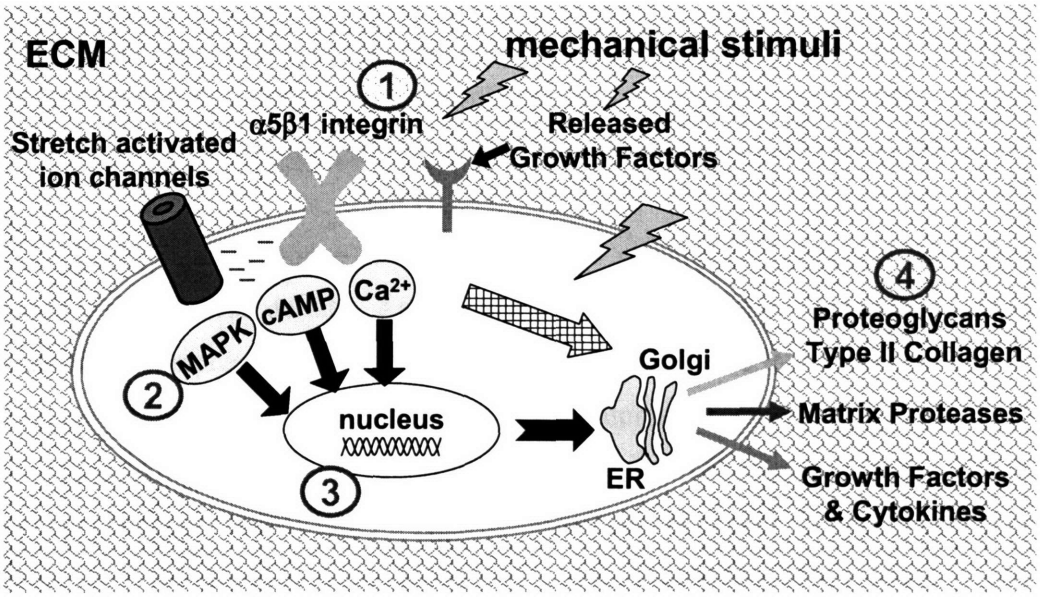

Figure 1.3: The transduction of a mechanical stimulus into biological outputs in a chondrocyte embedded in an extracellular matrix (ECM).

Identifying the mechanisms through which chondrocytes detect mechanical signals is an active research area. Due to technical difficulties of performing certain assays in explant tissue many experiments are performed on monolayer cultures of isolated chondrocytes. However, the differentiated state of chondrocytes is only preserved by culturing in three-dimensional scaffolds [36,37], and care must be taken when interpreting long-term monolayer culture studies. By increasing the pressure beneath a tissue culture plate, which stretches the plate base, researchers have been able to examine the immediate response of chondrocytes to pressure-induced strain [38]. Chondrocytes hyperpolarized in response to cyclic pressure-induced strain, a response that required $\alpha5\beta1$ integrin activated processes, calcium release, and interleukin-4 secretion. Hence, $\alpha5\beta1$ integrin, which is abundant on chondrocyte membranes, is considered a prime mechano-receptor candidate [39]. Application of oscillatory fluid flows across plated chondrocytes causes release of intracellular calcium [40,41], also suggesting that calcium release may be an early response to mechanical loading. Pressurized chambers have been used to apply hydrostatic pressures to isolated chondrocytes [42-45], and biological responses were observed. However, the mechanism of initial transduction was not determined and it is unclear how hydrostatic pressure in the absence of matrix deformation relates to *in vivo* loading. A major limitation to interpreting results from monolayer experiments is the fact that the ECM is absent, and hence the direct connection between the ECM and cytoskeleton is missing. Furthermore, the magnitude of flows and forces applied in monolayer experiments are typically much higher than experienced *in vivo* [46]. Therefore it is necessary to confirm the influence of physical stimuli and the mechanisms of action through explant experiments [47]. For example, there is evidence that the deformation induced by mechanical strain of cartilage affects the composition of organelles, particularly the Golgi apparatus [48,49], which may directly regulate the synthesis of matrix proteins.

The biosynthetic response of chondrocytes to mechanical loads has been thoroughly investigated over the last decade. Aggrecan and type II collagen biosynthesis decrease in response to static compression in cartilage explants [21,22,26], and hydrostatic pressurization of isolated chondrocyte [28,42]. In contrast, dynamic compression of cartilage explants increases synthesis of aggrecan and type II collagen, as does subjecting isolated chondrocytes to cyclic hydrostatic pressure gradients using pressurized chambers [28,42,45]. *In vivo* studies examining the effects of joint activity have found that limb immobilization results in decreased

proteoglycan (aggrecan) content [50,51], and that joint surfaces which undergo habitual loading have thicker cartilage and greater proteoglycan content [52]. Therefore, dynamic compression is considered an anabolic stimulus and many tissue engineering strategies utilize dynamic compression loading protocols to create stiffer pseudo-cartilage implants [53,54]. Recently dynamic tissue shear of cartilage explants was found to preferentially increase type II collagen, and also aggrecan biosynthesis [55], which suggests that isolated cyclic matrix deformation is an anabolic biophysical factor.

Regulation of matrix protein biosynthesis by mechanical forces has led to the speculation that the transcription of matrix proteins may also be mechano-regulated. The transcription of aggrecan increases during the first 4 hours of a displacement- or load-controlled static compression of cartilage explants [56,57]; however, by 24 hours aggrecan transcription is suppressed below control levels similar to biosynthesis studies. Cyclic pressure-induced strain increases aggrecan transcription in isolated chondrocytes [58], as does intermittent hydrostatic pressurization [44]. Chondrocytes subjected to hyperosmolarity media conditions suppress aggrecan transcription [59]. Therefore aggrecan transcription is strongly regulated by biophysical forces in a manner consistent with biosynthesis studies, suggesting that transcriptional regulation is part of the mechanotransduction pathway. Mechano-induced transcription is not expected to be restricted to aggrecan as type II collagen mRNA levels are also regulated by static compression of cartilage explants [57]. In monolayer systems there is evidence for matrix protease and/or TIMP transcriptional regulation in response pressure-induced strains [58], and fluid flow induced shear [60-62]. Prior to this thesis the extent of mechano-regulation of proteins involved in cartilage metabolism was unknown. Neither was it known how proteins might vary in response to different mechanical forces when chondrocytes were surrounded by their native ECM.

Cells utilize intracellular signaling pathways to convert external signaling events, such as receptor-ligand binding, into coordinated cellular responses. Hence, researchers are trying to identify roles for intracellular signaling molecules in cartilage mechanotransduction. Release of intracellular calcium was found to be necessary for aggrecan transcription induced by static compression of cartilage explants [63]. By performing static compression of cartilage explants in the presence of a variety of calcium chelators, calcium pump blockers, and inhibitors of calcium calmodulin, a causal relationship between static compression, intracellular calcium release, and aggrecan transcription was established. There is also evidence that cAMP activation of protein

kinase A is required for static compression induced aggrecan gene transcription [63], suggesting either cross talk exists between the two signaling pathways or that there is a downstream point of convergence. The mitogen-activated protein kinases (MAPKs) are enzymes known to respond to chemical and environmental stresses in other cell types [64], and were recently found to be activated in response to static compression [65]. Tyrosine kinases are phosphorylated in response to pressure-induced-strain of isolated chondrocytes [66]. In both cases the role of enzyme phosphorylation in mechanotransduction was not identified; however, the MAPK pathway has been implicated in aggrecan [67], and MMP [62] transcription in response to fluid flow induced shear.

The response of chondrocytes to other extracellular stimuli may help identify intracellular molecules important for chondrocyte behavior. The stimulation of MMP transcription and synthesis by cytokines, TNFα and IL-1β, was inhibited by blocking the MAPK pathway, NFκB, or transcription factor activating protein-1 (AP1), which is a c-Fos and c-Jun dimer [16,17]. Anabolic growth factors, IGF1 and TGFβ, stimulate MAPK phosphorylation in isolated chondrocytes [68,69], which has been shown to be involved in proteoglycan synthesis regulation [70,71]. The roles of the intracellular calcium, cAMP, and the MAPK pathway in chondrocyte metabolism makes them prime candidates for signaling pathways involved in mechanotransduction.

A major motivation for characterizing the mechanotransduction pathway in normal cartilage is the crippling disease osteoarthritis (OA), which affects 1 in 6 North Americans [72]. The progression of OA is characterized by increased matrix protease synthesis and activity, matrix protein fragments in the synovial fluid, and increased synthesis of matrix proteins in a failed attempt to repair the defective cartilage [9]. Acute joint injuries increase the chance of developing OA later in life [73-75], and also increase the concentration of matrix proteases and inflammatory cytokines in the synovial fluid in the years following the injury [10,15]. It is postulated that chondrocytes within injured or OA cartilage respond to the altered mechanical and chemical environment, and incorrectly respond to physiological mechanical forces. Chondrocytes from OA tissue do not regulate aggrecan transcription in response to pressure-induced-strain [58], and in contrast to normal chondrocytes, actually depolarize the cell cytosol [76]. Chondrocytes within mechanically injured cartilage explants to not increase proteoglycan synthesis in response to dynamic compression [24]. It is possible that injury and OA induce

fundamental changes in the cartilage mechanotransduction pathway. By comparison with a well characterized model of normal cartilage mechanotransduction that links signaling pathways with transcriptional responses new insight into the mechanisms driving the progression of OA will be discovered.

1.3 Thesis Outline

The objectives of this thesis were to quantify temporal gene expression changes in chondrocytes within their native extracellular matrix, induced by a set of mechanical loading conditions designed to represent components of *in vivo* loading, and to associate mechanically-induced changes in gene transcription with intracellular signaling pathways.

Chapter 2 describes the effects of static compression load and duration on the gene expression of 28 genes involved in cartilage homeostasis using real time polymerase chain reaction. The roles of intracellular calcium release and cAMP activation on compression-induced gene expression were examined by using molecular inhibitors. Data analysis techniques were developed to cluster and visualize the gene expression patterns and are described in Section 2.5.

Chapter 3 investigates the effects of time-varying mechanical loading regimes, dynamic compression and dynamic shear, on chondrocyte gene expression. A comparison is made of the effects of all three loading types in an effort to elucidate the roles of the specific physical stimuli induced by *in vivo* loading. The involvement of intracellular calcium and cAMP in dynamic compression and dynamic shear induced gene transcription is also described.

Chapter 4 examines the role of two MAP kinases, ERK1/2 and p38, in the regulation of transcription by the three mechanical loading regimes. Chapter 5 re-examines the relationship between physical stimulus and gene transcription by subdividing cartilage explants into regions of high hydrostatic pressures or high fluid velocities following application of the three loading regimes.

Appendix A summarizes changes in gene expression following a mechanical injury and/or culturing cartilage with injured synovial tissue. Appendix B details the development of the RNA-RT-PCR technique and includes the RNA extraction, reverse transcription, real-time PCR, and primer design protocols.

Chapter 2

Mechanical Compression of Cartilage Explants Induces Multiple Time-Dependent Gene Expression Patterns and Involves Intracellular Calcium and Cyclic AMP

This chapter was published in the Journal of Biological Chemistry in 2004 [77].

2.1 Introduction

Articular cartilage is responsible for the smooth articulation of synovial joints during locomotion. Chondrocytes within cartilage constantly remodel the tissue's extracellular matrix (ECM) throughout life. The major load-bearing constituents of the ECM are type II collagen and aggregates of the proteogylcan, aggrecan, which provide the tissue's tensile and compressive stiffness, respectively. Also present in the ECM are families of matrix proteinases, tissue inhibitors of matrix metalloproteinases (TIMPs), growth factors and cytokines that together regulate ECM remodeling and turnover in health and disease [78]. It is known that mechanical exercise of the knee joint *in vivo* increases the density of aggrecan in cartilage [79], whereas knee joint inactivity results in decreased aggrecan deposition [51,52]. Traumatic injury to cartilage diminishes mechanical strength and leads to excessive catabolism of the ECM, increasing the risk of osteoarthritis later in life [10].

A number of model systems have been developed to simulate various aspects of the mechanical loading forces experienced by articular cartilage *in vivo*. Compressive and shear forces have been applied to cartilage explants and chondrocyte cultures *in vitro* to examine the transduction of mechanical signals into biological responses. Application of 50% static

compression to cartilage explants decreased synthesis of type II collagen and proteoglycans (PG) within the first 1-2 hours of loading, and synthesis remained suppressed throughout a 24 hour loading period [22,26,80]. Dynamic compression [22,81] and shear [55] increased type II collagen and PG synthesis at low amplitudes and frequencies (1-5% strain, 0.01-1Hz); however, compression also increased the activation of MMP-2 and MMP-9 [32]. Injurious compression of cartilage explants results in increased PG loss to medium and damage to the collagen network [82,83]. Currently, many cartilage tissue engineering strategies employ some form of mechanical stimulation to enhance matrix production by chondrocytes during culture [54,84-87].

Recent studies of mechano-regulation of chondrocyte gene expression showed that application of 25-50% static compression to bovine cartilage explants caused a transient increase in expression of aggrecan [56,57] and type II collagen [57] mRNA levels during the first 4 hours of loading (>1.5-fold), followed by a decrease in expression to levels below non-loaded controls by 24 hours. Intermittent hydrostatic pressure (IHP) applied to human chondrocytes in monolayer culture at 1 Hz frequency (4 hour/day for 4 days) increased aggrecan and type II collagen gene and protein expression (>1.4-fold) [43]; IHP did not deform the chondrocytes. Millward-Sadler et al. applied hydrostatic pressure to chondrocyte in monolayer at 0.33 Hz for 20 minutes in a manner that induced strain on the culture dish and plated cells (pressure-induced strain, PIS) [58]. They observed an increase in aggrecan mRNA and a decrease in MMP-3 mRNA within 1 hour following stimulation, with a return to baseline levels by 24 hours. In a single experiment applying hydrostatic pressure (IHP) to human chondrosarcoma cells, changes in the expression of 51 genes were measured by cDNA array technology without widespread change in RNA stability [88], indicating that many genes may be influenced by mechanical stimuli.

Studies have also focused on cellular mechanotransduction events that may initiate changes in gene expression. Application of intermittent PIS to chondrocytes induced $\alpha 5\beta 1$ integrin activation of interleukin-4, which caused cell hyperpolarization via intracellular calcium release [38]. Inhibition of interleukin-4 suppressed the upregulation of aggrecan gene expression observed due to PIS [58]. Intracellular calcium release, cAMP and the PLC pathway have been implicated for aggrecan gene upregulation in response to static compression in cartilage explants [63]. Static compression also increased ERK1/2 phosphorylation within minutes of application, with sustained increases during 24 hours of compression [65]. While such signaling pathways

have been identified in the mechanical regulation of aggrecan gene expression, less is known about chondrocyte gene expression patterns of other ECM-related molecules or whether common upstream signaling pathways are responsible for their regulation.

Given these observations regarding the sensitivity of chondrocyte biosynthesis to mechanical forces *in vivo* and in the cartilage explant model, we hypothesized that mechanical loading would also induce widespread transcriptional changes, particularly for molecules involved in ECM maintenance. Our objective was to characterize the transcriptional response to static compression of chondrocytes within normal intact cartilage, focusing on a range of anabolic, catabolic, and signaling genes involved in tissue homeostasis. Temporal expression profiles of 28 genes were measured to compare immediate and long-term changes in response to sustained compression. Molecular inhibitors of intracellular calcium, cAMP and activating protein-1, were used to identify possible upstream signaling pathways involved in the mechanotransduction of the genes studied here. Clustering analysis [89,90] and principal component analysis [91,92] were used to elucidate the main expression trends and to highlight genes that appeared to be co-regulated by mechanical compression. These computational techniques can help to classify groups of genes with common upstream signaling pathways, and may help to predict certain cell behavior [90,92]. We found that both anabolic and catabolic genes were induced by static compression, but with contrasting expression patterns. Intracellular calcium and cAMP were found to play a fundamental role in the mechanical regulation of gene transcription.

2.2 Experimental Procedures

2.2.1 Cartilage Extraction & Mechanical Loading

Articular cartilage explant disks (3mm diameter, 1mm thick) were obtained from the middle zone of the patello-femoral groove of 1-4 week old calves as described previously [22]. Explants were washed with PBS and maintained in low glucose Dulbecco's modified essential medium supplemented with 10% FBS, 10mM Hepes Buffer, 0.1mM nonessential amino acids, 20μg/ml ascorbate, 100U/ml penicillin, 100μg/ml streptomycin and 0.25μg/ml amphotericin B. Explants were allowed to equilibrate for 2-5 days before loading, with media changes every second day and 12hrs before loading. Anatomically matched explants (6 explants per timepoint per loading treatment) were transferred into polysulphone loading chambers [22], slowly

compressed over a ~3 minute period to 25% or 50% of cut thickness, and maintained at these static strain levels for 1, 2, 4, 8 or 24hrs (25% strain, n = 4; 50% strain, n = 11), with explants kept in free-swelling conditions as controls (Figure 2.1A,B). Upon completion of loading explants were stored at -80°C in RNA-later solution (QIAGEN, CA).

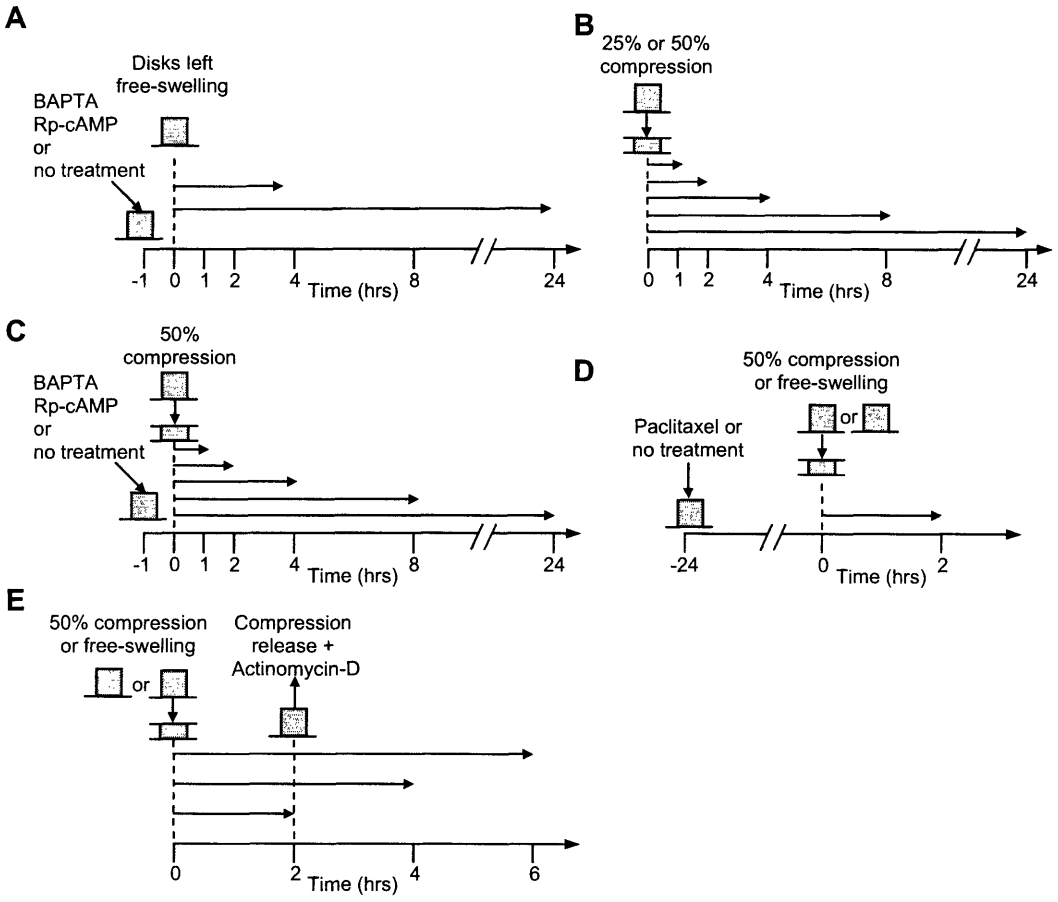

Figure 2.1: Protocols for mechanical compression of cartilage explants with and without inhibitor treatment. A) Free-swelling cartilage explants incubated for 4 or 24hrs with or without inhibitor treatment were used as controls for compression time-series. B) Continuous 25% or 50% compression was applied for 1-24hrs. C) No treatment, 10μM BAPTA-AM, or 50μM Rp-cAMP was added to media 1hr before commencement of a 50% compression time-series, with controls shown in (A). D) 10μM Paclitaxel was added 24hrs before application of 2hrs of 50% compression or a 2hr extended period of free-swelling. E) Cartilage explants were subject to 50% compression or kept free-swelling for 2hrs. Compression was released, 30μM Actinomycin-D was added to media, and explants were kept free-swelling for up to 4hrs. Six cartilage explants were used for every timepoint of each condition for all repeated experiments.

2.2.2 Inhibitor Studies

To investigate the role of intracellular signaling pathways during static compression, molecular inhibitors were added to media prior to application of 50% compression (Figure

2.1C,D). Cartilage explants were pre-incubated for 1hr with 10μM BAPTA-AM, a chelator of intracellular calcium (A.G.Scientific, CA) or 50μM Rp-cAMP, an inhibitor of cyclic-AMP activated protein kinase A (PKA) (Sigma, MO), which have been previously shown to completely inhibit mechanically-induced aggrecan gene regulation [56,63]. For each timepoint six untreated and six treated explants were placed into a 12-well polysulphone chamber to allow identical compression (n = 4-5). In separate experiments, Paclitaxel, an inhibitor of transcription factor activating protein-1 (AP-1) binding to DNA, (10μM, Sigma, MO) was added 24hrs prior to 2hrs of 50% static compression (n = 5), at concentrations previously shown to inhibit AP-1 activity in bovine chondrocytes [20]. To assess RNA stability, explants were either maintained in free-swelling conditions or loaded for 2hrs at 50% strain, and then released to free-swell for up to 6hrs before being stored at -80°C (n = 2). Actinomycin-D was added to media immediately upon completion of loading (Figure 2.1E) at concentrations shown previously to inhibit transcription in bovine chondrocytes and cartilage explants (30μM, Sigma, MO) [88].

2.2.3 RNA Extraction, Primer Calibration & Real-time PCR

For each timepoint and loading treatment, six cartilage explants were pulverized using liquid-nitrogen cooled mortar and pestles, and homogenized in QIAshredder tubes (QIAGEN, CA) spun at 10,000rpm for 2 minutes. RNA was then extracted from the clear supernatant using the QIAGEN RNAeasy Mini kit protocol with the DNase digest (QIAGEN, CA). RNA was stored in 40μl of RNase free water at -80°C until reverse transcription was performed using Applied Biosystems Reagents. Real-time PCR was performed on a 384-wells/plate ABI7900HT machine (2 min 50°C, 10 min 95°C, 50 cycles of 15 sec 94°C and 1 min 60°C) using SybrGreen MasterMix (Applied Biosystems, CA). The SybrGreen Master mix and H_2O were combined, and aliquots dispersed into cDNA containing tubes. A multipipette was used to distribute 9μl aliquots into a 384-well plate, followed by 1μl of 10μM forward and reverse primer mix. Free-swelling controls, and inhibitor treated samples were always run on the same plate as untreated compressed samples. A total of 28 primer pairs for the 28 genes listed in Table 2.1 were designed with amplification product length 85-130bp and annealing temperature ~60°C. All primers were tested to produce proportional changes in threshold cycle with varying starting cDNA quantity. Measured threshold cycles (C_T) were converted to relative copy numbers using primer-specific standard curves.

Matrix Proteins	Matrix Proteases	Protease Inhibitors	Transcription Factors	Cytokines/ Growth Factors	Intracellular signaling	Reference Genes
Aggrecan	MMP1	TIMP1	Sox9	IL-1β	COX-2	HSP70
Type I Collagen	MMP3	TIMP2	c-Fos	TNFα	MAPk1	Ribosomal-6P
Type II Collagen	MMP9	TIMP3	c-Jun	TGFβ	NOS2	
Type X Collagen	MMP13			IGF1		Housekeeping
Fibromodulin	ADAMTS4					18S
Fibronectin	ADAMTS5					G3PDH
Link Protein						

Table 2.1: Genes examined using real-time PCR, categorized by function. Primers were designed using Primer Express Software (Applied Biosystems) and Primer3 software (http://www-genome.wi.mit.edu/cgi-bin/primer/primer3_www.cgi), to have optimum annealing temperatures of 60°C and PCR product length between 85 & 130bp. Serial dilution standard curves comparing threshold cycle, C_T, and relative starting cDNA quantity, were created for all primers and had correlations $R \equiv 0.98$, and slopes close to unity.

2.2.4 Data Normalization & Statistical Analyses

For each experiment and every loading condition, gene expression levels were normalized by the average levels of mean-centered housekeeping genes 18S and G3PDH. The time-course of each gene was then normalized by the corresponding free-swelling expression level. For example, the BAPTA-AM treated time-courses were normalized by BAPTA-AM treated free-swelling controls after normalizing by housekeeping genes. Expression levels further than three standard deviations from the mean were considered outliers and removed. Gene expression levels induced by compression were compared to free-swelling expression levels using two-tailed Student's t-tests. Comparison between compression time-courses with and without the presence of inhibitors was performed using comparison of means two-tailed t-tests, with Welch corrected degrees of freedom for unequal variance. Games-Howell corrected standard deviations were used to account for unequal sample sizes, as F-tests had revealed significant differences between untreated and treated gene expression level variances (data not shown). Skew and Kurtosis criteria were used to confirm that the data were approximately normally distributed. A p-value of less than or equal to 0.05 was used to assess statistical significance.

2.2.5 Clustering Analysis

To further analyze the expression patterns and pathways activated by compression, the expression levels for each gene from the 50% compression, BAPTA-AM treated and Rp-cAMP

treated time-courses were combined into fifteen point expression vectors (23 genes had complete time-courses). These expression vectors were then standardized to have equal variance, to emphasize expression patterns rather than amplitudes, and were then iteratively clustered using two different *k*-means clustering techniques (see Section 2.5). First, principal component analysis (PCA) [91,92] was used to determine the principal components of the data matrix comprised of the genes and timepoints. Each standardized expression vector was then projected onto the three main principal components and the resulting three-dimensional coordinates were *k*-means clustered using a Euclidean distance metric. The second approach was to cluster the standardized expression vectors directly using correlation as a metric [89,90]. The main expression trends were then identified from comparison of the two techniques. Projection coordinates for each group centroid were calculated by averaging the projection coordinates of each gene within a group. Centroid vectors were formed by adding the three main principal components weighted by the centroid projection coordinates. Centroid variances were calculated, and the Euclidean distance between the projection coordinates of centroids was used to perform comparison of means Student's t-tests to assess the distinctiveness of expression trends (see Section 2.5.4 for details).

2.3 Results

2.3.1 Effect of Static Compression on Gene Expression

Static compression was applied for 1-8hrs at 25% strain and 1-24hrs at 50% strain, and expression levels of 28 ECM maintenance genes were monitored. For ease of presentation and discussion, selected results for specific genes are reported in Figure 2.2, Figure 2.3 & Figure 2.4; the complete results for all 28 genes in this study are given in the Section 2.6, Figure 2.11 & Figure 2.12. Consistent with previous findings aggrecan [56,57] and type II collagen [57] were transiently upregulated in a strain-dependent manner during the first 8hrs of compression (up to 2.5-fold) before decreasing below free-swelling expression levels by 24hrs of 50% compression; link protein was similarly affected (Figure 2.2). In contrast, type I collagen was downregulated in response to 25% compression, and increasingly upregulated during 50% compression, greater than 3-fold after 24hrs (Figure 2.2); however, comparison of C_T values showed that absolute mRNA abundance of type I collagen was two orders of magnitude lower than type II collagen (data not shown). MMP3 and ADAMTS4 were increasingly upregulated with 50% compression

duration up to 16-fold and 4-fold respectively (Figure 2.2), and TNFα, IL-1β, and COX-2 were similarly affected (Figure 2.12). MMP9 and 13 were upregulated 2-fold and 8.6-fold by 24hrs of 50% compression, whereas MMP1 and ADAMTS5 were downregulated by 30% (Figure 2.11).

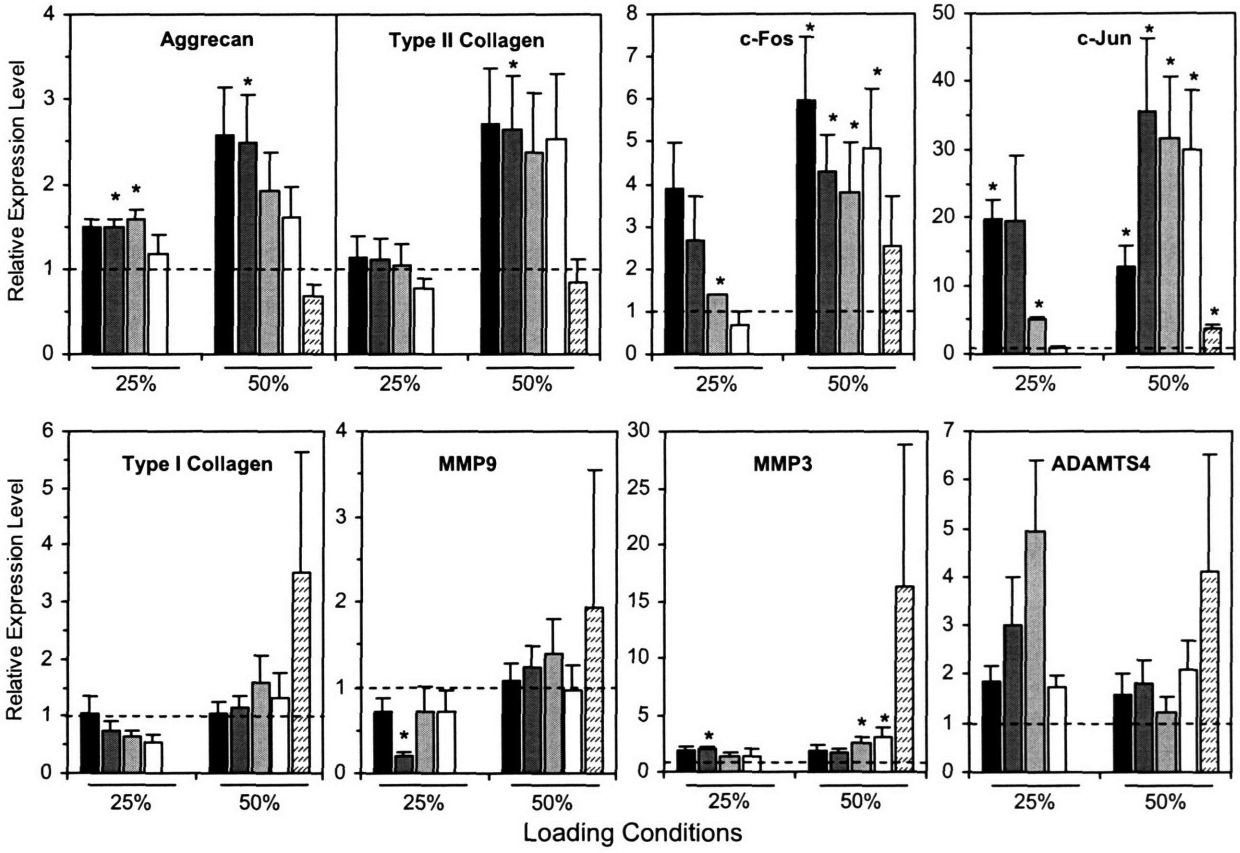

Figure 2.2: Selected gene expression levels induced by static compression, measured by real-time PCR. 25% = 1-8hrs of 25% static compression (n = 4). 50% = 1-24hrs of 50% static compression (1-8hrs, n =11 & 24hrs, n = 4). Expression levels were normalized by 18S and G3PDH housekeeping genes and divided by free-swelling expression levels. Mean + SE. * = $p<0.05$ compared to free-swell control using Students two tailed t-test. ■1hr, ■2hr, ■4hr, □8hr, ⊟24hr, relative free-swelling expression level = 1 (dashed line).

Transcription factor Sox9 was upregulated more by 25% compression (up to 1.7-fold) than 50% compression; in both cases the effect was transient lasting 4hrs or less (Figure 2.12). c-Fos and c-Jun showed marked upregulation during the 25% compression time-course as well as peaked upregulation (6 & 35-fold respectively) during the 50% compression time-course (Figure 2.2). The TIMPs were generally downregulated by 50% compression with upregulation only occurring at initial timepoints (Figure 2.12). Fibromodulin, fibronectin, and ribosomal-6-phosphate were in general unaffected by static compression (Figure 2.11 & Figure 2.12). HSP70

was slightly upregulated throughout the 50% compression time-course (Figure 2.12). IGF1 and NOS2 were highly upregulated at certain timepoints but their expression levels were scarcely detectible even with real-time PCR (Figure 2.12).

2.3.2 Effect of BAPTA-AM Treatment

To determine if intracellular calcium release was a prevalent step in the mechanotransduction pathway, 10μM BAPTA-AM was added to the medium 1 hour before application of the 50% compression time-course (Figure 2.1C). The addition of BAPTA-AM did not appear to affect free-swell gene expression levels; however, genes which did show a greater than 70% or significant change are summarized in Figure 2.3.

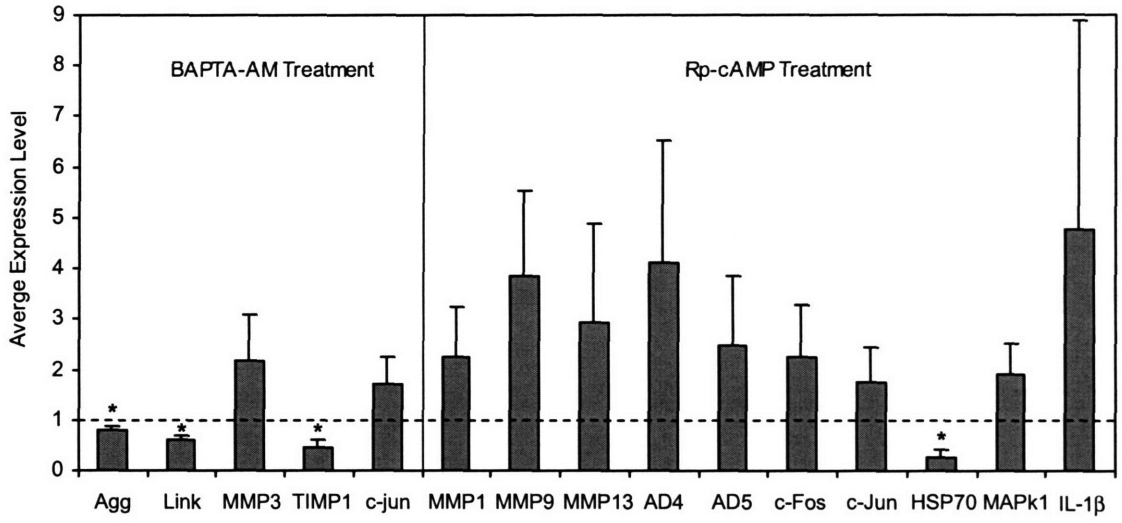

Figure 2.3: Expression levels of genes affected by the addition of BAPTA-AM or Rp-cAMP to media under free-swelling conditions. Six cartilage explants were incubated in media with or without the addition of 10μM BAPTA-AM or 50μM Rp-cAMP for 4 hours or 24hrs. Most of the 28 genes examined were unaffected by the addition of either inhibitor under free-swell conditions, and only genes for which the inhibitor treated expression level changed by > 70% or were statistically significantly affected are shown. Mean + SE (n = 3-6). * $p < 0.05$ Student's t-test comparing inhibitor-treated expression to the untreated relative expression level = 1 (dashed line). Agg = aggrecan, AD4 = ADAMTS4, AD5 = ADAMTS5.

Aggrecan, link protein and TIMP1 free-swelling expression levels were significantly downregulated by 20%, 38% and 54% respectively. In general BAPTA-AM treatment suppressed the regulation induced by 50% compression (Figure 2.4, Figure 2.11 & Figure 2.12). In particular, aggrecan, link protein, and fibromodulin expression remained close to free-swelling expression levels throughout the BAPTA-AM treated time-course, while type II collagen was

partially suppressed (Figure 2.4 & Figure 2.11). The expression pattern of c-Fos was unaffected by the presence of BAPTA-AM; however, c-Jun levels, though upregulated compared to free-swelling controls, were reduced by approximately half compared to the untreated 50% compression time-course (Figure 2.4). MMP1,9&13 were downregulated below free-swelling controls throughout the BAPTA-AM treated time-course, and the upregulation of MMP3 was largely suppressed, particularly at 24hrs (Figure 2.4 & Figure 2.11). In contrast, ADAMTS-4 was mainly unaffected by the presence of BAPTA-AM during 50% static compression and HSP70 was actually increased (Figure 2.11 & Figure 2.12). IL-1β was suppressed below free-swelling expression levels; however, COX-2 remained upregulated (Figure 2.12).

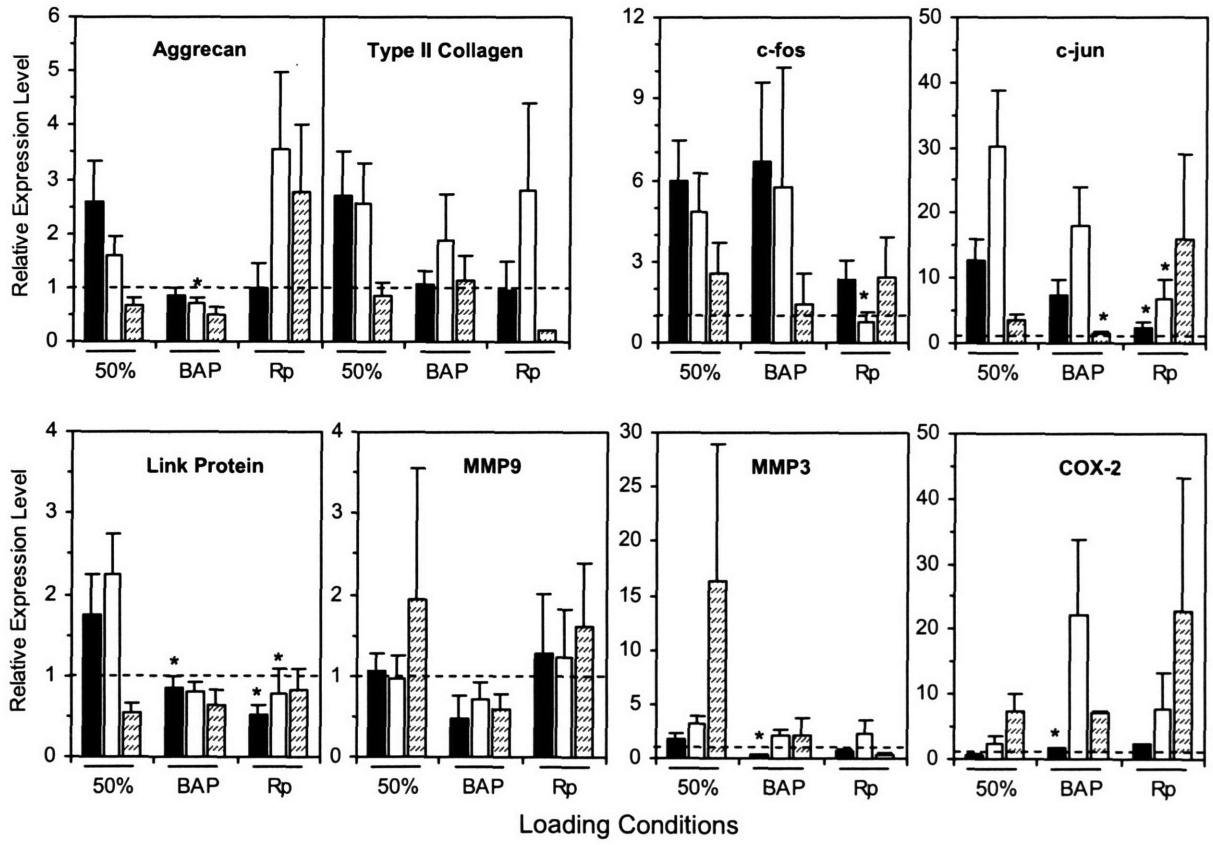

Figure 2.4: Effect of BAPTA-AM or Rp-cAMP pretreatment on gene expression levels induced by 50% static compression for a selection of genes. 50% = untreated 50% compression time-course (1-8hrs, n = 11 & 24hrs, n = 4), BAP = BAPTA treated 50% compression time-course (n = 4), Rp = Rp-cAMP (n = 3) treated 50% compression time-course. Expression levels were normalized using 18S and G3PDH housekeeping genes, and divided by the appropriately treated free-swelling expression levels. Mean + SE. * = $p<0.05$ compared to untreated 50% compression time-course, using Welch and Games-Howell corrected, comparison of means, two-tailed t-tests. ■1hr, □8hr, ▨24hr, relative free-swelling expression level = 1.

2.3.3 Effect of Rp-cAMP Treatment

To determine if cAMP activation of PKA was a prevalent step in the mechanotransduction pathway, Rp-cAMP was added 1 hour prior to application of the 50% compression time-course (Figure 2.1C). Rp-cAMP had a more pronounced effect on free-swelling expression levels than BAPTA-AM, though still only affected a subset of genes (Figure 2.3). Notably HSP70 was suppressed by 70%, IL-1β was upregulated 4.7-fold, and MMP1,9,13, ADAMTS4,5 were upregulated >2-fold. In general, Rp-cAMP suppressed gene induction by compression similar to BAPTA-AM, but also enhanced the regulation of a number of genes (Figure 2.4, Figure 2.11 & Figure 2.12). The initial timepoints of aggrecan and type II collagen were suppressed by Rp-cAMP; however, after 8hrs of loading, the expression levels of both genes were higher than corresponding untreated levels, and also after 24hrs for aggrecan (Figure 2.4). Although c-Jun was still upregulated in the presence of Rp-cAMP, overall expression levels were much lower than in response to BAPTA-AM treatment or 50% compression alone, and increased with compression duration (Figure 2.4). In contrast to the BAPTA-AM treated time-course, the upregulation of c-Fos was mostly suppressed during the first 8hrs of Rp-cAMP treated compression (Figure 2.4). Type I collagen and MMP expression were suppressed even below free-swelling expression levels for most timepoints, particularly MMP3 which was reduced to 0.30-fold after 24hrs compression (Figure 2.4). In contrast, ADAMTS4 remained upregulated after 24hrs and COX-2, HSP70, and TIMP3 gene expression levels were higher with Rp-cAMP treatment during compression, peaking after 24hrs at 23-fold, 10.5-fold and 4-fold, respectively (Figure 2.11 & Figure 2.12). Notably, Sox9 was downregulated to 0.06-fold after 24hrs (Figure 2.12).

2.3.4 Main Expression Trends Induced by Static Compression

PCA revealed three main eigenvectors (principal components) that accounted for 60% of the variance in the data. The coordinates of each standardized gene expression vector when projected onto the three main principal components are shown in Figure 2.5. Visual examination of the projection plot and varying the number of groups while clustering revealed that the genes were best divided using 4 groups. *k*-means clustering of the projection coordinates using Euclidean distance produced four clusters with 4-7 genes each, shown in Figure 2.5 and Table 2.2A. *k*-means clustering using a correlation metric and the standardized gene expression vectors

produced almost identical results, with only aggrecan and ADAMTS4 swapping groups. Examination of the top five groupings showed only 1 to 2 gene placement variations from the optimal solutions produced by either clustering method indicating that the groupings were very robust. The optimal groupings produced by either method were significantly better than randomly assigning genes to groups ($p << 0.001$, see Section 2.5.4). Comparing inter-centroid distances using comparison of means Student's t-tests revealed that the four clusters were significantly separated and distinct (Table 2.2B).

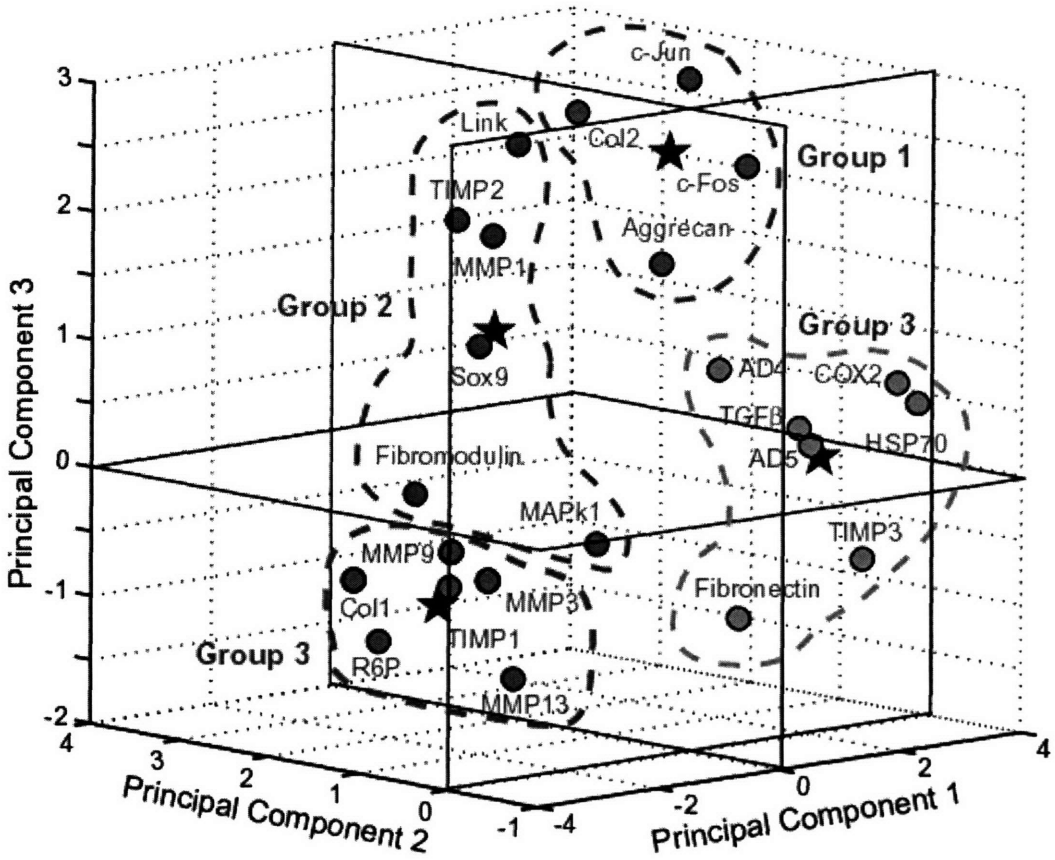

Figure 2.5: Three-dimensional plot of gene expression profiles induced by static compression with and without inhibitors. The standardized gene expression vectors were projected onto the three main principal components found using PCA, with groupings found using *k*-means clustering. '★' marks the projection coordinates of the four cluster centroids. Abbreviations: Col = collagen, AD = ADAMTS, R6P = ribosomal 6 phosphate.

A

Group #	Grouped Genes	Centroid Coordinates (PC1, PC2, PC3)
1	Aggrecan, Type II Collagen, c-Fos, c-Jun	(1.45,1.21, 2.45)
2	Link Protein, MMP1, TIMP2, Sox9, Fibromodulin, MAPk1	(-2.11, 0.77, 1.35)
3	Type I Collagen, MMP3, MMP9, MMP13, TIMP1, Ribosomal 6-P	(-0.12, 2.71, -1.19)
4	ADAMTS4, ADAMTS5, TIMP3, Fibronectin, HSP70, TGFβ, COX-2	(2.42, 0.18, 0.1)

B

p-values for Centroid separation	Centroid 1	Centroid 2	Centroid 3
Centroid 2	1.3×10^{-3}		
Centroid 3	2.8×10^{-4}	4.5×10^{-4}	
Centroid 4	4.8×10^{-3}	4.7×10^{-5}	1.7×10^{-4}

Table 2.2: Optimal groupings found by gene clustering. The 50% compression time-course, and BAPTA-AM treated and Rp-cAMP treated time-courses were combined into gene expression vectors. A) Groupings found by *k*-means clustering the standardized gene expression vectors projected onto the three main principal components. Centroid coordinates represent the location of the average of all genes within a group projected onto the three main principal components. B) p-values for comparison of centroid locations. The Euclidean distance between the projection coordinates of two centroids was used for comparison of means Student's t-test, with the number of genes within each group representing the degrees of freedom. Intra-centroid variance was calculated using Equation 2.13.

The centroids of the four main expression patterns induced by compression with and without the presence of inhibitors are shown in Figure 2.6. Group 1 paired aggrecan and type II collagen, which was expected from previous experiments, along with the AP-1 binding protein elements c-Fos and c-Jun. Both Centroids 1 and 2 transiently increased during the first 4 to 8hrs of static compression followed by a decrease towards free-swelling expression levels by 24hrs (Figure 2.6). However, Centroid 2 was suppressed by the addition of either BAPTA-AM or Rp-cAMP, whereas Centroid 1 was only partially suppressed by BAPTA and only suppressed at initial timepoints by Rp-cAMP (Figure 2.6). Group 3 contained mainly matrix metalloproteinases and type I collagen, and exhibited a 50% compression induced upregulation that peaked after 24hrs (Figure 2.6). Group 4 had a similar pattern during 50% compression with a less pronounced peak at 24hrs. However, in contrast to Centroid 3 which was almost

completely suppressed by either BAPTA-AM or Rp-cAMP, Centroid 4 mechano-induction was enhanced by BAPTA-AM and even more so by Rp-cAMP.

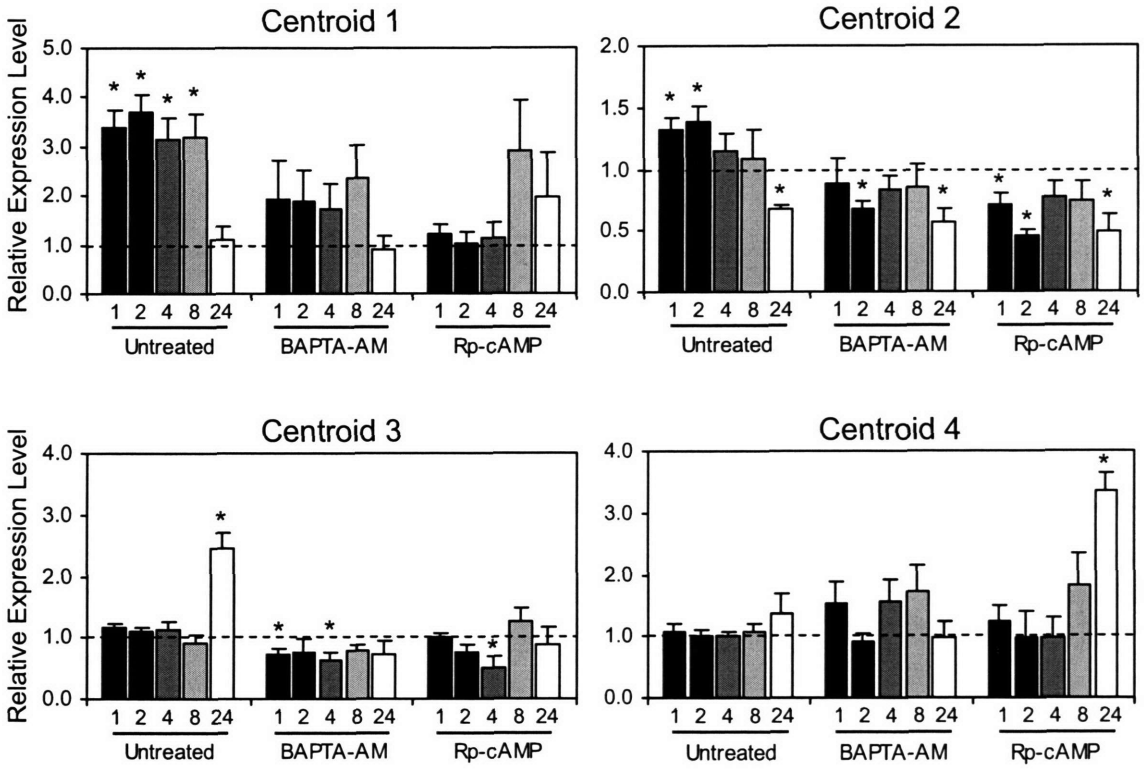

Figure 2.6: Four main expression trends induced by 1-24hrs of 50% static compression with and without the presence of BAPTA-AM or Rp-cAMP. Centroid-vectors were calculated from the average projection coordinates of genes within each group, re-constructed using the three main principal components. Optimal groups were found using *k*-means clustering of gene-projection coordinates using Euclidean distance. Group expression profiles were calculated from the average profiles of genes in a group using Equation 2.12. Mean + SE, * $p < 0.05$ compared to free swelling control expression level (dashed line).

2.3.5 Effect of Paclitaxel Treatment

To determine if the upregulation of c-Fos and c-Jun by compression, which may increase AP-1 signaling, was involved in regulating gene transcription during mechanical loading, paclitaxel was added 24 hrs before 50% compression (Figure 2.1D). Genes in Group 1 remained upregulated after 2hrs of compression with paclitaxel present, and free-swelling controls remained unaffected (Figure 2.7). Sox9 levels were reduced below controls, and c-Fos upregulation was suppressed by 50% (Figure 2.7), though c-Jun expression was unaffected. MMP3 expression was reduced below free-swelling expression levels, MMP13 was upregulated by >2-fold, and COX-2 remained upregulated by 4-fold during paclitaxel treated compression (Figure 2.7). MMP1 and MMP9 remained upregulated to the same extent with paclitaxel present;

however, TIMP expression was further increased ~1.5-fold and type I collagen was further doubled by the presence of paclitaxel during compression (data not shown).

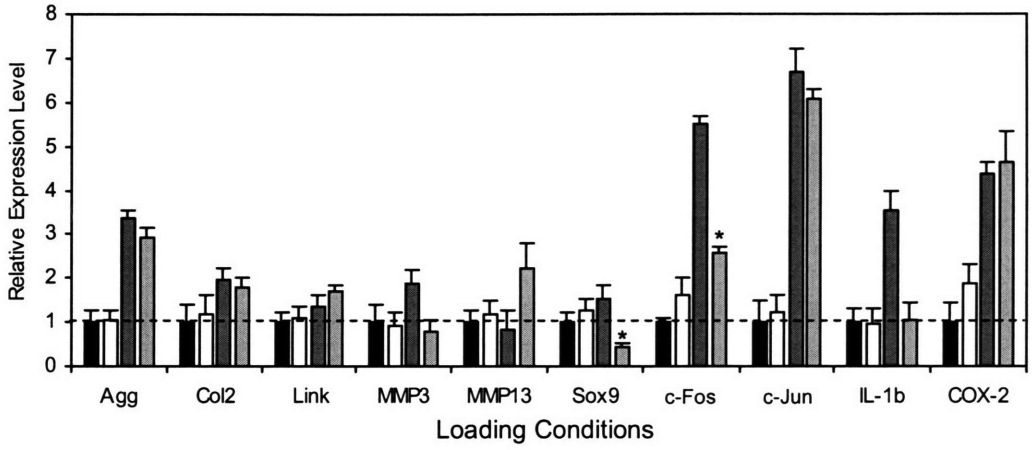

Figure 2.7: Effect of paclitaxel on gene expression changes induced by 2hrs of 50% compression. Paclitaxel was added 24hrs before loading. Gene expression levels were normalized by housekeeping genes, repeated experiments were averaged, and then scaled by free-swelling expression levels. ■free-swell, □free-swell + 10μM paclitaxel, ■2hrs 50% compression, ■2hrs 50% compression + 10μM paclitaxel. Mean + SE. *= $p < 0.05$ using Games-Howell corrected comparison of means, t-test (n = 5). Abbreviations: Agg = aggrecan, Col2 = type II collagen and Link = link protein.

2.3.6 RNA Stability

To determine if the changes in mRNA expression were due to changes in transcription or changes in RNA half-life, actinomycin-D was added upon release of compression, and gene expression was monitored for up to 6hrs post-compression (Figure 2.1E). Individual and group expression trends were examined for the genes listed in Table 2.1. However, transcript half-lives exceeded the 6hr timepoint and no clear differences between compressed and free-swelling conditions could be determined (data not shown). Therefore, 2hrs of 50% static compression did not appear to modify RNA stability over the time-period examined.

2.4 Discussion

In this study, we demonstrated that most genes investigated responded to static compression, with expression profiles that were both strain and time dependent. The effects of static compression on transcription evolved with time, and after 24hrs the transcription of proteases and signaling molecules dominated over matrix molecules and early response genes. Cluster analysis revealed four group expression patterns induced by compression, with two groups requiring intracellular calcium and cAMP as common upstream mechano-regulators.

To further interpret the changes in gene expression in response to compression, we can compare our results to the kinetics of the intratissue mechanical forces and flows caused by compression. During joint loading *in vivo*, cartilage experiences a complex mixture of compressive and shear deformation having both static and dynamic components. For example, *in vivo* joint loading can result in high peak mechanical stresses (15-20 MPa) that occur over very short durations (< 1 sec) causing cartilage compressive strains of only 1-3% [93]. In contrast, sustained (static) physiological stresses applied to knee joints for 5-30 minutes can result in compressive strains in certain knee cartilages as high as 40-45% [23]. In the present study, application of a slow compression over ~3min to a final strain of 25% or 50% causes an initial transient intratissue pressurization and fluid flow within the matrix immediately following compression and during a 15-30 minute period of stress relaxation [22,33]. After stress relaxation has ended, fluid flow ceases and intratissue pressure returns to zero (i.e., that of the medium) as the new equilibrium compressed state of the tissue is reached. Thus, the initial compression transient has certain physical attributes of slow dynamic compression, while the final compressed state mimics the static component of *in vivo* compression. Therefore, our objective was to explore the kinetics of changes in gene expression to both the initial transient loading and final static loading phases.

Static compression has been previously shown to decrease PG and type II collagen synthesis within 1-2hrs [22,94]. In our experiments, 25% compression transiently upregulated aggrecan gene expression and did not alter type II collagen during 8hrs of loading (Figure 2.2). Consistent with previous studies that used Northern analyses [57], 50% compression caused transient upregulation of both aggrecan and type II collagen during the first 8hrs and a subsequent decrease in expression below free-swelling levels by 24hrs (Figure 2.2). Thus, the temporal kinetics of transcriptional and biosynthetic responses to loading are considerably different, though they converge by 24hrs after application of static compression. Therefore, the initial transient upregulation of aggrecan and type II collagen genes may be more sensitive to the dynamic components of the applied compression. Recent experiments have shown that ERK1/2 and p38 phosphorylation levels peak within 10 minutes of static compression but only ERK1/2P levels remained upregulated after 24hrs [65]. It was suggested that such an initial transient response was due to the dynamic components of static compression, consistent with the results of Li et al. [95], which may similarly explain the transient transcriptional upregulation of matrix

proteins observed here. In addition, loading may affect the apparatus for transcription and translation differently. Studies have shown that high pressure can cause changes in cell morphology and disorganization of the Golgi and microtubules in chondrocytes [48]. Compression of cartilage explants also reduces cell volume and the volumes of several intracellular organelles; however, the volume of the Golgi remains unaffected by static compression of up to 50% strain [1,49]. Thus, the synthesis of proteins which require significant post-translation modification may be affected by compression differently than transcription.

Dynamic compression, a known stimulator of matrix protein synthesis, was also found to induce MMP2&9 gene expression and activity [32]. In our study, matrix protease gene expression followed a common trend of increasing upregulation with 50% compression duration (Figure 2.2 & Figure 2.11). COX-2 and IL-1β were upregulated in a similar pattern to the matrix proteases and TNFα was highly upregulated after 24hrs (Figure 2.12). IL-1β is a known modulator of COX-2 gene and protein expression [19] and IL-1β, TNFα and COX-2 are known to regulate the gene and protein expression of matrix proteases [14,16-18,96,97]. Hence, the regulation profile of the MMPs may follow the regulation of IL-1β, TNFα and COX-2. IL-1β did not increase above control levels until after 8hrs of compression, and a similar delay of 3hrs was seen during 50% loading experiments by another group [98]. Furthermore, blocking IL-1β signaling during compression suppressed the expected decrease in PG synthesis, but only at longer timepoints (6hrs) [98], confirming the involvement of IL-1β signaling during prolonged periods of static compression.

The early upregulation of transcription factors c-Fos and c-Jun (Figure 2.2), which form the AP-1 binding protein, may be another signal for compression-induced matrix remodeling or catabolism. Increased AP-1 activity is a precursor to the IL-1β induction of matrix proteases, which can take up to several hours [17,97,99]. ERK1/2, p38 and JNK phosphorylation is also upregulated as early as 10-60 minutes after compression [65], indicating activation of MAPK pathways possibly responsible for c-Fos and c-Jun upregulation.

ECM gene expression was unaffected by the presence of the AP-1 inhibitor, paclitaxel, during 2hrs of 50% compression (Figure 2.7), demonstrating that AP-1 activation was not responsible for the early upregulation of aggrecan and type II collagen (Figure 2.2). Another role for the pronounced upregulation of c-Fos and c-Jun is suggested by studies in which chondrocytes were transfected with c-Fos, causing a decrease in PG synthesis [100] similar to

static compression [22,26]. COX-2, which was upregulated in response to 50% compression (Figure 2.12), and by PIS [101], is known to cause PG destruction via prostaglandin E-2 (PGE-2) [102]. Interestingly, in chondrocyte cell lines, PGE-2 regulated cAMP and intracellular calcium pathways [103]. Thus, the anti-anabolic effects of static compression may be mediated in part by mechanisms dependent on short-term c-Fos/c-Jun upregulation and long-term COX-2 upregulation.

When the 50% compression data were formed into gene expression vectors and clustered, two main untreated 50% compression expression profiles were found. Groups 1 and 2 (Table 2.2) were characterized by a transient 4-8hr upregulation followed by a decline towards free-swell levels after 24hrs (Figure 2.6) while Groups 3 and 4 showed increased upregulation with compression duration (Figure 2.6). Each group behaved distinctly in response to BAPTA-AM or Rp-cAMP, further dividing the transcriptional responses induced by static compression into a total of four groups. Chelation of intracellular calcium using BAPTA-AM suppressed aggrecan gene upregulation in response to compression (Figure 2.4) similar to previous findings [63]. Calcium-dependent K^+ channels have been implicated in the mechanotransduction pathway of isolated chondrocytes [38], suggesting intracellular calcium release is an initial event in mechanotransduction. We found that the presence of BAPTA-AM during mechanical loading suppressed the upregulation of many genes, including, aggrecan, type II collagen, link protein, c-Jun, and many MMPs (Figure 2.4, Figure 2.11 & Figure 2.12). In particular Centroids 2 and 3 were completely suppressed when BAPTA-AM was present during loading, Centroid 1 was partially suppressed and Centroid 4 was mainly unaffected. The selective suppression by BAPTA-AM supports the idea that intracellular calcium is a common but not complete upstream signaling event controlling the mechano-regulation of anabolic, catabolic, and anti-catabolic genes. Interestingly, expression of stress protein HSP70 during compression was significantly greater when in the presence of BAPTA-AM (up to 3.8-fold) (Figure 2.12). Hence, intracellular calcium release may also be required to elicit the stress-protective response seen in chondrocytes during loading [104]. IL-1β was downregulated below free-swelling controls and c-Jun expression was significantly suppressed during BAPTA-AM treated compression, which may explain the downregulation and suppression of matrix proteases, even though COX-2 expression remained upregulated (Figure 2.12).

The inhibition of cAMP activated PKA during 50% compression prevented aggrecan gene upregulation, although only during the first 4hrs of loading (Figure 2.4), consistent with previous findings [56]. Cluster analysis revealed that the effect of Rp-cAMP was distinct from that of intracellular calcium chelation. The presence of Rp-cAMP during loading suppressed Centroids 2 and 3 similar to BAPTA-AM; however, the upregulation of Centroid 4 was enhanced at later timepoints. In contrast to BAPTA-AM treatment, the early upregulation of both c-Fos and c-Jun was suppressed during Rp-cAMP treated compression (Figure 2.4) which might prevent the AP-1 signaling necessary for MMP upregulation. The dominant change in Centroid 1 in response to Rp-cAMP treatment during loading was a shift from a transient initial upregulation to increasing upregulation during longer time periods. These results confirm cAMP activation as a prevalent upstream component of the intracellular mechanotransduction pathway. Both intracellular calcium and cAMP were necessary for Group 2 and 3 mechano-induction, suggesting that common downstream mechanisms may be involved. Suppression of c-Fos by only Rp-cAMP, and the differing regulation of Groups 1 and 4 by the two inhibitors, suggests that cAMP is not simply downstream of intracellular calcium as was previously proposed [63]. The failure of either BAPTA-AM or Rp-cAMP to suppress the mechano-induction of Group 4 genes suggests that additional upstream signaling mechanisms exist.

The widespread impact of mechanical loading on the transcription of genes involved in ECM maintenance has been demonstrated in this study. It is possible to speculate that gene mechano-regulation may play a role in maintaining a healthy cartilage ECM throughout life and that the inferior cartilage phenotype developed during OA may include improper gene mechano-regulation. Ongoing studies are examining gene mechano-regulation in response to the dynamic compression and shear components of *in vivo* mechanical loading. The exact order in which intracellular pathways are activated and the role of the transcribed signaling molecules cannot be directly inferred from the inhibitor studies and gene expression data presented. Further studies are required to determine what factors are responsible for the divergent anabolic and catabolic temporal expression profiles. Four main expression patterns were identified in response to static compression and could represent genes co-regulated by intracellular calcium and/or cAMP. The dramatic upregulation of c-Fos and COX-2 by static compression suggests a possible role in mechanically-mediated cartilage remodeling and/or degradation, and it will be worthwhile to

further examine these molecules in the presence of injurious mechanical compression of cartilage.

2.5 Statistical & Clustering Analysis Techniques

2.5.1 Gene Vector Standardization & PCA

The 23 genes containing complete 50% compression untreated, BAPTA-AM and Rp-cAMP treated time-courses represent an intermediate size dataset. It is possible to visually group certain genes together, but to do so in a mathematically rigorous manner required the use of clustering techniques. Principal component analysis (PCA) is a tool commonly used to reduce large data matrices, in our case 23 genes x 15 timepoints, into a smaller number of essential characteristics. PCA requires solving the eigenvalue problem for the squared dataset ($data^T \times data$) and produces the eigenvectors (principal components) and corresponding eigenvalues. These principal components form a set of basis vectors (the number of vectors equal to the length of the shortest dimension of the matrix). Each gene vector can then be represented as a weighted, linear combination of the principal component vectors.

$$\mathbf{X}_i = \alpha_1 \mathbf{V}_1 + \alpha_2 \mathbf{V}_2 + \ldots + \alpha_{15} \mathbf{V}_{15} \qquad (2.1)$$

$\mathbf{X}_i$ is a gene expression vector, $\mathbf{V}_i$ is a principal component, and α_i is the weighting of $\mathbf{V}_i$ required for $\mathbf{X}_i$ and is calculated as the projection of $\mathbf{X}_i$ on $\mathbf{V}_i$ (which is simply the dot product of $\mathbf{X}_i$ and $\mathbf{V}_i$ as $\mathbf{V}_i$ is unit length). The reason PCA provides dimensional reduction is that many of the eigenvalues, which represent the variance accounted for by the corresponding eigenvector, are close to zero, and may be considered unimportant or simply noise and removed before clustering the data [105,106]. Therefore each gene vector can be accurately recreated from a few principal components and the weightings visualized as gene coordinates (α_1,α_2,α_3) in two or three dimensions. A drawback of this technique when applied to gene expression data is that it is difficult to define noise in expression patterns since some of the lesser eigenvectors may represent important traits [107]. However, the ability of PCA to produce meaningful insights has been shown when the data are properly pre-processed [91,92,108].

Our initial attempts applying PCA to the data matrix revealed two main principal components as shown in the Scree plot in Figure 2.8, with PC1 accounting for ~75% of the variance in the data. Projection of the gene expression vectors onto the two principal components

highlighted that PC1 was primarily composed of c-Jun and PC2 of COX-2 (Figure 2.8). This was confirmed by performing Euclidean distance based clustering which formed groups of COX-2 alone, c-Jun alone, and then one large group containing the remainder of the genes. Hence, our initial PCA-based clustering method was not able to distinguish the distinct but lower amplitude trends of other genes such as aggrecan, MMP9 and ADAMTS4 (Figure 2.2).

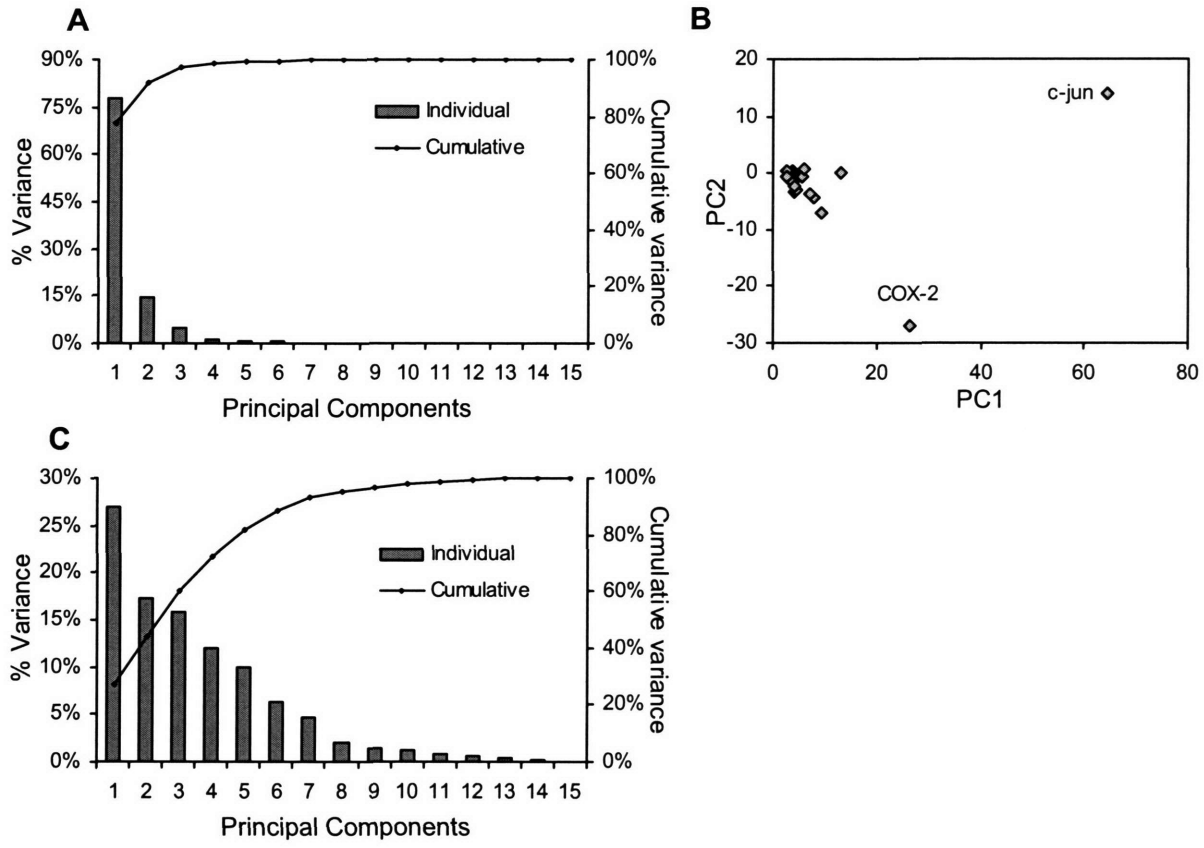

Figure 2.8: Principal Component Analysis of expression levels induced by static compression before (A) and after (C) standardization of gene expression vector variance. The 1-24hrs 50% compression untreated, BAPTA-AM and Rp-cAMP treated time-courses were combined to form a data matrix for PCA. A) Scree plot showing the variance accounted for by each principal component of the unstandardized expression vectors, in descending order. B) Projection plot of unstandardized expression vectors onto first two principal components. C) Scree plot showing variance accounted for by each principal component of the standardized expression vectors, in descending order.

The main purpose of clustering was to establish the general expression patterns activated by mechanical loading. Therefore, to improve our PCA-based clustering method the data matrix was pre-processed using the following standardization equations to re-weight each expression vector to have equal variance and thus remove the bias of the highly changing genes, such as COX-2 and c-Jun.

$$\mathbf{Z} = \frac{\mathbf{X} - \mathbf{F}}{S_X} \tag{2.2}$$

$$S_X^2 = \frac{\|\mathbf{X} - \mathbf{F}\|^2}{T} \tag{2.3}$$

X is a gene expression vector, **F** = free-swelling expression vector of 1's, S_X is the modified standard deviation of gene X with respect to the free-swelling expression level, T is the number of timepoints in the expression vector, and **Z** is the resulting standardized expression vector. Standardization with reference to the free-swelling expression level (or corresponding control in other data sets) was chosen instead of the mean of the gene expression vector to ensure that the direction of regulation was preserved when averaging a group of genes. Subsequently, the standardized free-swelling expression level is equal to zero. When PCA was applied to the standardized dataset, the variance was spread over a larger number of principal components (Figure 2.8C), indicating that a greater number of trends had been detected. Methods for deciding the number of principal components to retain include keeping principal components with greater than 1/T variance, or sum to greater than 50% variance, or by observation of steps in the Scree plot [105]. The three methods suggest choosing either three or five principal components, and the main three components, which accounted for 60% of the variance, were finally chosen to allow visualization to aid in the selection of the number of clusters.

The profile of principal component 1 (PC1) is increasingly upregulated with 50% compression duration with or without Rp-cAMP treatment, and is constantly upregulated during BAPTA-AM treated compression (Figure 2.9). The profile of PC2 is similar to PC1 during 50% compression but remains close to free-swelling expression levels during BAPTA-AM and Rp-cAMP treated time-courses. PC3 contains a transient upregulation during 50% compression and to a lesser extent during BAPTA-AM treatment, and remains close to free-swelling expression levels during Rp-cAMP treated compression.

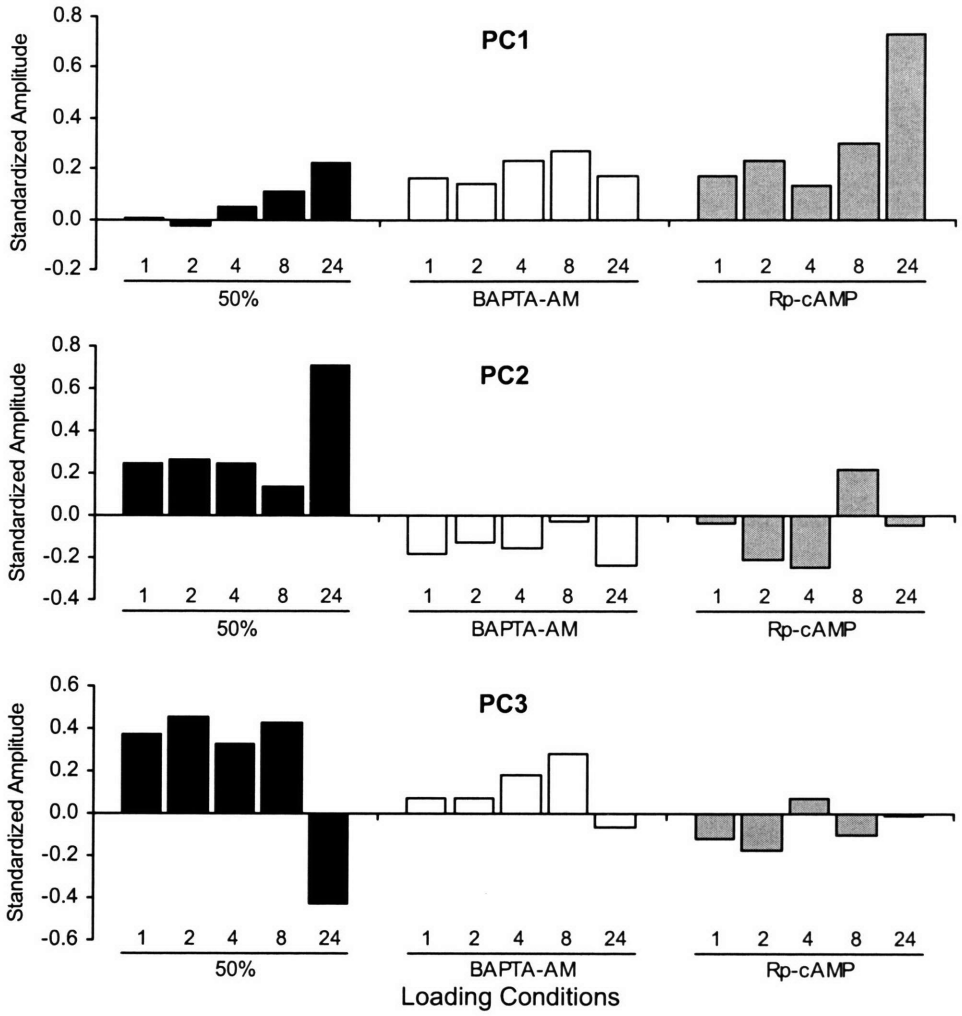

Figure 2.9: The three main principal components found by applying PCA to the standardized static compression dataset. The 50% untreated, BAPTA-AM and Rp-cAMP treated time-courses were combined into 15-point expression vectors and standardized by gene-vector variance before application of PCA. The variance in expression patterns accounted for by PC1, PC2 & PC3 was 26.9%, 17.3%, & 15.8%, respectively. Standardized free-swelling expression level = 0. Standardized amplitudes represent relative changes from control level within an expression vector. For example, the 24hr timepoint in PC1's 50% compression time-course is upregulated twice as much as the corresponding 8hr timepoint.

2.5.2 Clustering using PCA

The coordinates $(\alpha_1,\alpha_2,\alpha_3)$ of each standardized gene expression vector projected onto each main principal component were used to create the projection plot in Figure 2.5. From examination of Figure 2.5, four clusters were chosen as the minimum number capable to represent the data, though 3-6 clusters were tested for comparison. The following Euclidean

distance metrics were used to cluster the data (PCA does not preserve correlation between genes).

$$d(\mathbf{P}_a, \mathbf{P}_b) = \left\| \mathbf{P}_a - \mathbf{P}_b \right\| \tag{2.4}$$

$$D^2 = \sum_{i=1}^{k} \sum_{j=1}^{N_k} d(\mathbf{P}_{ij}, \mathbf{P}_{iC})^2 \tag{2.5}$$

$d(\mathbf{P}_a,\mathbf{P}_b)$ is the Euclidean distance between the three dimensional projection coordinates of gene a ($\mathbf{P}_a$) and gene b ($\mathbf{P}_b$), D is the sum over all genes of the distance between the projection coordinates of the j^{th} gene in group i, $\mathbf{P}_{ij}$, from the projection coordinates of centroid i, $\mathbf{P}_{iC}$, k is the number of groups, and N_k is the number of genes in each group.

To initiate clustering the coordinates of k genes were randomly chosen as the starting centroid positions. The distance of each gene coordinate to these centroids was calculated and genes were grouped with their closest centroid. Centroid positions were then recalculated as the average of the coordinates of the genes in a group. The new distance between a gene and centroid was calculated and genes were regrouped. This process continued in an iterative fashion until gene clusters stabilized. Each combination of initial starting genes deterministically clusters to a final solution. The set of all final solutions is much smaller than the set of all possible random groupings (see Section 2.5.4), and the number of repetitions was chosen so that it was highly likely that all final solutions were covered (in this case 6000 trials were performed). The optimal clustering is chosen as the grouping with the minimum total distance (D) after many repetitions and is shown in Figure 2.5 and Table 2.2. It is the cluster centroids, not the principal components, which represent the main expression patterns of the dataset. Each centroid is the sum of the three principal components weighted by the centroid projection coordinates (see Table 2.2).

$$\begin{aligned} \mathbf{C}_k &= \alpha_{k1}\mathbf{V}_1 + \alpha_{k2}\mathbf{V}_2 + \alpha_{k3}\mathbf{V}_3 \\ \alpha_{k1} &= \frac{1}{N_k}\sum_{i=1}^{N_k} \alpha_{i1} \end{aligned} \tag{2.6}$$

$\mathbf{C}_k$ represents the centroid vector for the k^{th} group, ($\alpha_{k1},\alpha_{k2},\alpha_{k3}$) represent the centroid coordinates of $\mathbf{C}_k$ in the first three dimensions, which are the average of the gene coordinates ($\alpha_{i1},\alpha_{i2},\alpha_{i3}$) for the genes in the k^{th} group. N_k is the number of genes in the k^{th} group.

Centroid 1 (Figure 2.6) includes a transient increase during the 50% compression time-course, thus, contains PC3, but also was highly upregulated by Rp-cAMP treated compression and so contains PC1. In contrast, Centroid 2 which also includes a transient upregulation during 50% compression, was mainly composed of PC3 minus PC1, as the BAPTA-AM and Rp-cAMP treated time-courses are suppressed below control levels. Centroid 3 was mainly composed of PC2 reflecting the increasing with duration profile during 50% compression, and suppressed expression with BAPTA-AM and Rp-cAMP. However, Centroid 4, which has a similar 50% compression profile as Centroid 3, is mainly composed of PC1 due to the upregulation seen during the BAPTA-AM and Rp-cAMP treated time-courses.

2.5.3 Alternative Clustering Technique

To confirm the expression trends found by PCA-based clustering, an alternative distance metric, correlation, was used to *k*-means cluster the full-length standardized gene expression vectors. The correlation between genes was conserved after standardization, using the following definitions:

$$S(\mathbf{X}_1,\mathbf{X}_2)=\frac{1}{T}\sum_{i=1}^{T}\frac{(X_{1i}-F_i)}{S_{X1}}\frac{(X_{2i}-F_i)}{S_{X2}}=\frac{\mathbf{Z}_1^T\mathbf{Z}_2}{T} \qquad (2.7)$$

$$S(\mathbf{Z}_1,\mathbf{Z}_2)=\frac{1}{T}\sum_{i=1}^{T}\frac{(Z_{1i}-0)}{S_{Z1}}\frac{(Z_{2i}-0)}{S_{Z2}}=\frac{\mathbf{Z}_1^T\mathbf{Z}_2}{T} \qquad (2.8)$$

$\mathbf{X}_1$ and $\mathbf{X}_2$ are two gene expression vectors, S_{X1} and S_{X2} are defined by Equation 2.3, $\mathbf{Z}_1$ and $\mathbf{Z}_2$ are the standardized gene vectors, with S_{Z1} and S_{Z2} equal to 1 by the standardization process. $S(\mathbf{a},\mathbf{b})$ represents the correlation between two vectors but is not the standard form of Pearson's correlation, as the reference point is taken from the free-swelling expression level (or corresponding control in other data sets) of the standardized and unstandardized vectors (0 and 1 respectively), and not the mean. To initiate the clustering random gene expression vectors were chosen as the starting centroids. The correlation between a gene and starting centroid was calculated and genes were placed with their highest correlating centroid. Centroids were recalculated as the average expression profile of genes in a group. The new correlation between genes and centroids was calculated and genes were regrouped with their highest correlating centroid. The process continued until the clusters stabilized. As described for the Euclidean

distance PCA-based method of clustering, multiple trials must be performed and the optimal clustering was chosen by comparing the overall gene-centroid correlation, R, over many repetitions.

$$R = \frac{\sum_{i=1}^{k}\sum_{j=1}^{N_k}\mathbf{Z}_{ij}^{T}\mathbf{C}_i}{N} \tag{2.9}$$

$\mathbf{Z}_{ij}$ is the expression vector for the j^{th} gene in group i, $\mathbf{C}_i$ is the standardized centroid of the i^{th} group and N is the total number of genes, in this case 23. The optimal grouping produced using the correlation metric and the full-length standardized expression vectors was different from the Euclidean distance based clustering of the gene projections by only the reversed placement of aggrecan and ADAMTS4, demonstrating that the four clusters were robust features of the dataset.

The following improvement was incorporated after publication. The centroid expression vectors were computed using Equation 2.6 or simply the average of the standardized expression vectors in a group.

$$\mathbf{C}_k = \frac{1}{N_k}\sum_{j=1}^{N_k}\mathbf{Z}_j = \frac{1}{N_k}\sum_{j=1}^{N_k}\frac{\mathbf{X}_j - 1}{S_{Xj}} \tag{2.10}$$

The standardized centroids, for which the control level is equal to zero, were converted into the same representation as the individual gene expression vectors. This was achieved by creating centroids, $\mathbf{G}_k$, related to the standardized centroids, $\mathbf{C}_k$, via a relationship analogous to Equation 2.2.

$$\frac{\mathbf{G}_k - 1}{S_k} = \mathbf{C}_k = \frac{1}{N_k}\sum_{j=1}^{N_k}\frac{\mathbf{X}_j - 1}{S_{Xj}} \tag{2.11}$$

S_k is a scaling factor which is not equal to the standard deviation of $\mathbf{G}_k$, as this would force the standard deviation of $\mathbf{C}_k$ be equal to one. The form of the above equation allows it to be solved as follows;

$$\begin{aligned} &\frac{\mathbf{G}_k}{S_k} - \frac{1}{S_k} = \mathbf{C}_k = \frac{1}{N_k}\sum_{j=1}^{N_k}\frac{\mathbf{X}_j}{S_{Xj}} - \frac{1}{N_k}\sum_{j=1}^{N_k}\frac{1}{S_{Xj}} \\ &\mathbf{G}_k = \mathbf{C}_k S_k + 1 \;\Leftarrow\; S_k = N_k\left(\sum_{j=1}^{N_k}\frac{1}{S_{Xj}}\right)^{-1} \end{aligned} \tag{2.12}$$

The group centroids, $\mathbf{G}_k$, are more easily interpreted when represented in the same manner as the individual gene expression profiles.

2.5.4 Group Centroid Robustness & Distinctiveness

To further test the robustness of the optimal groupings, genes were randomly assigned into four groups, and the overall correlation was calculated. 100,000 repetitions were performed in an attempt to gain a cross-section of all possible combinations (>1 billion). The mean and standard deviation of the overall correlation was 0.49 ± 0.03 (Figure 2.10). The distribution of the overall correlation was not centered on zero indicating that the dataset contained positively correlated genes further suggesting the genes may be co-regulated. The optimal groupings found using PCA-based clustering and correlation-based clustering of gene expression vectors, had overall correlations of 0.7440 and 0.7466 respectively. Therefore, compared to random groupings, both solutions appear to be very optimal ($p << 0.001$). Examination of the top five correlation-based clustering groupings showed only 1 to 2 gene placement differences from either PCA-based or correlation-based solutions, further demonstrating the robust nature of the main expression trends.

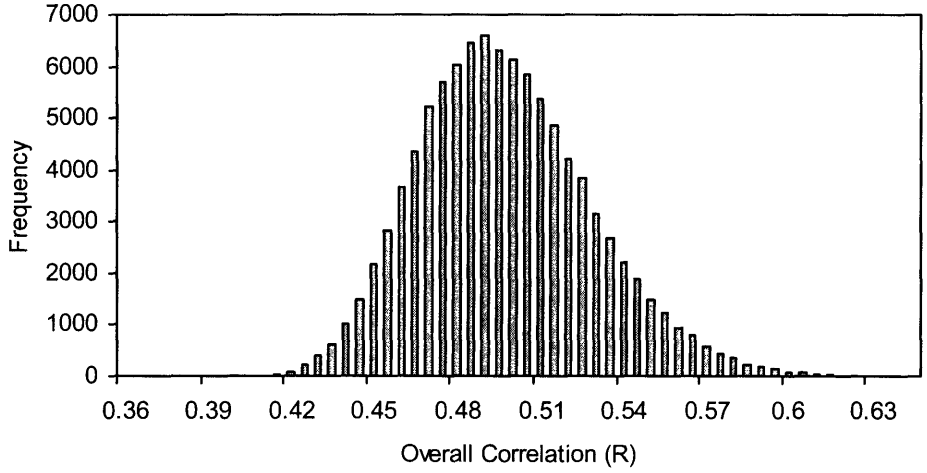

Figure 2.10: Distribution of the overall correlation metric from 100,000 random grouping trials. The twenty-three genes used for the clustering algorithm were each randomly assigned a group number from 1 to 4. Overall correlation for each trial was calculated using Equation 2.9. Mean ± SE = 0.49±0.03.

The variance of each group centroid was calculated using the distance between the projection coordinates of the centroid and each gene within a group.

$$U_k = \sum_{j=1}^{N_k} \frac{d(\mathbf{P}_{kC}, \mathbf{P}_{jk})^2}{N_k} \qquad (2.13)$$

U_k is the variance of the k^{th} centroid, which is different from S_{qk} which is standard deviation along a centroid vector. The Euclidean distance between centroid projection coordinates $d(\mathbf{P}_{iC},\mathbf{P}_{jC})$, and centroid variances U_i, U_j were used to perform comparison of means Student's t-tests. All centroids were found to be significantly spatially separated (Table 2.2B) indicating the group expression patterns represented distinct trends.

2.6 Supplementary Figures

Figure 2.11: Relative gene expression levels measured by real-time PCR in compressed cartilage explants. A&B) Matrix Proteins and C&D) Matrix Proteinases. Static compression was applied for 1-24hrs in one of four loading conditions: 25% = 25% compression of cut thickness (n = 4), 50% = 50% compression of cut thickness (1-8hrs, n = 11 & 24hr, n = 4), BAP = pretreated with 10μM BAPTA-AM before 50% compression (n = 5), and Rp = pretreated with 50μM Rp-cAMP before 50% compression (n = 3). Expression levels were normalized using 18S and G3PDH housekeeping genes and divided by free-swelling expression levels. * = $p < 0.05$ compared to free-swelling controls using Students two tailed t-test. ‡ = $p < 0.05$ compared to untreated 50% compressed expression levels, using Welch and Games-Howell corrected, comparison of means, two-tailed t-tests. ■1hr, ■2hr, 4hr, □8hr, ⊟24hr, relative free-swelling expression level = 1.

Figure 2.12: Relative gene expression levels measured by real-time PCR in compressed cartilage explants. A) Tissue inhibitor of matrix proteinases, B) Transcription factors, and C&D) Cytokines, growth factors and reference genes. Static compression was applied for 1-24hrs in one of four loading conditions: 25% = 25% compression of cut thickness (n = 4), 50% = 50% compression of cut thickness (1-8hrs: TIMPs & TFs, n = 4-11, others n = 4-7, 24hrs: all, n = 4), BAP = pretreated with 10μM BAPTA-AM before 50% compression (n = 4-5), and Rp = pretreated with 50μM Rp-cAMP before 50% compression (n = 3). Expression levels were normalized using 18S and G3PDH housekeeping genes and divided by free-swelling expression levels. * = $p < 0.05$ compared to free-swelling controls using Students two tailed t-test. ‡ = $p < 0.05$ compared untreated 50% compressed expression levels, using Welch and Games-Howell corrected, comparison of means, two-tailed t-tests. ■1hr, ■2hr, 4hr, □8hr, ⊟24hr, relative free-swelling expression level = 1.

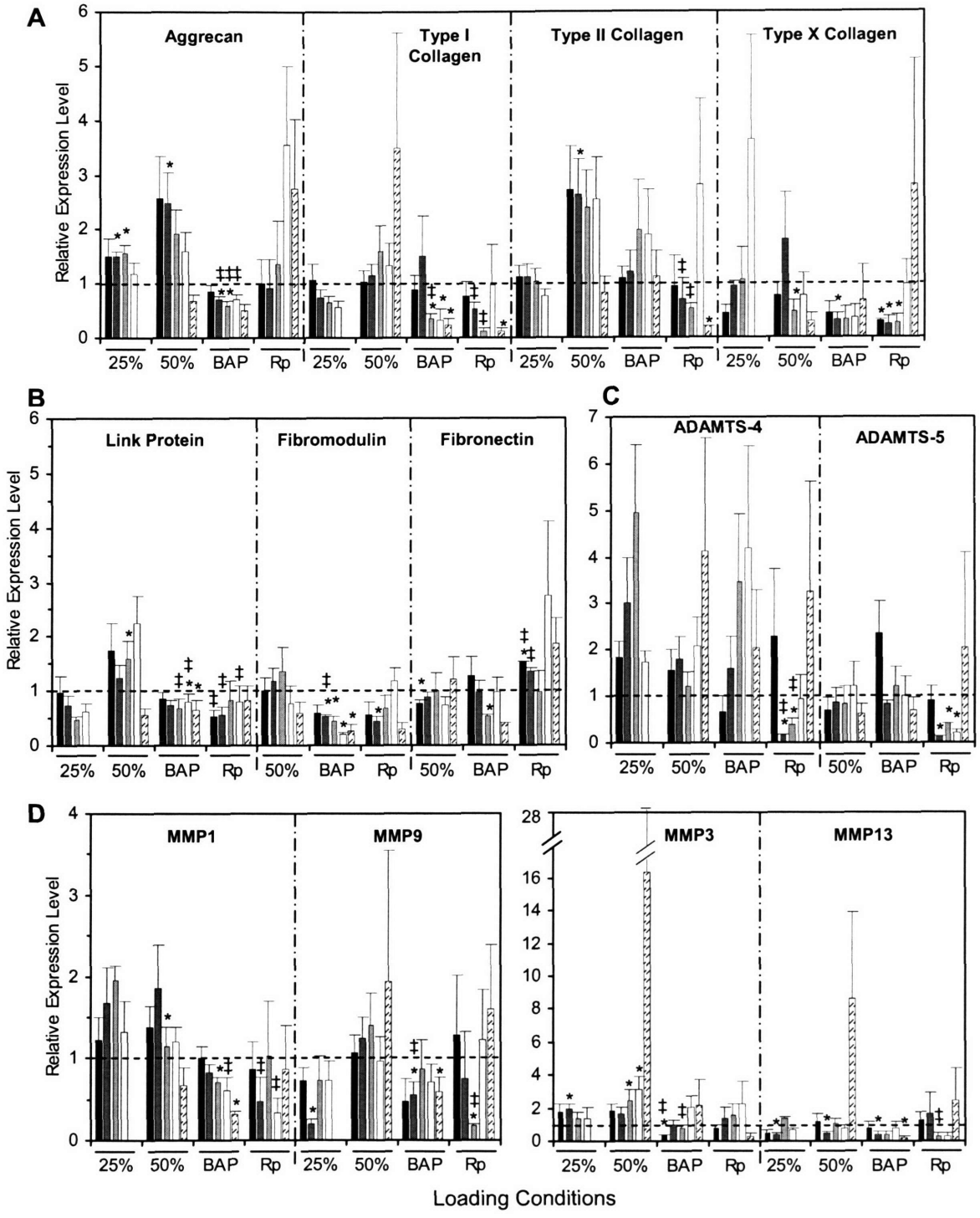
A
Aggrecan
Type I Collagen
Type II Collagen
Type X Collagen
Relative Expression Level
B
Link Protein
Fibromodulin
Fibronectin
C
ADAMTS-4
ADAMTS-5
D
MMP1
MMP9
MMP3
MMP13
25%
50%
BAP
Rp
Loading Conditions

Figure 2.11

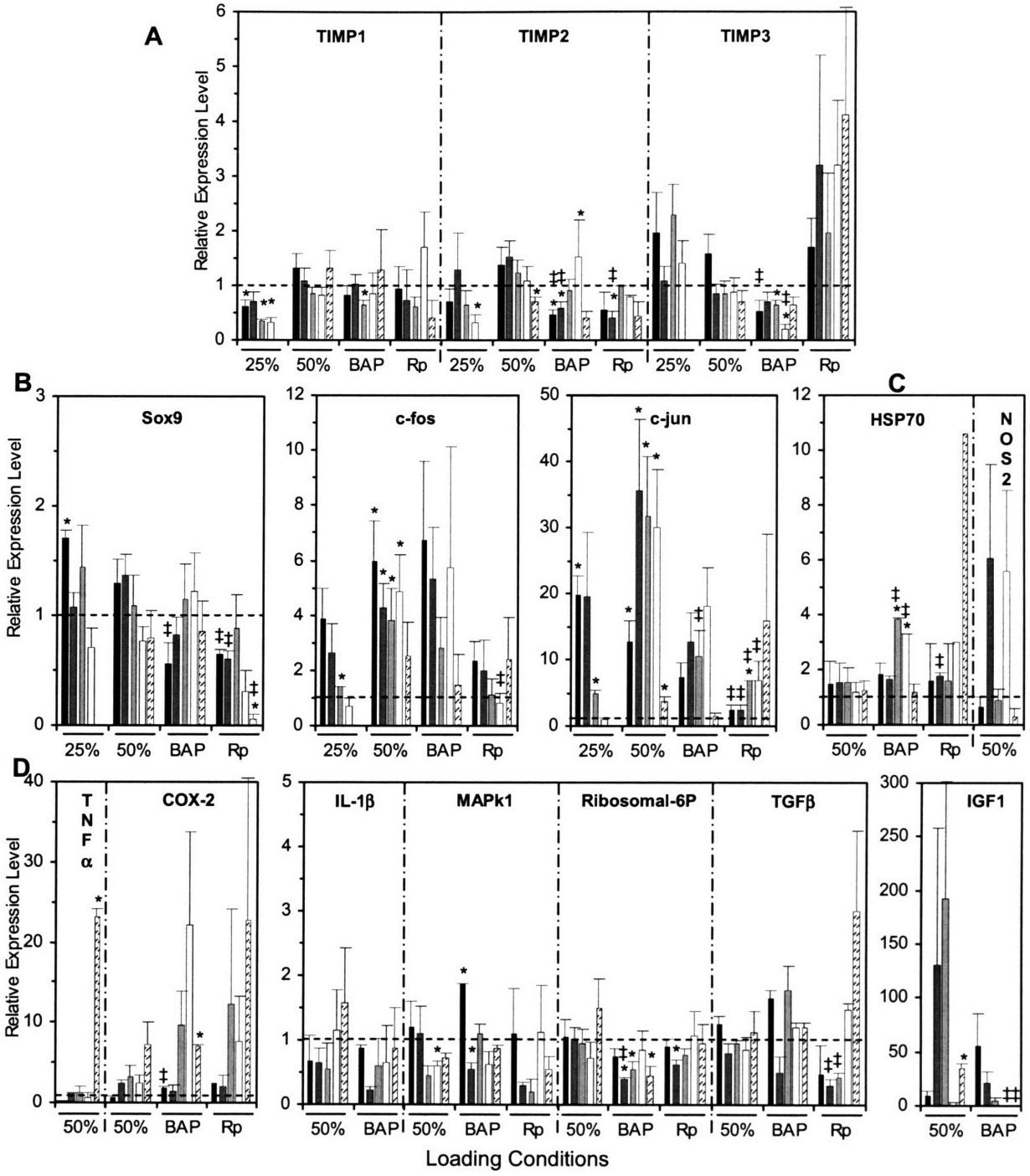
A
TIMP1
TIMP2
TIMP3
Relative Expression Level
25% 50% BAP Rp 25% 50% BAP Rp 25% 50% BAP Rp
B
Sox9
c-fos
c-jun
C
HSP70
NOS2
Relative Expression Level
25% 50% BAP Rp 25% 50% BAP Rp 25% 50% BAP Rp 50% BAP Rp 50%
D
TNFα
COX-2
IL-1β
MAPk1
Ribosomal-6P
TGFβ
IGF1
Relative Expression Level
50% 50% BAP Rp 50% BAP 50% BAP Rp 50% BAP Rp 50% BAP Rp 50% BAP
Loading Conditions

Figure 2.12

Chapter 3

Shear and Compression Duration, Rate, and Magnitude Differentially Regulate the Temporal Transcription Profiles of Functionally-related Genes in Cartilage Explants

3.1 Introduction

Mechanical forces within synovial joints are known to influence the metabolic behavior of chondrocytes, the sole cell type of cartilage [50,51,79]. Chondrocytes are responsible for the maintenance and turnover of the cartilage extracellular matrix (ECM), in particular the biosynthesis of type II collagen and the proteoglycan (PG), aggrecan, which in combination provide the tensile, shear, and compressive stiffness of cartilage. Cartilage thickness and PG content were found to be enhanced in load-bearing areas [52]. Joint inactivity [50,51] and injury [10] have been found to promote degradation of the ECM and to reduce cartilage load bearing capacity. The exact mechanisms by which mechanical forces influence the biological activity of chondrocytes are under intense study. In addition, the precise component(s) of the physical stimuli that induce such cell biological changes following joint movement are not known.

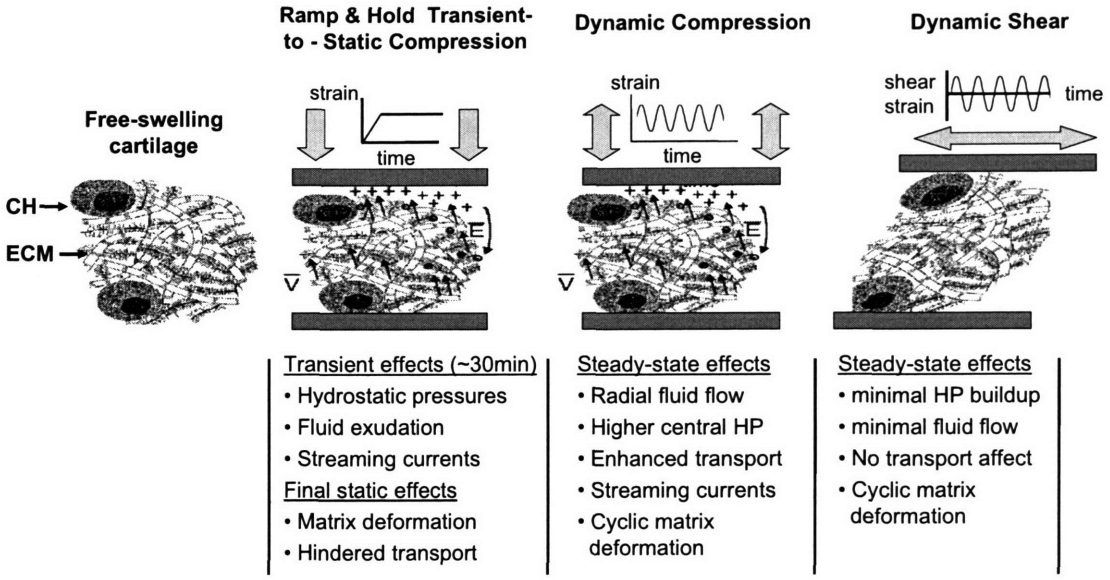

Figure 3.1: Fields, forces, and flows, induced by static and time varying mechanical stimuli. CH = chondrocyte, ECM = extracellular matrix. Adapted from [1].

The effects of mechanical loading on cartilage have been studied using intact bovine cartilage explants to determine the precise biophysical forces and physicochemical changes that result (for reviews, see [1] and [109]). Application of a transient compressive deformation (using displacement or load control) induces an initial build up of hydrostatic pressure (HP) within the tissue and a concomitant intratissue fluid flow and flow-induced electrical streaming potentials (Figure 3.1). After fluid exudation and volumetric compaction have ceased, mechanical stress-relaxation (at constant displacement) or creep relaxation (at constant load) lead to a new static equilibrium compressed state of the tissue [1,22]. Compression of up to 50% strain inhibited chondrocyte biosynthesis for over 24 hours [22,26,33]. In contrast, dynamic compression leads to cyclic changes in pressure, deformation, and fluid flow within the tissue (Figure 3.1). For the case of unconfined dynamic compression of cylindrical cartilage explant disks using impermeable compression platens, theoretical models have predicted increases in dynamic amplitude of the hydrostatic pressure and radial strain at the explant center, radially-directed fluid flow with greatest amplitudes at the explant periphery, and corresponding radially-directed streaming potential gradients [34,35]. Dynamic tissue shear induces cyclic matrix deformation in a nearly uniform manner throughout the explant disk with minimal fluid flow or increased hydrostatic pressure (Figure 3.1)[55]. Both types of dynamic loading were found to increase type II collagen and PG synthesis [33,55]. However, quantitative autoradiography studies showed that

dynamic compression only increased PG biosynthesis by chondrocytes located near the explant periphery [34] in the region of maximal fluid flow, while the stimulatory effects of dynamic shear were observed throughout the explant [55], consistent with the more spatially uniform cyclic shear deformation. Studies applying HP to bovine articular chondrocyte (BAC) cultured in monolayer showed that moderate cyclic HP (0.5-5MPa, 0.1-1Hz) increased biosynthesis [42,45], whereas high continuous HP (>15MPa) decreases biosynthesis [42].

Recent studies have focused on intracellular signaling and gene expression pathways that may be linked to the observed changes in biosynthesis caused by mechanical loading of cartilage tissue. Ramp-and-hold (transient to static) compression of cartilage explants up to 50% strain and durations of 1-24 hours induced time-dependent gene expression patterns that involved intracellular calcium and cyclic AMP (Figure 2.4). Expression of matrix proteins such as aggrecan [56], type II collagen, and link protein were transiently upregulated but downregulated by 24 hours, and matrix proteases were increasingly upregulated with longer duration of static compression (Figure 2.2). Cyclic HP applied to BAC monolayer cultures for 2-24 hours, or intermittently for 4 days, increased type II collagen and aggrecan transcription by 3 fold [43,44]. Twenty minutes of cyclic pressure-induced strain (PIS) applied to human chondrocytes upregulated aggrecan transcription within 1 hour of loading; however, no effect was observed 24 hours after loading [58]. PIS have also been found to induce inositol-triphosphate mediated calcium release in human chondrocytes [38,110]. Constant and cyclic fluid shear increased the frequency of intracellular calcium oscillations in bovine articular chondrocytes [40,46]. In cartilage explants, chelating intracellular calcium inhibited the upregulation of gene transcription induced by static compression in a majority of matrix proteases and proteins (Figure 2.6), notably aggrecan [63].

Although cyclic loading has been shown to affect chondrocytes metabolic activities in culture, little is known about the intracellular effects of dynamic loading on intact cartilage explants. Motivated by the widespread induction of gene transcription by static compression (Figure 2.6), we applied dynamic loading to cartilage explants and measured the response of 25 genes involved in cartilage ECM homeostasis. To distinguish the effects of matrix deformation from HP gradients, fluid flow, and streaming potentials, we separately applied dynamic compression and dynamic shear. In order to identify certain intracellular signaling pathways modulated by particular mechanical forces we used inhibitors of intracellular calcium and cAMP

mediated signaling during loading. Clustering analysis [89,90] and principal component analysis (Section 2.5)[91,92] were used to group similarly responding genes and identify the main expression patterns induced by each loading regime. We found that dynamic compression and dynamic shear induced similar expression patterns for anabolic and catabolic genes, which were distinct from those induced by static compression. Furthermore, both loading regimes required intracellular calcium release to induce gene transcription.

3.2 Experimental Procedure

3.2.1 Cartilage Preparation

Cylindrical cartilage explant disks (3mm diameter, 1mm thick) were obtained from the middle zone of the patella-femoral groove of 1-2 week old calves as described previously [22]. Explants were washed with phosphate-buffered saline and allowed to equilibrate for 2 to 5 days in low glucose Dulbecco's modified essential medium supplemented with 10% fetal bovine serum, 10mM Hepes buffer, 0.1mM nonessential amino acids, 20μg/ml ascorbate, 100 units/ml penicillin, 100μg/ml streptomycin and 0.25μg/ml amphotericin, with medium exchanged every second day. To avoid pH or temperature changes at the onset of loading, medium was changed sixteen hours before loading, and anatomically matched explants were distributed amongst the loading conditions. In selected experiments BAPTA-AM, a chelator of intracellular calcium (10μM, A.G. Scientific), or Rp-cAMP, a competitive inhibitor of cAMP activation of protein kinase A (50μM, Sigma), were added to medium 1 hour before loading, at concentrations previously shown to suppress compression induced aggrecan gene transcription (Figure 2.4)[56,63].

3.2.2 Mechanical Loading

Dynamic compression: for each timepoint of the dynamic compression experiments, 12 explants (4 inhibitor-free, 4 BAPTA-AM treated, 4 Rp-cAMP treated) were placed in a polysulphone loading chamber which was mounted into an incubator-housed loading apparatus [25]. Cartilage explants were dynamically compressed by 3% strain at 0.1Hz with a 5% strain offset for 1, 4, 8 or 24 hrs. Control explants were statically loaded by 5% strain for 4 or 24 hrs. *Dynamic shear*: for each timepoint of the dynamic shear experiments, 12 explants (6 untreated, 6 BAPTA-AM treated) were placed in a polysulphone shear chamber that was mounted into the

loading apparatus [25]. Cartilage explants were maintained at cut thickness to minimize hydrostatic pressure buildup and dynamically sheared by 3% strain at 0.1Hz for 1, 4 or 24 hrs. These tissue shear loading conditions were previously shown to produce minimal fluid flow [55]. Control explants were maintained at cut thickness for 4 or 24 hrs within similar chambers but not dynamically loaded. Immediately upon loading completion, cartilage explants subjected to identical mechanical loading and inhibitor treatment were pooled, flash frozen in liquid nitrogen, and stored at -80°C.

3.2.3 RNA Extraction & Real-Time PCR

Pooled cartilage explants were disrupted with a liquid nitrogen cooled tissue pulverizer, placed in a Trizol lysis buffer (Invitrogen) and lysed using a tissue homogenizer (BioSpec Products Inc). The lysate was separated using phase-gel spin columns (Eppendorf) spun at 10,000rpm for 10 minutes, and the supernatant was transferred to QIAGEN RNeasy Mini columns. Total RNA was purified according to the manufacturer's protocol with the on-column DNA digest. Approximately 1-2μg of total RNA was reverse transcribed (Applied Biosystems) on an Eppendorf Mastercycler. Real-time polymerase chain reaction (PCR) was performed on an MJResearch Opticon 2 machine using Applied Biosystems SybrGreen master mix. Primers were designed for the genes listed in Table 3.1 and were tested and calibrated as described in Section B.5. Loaded samples were always run on the same PCR plate as unloaded controls and housekeeping genes 18S and G3PDH were run on every plate. Cycle threshold values were converted to relative copy numbers using primer specific standard curves. To normalize for starting cDNA content, copy numbers were divided by the average of the mean-centered housekeeping genes for each sample on a plate. Relative expression levels were calculated by dividing dynamically loaded samples by controls.

	GENE	ACCESSION #	Forward Primer	Reverse Primer
Matrix Proteins	Aggrecan	U76615	CCTGAACGACAAGACCATCGA	TGGCAAAGAAGTTGTCAGGCT
	Type I Collagen	AB008683	AATTCCAAGGCCAAGAAGCATG	GGTAGCCATTTCCTTGGTGGTT
	Type II Collagen	X02420	AAGAAGGCTCTGCTCATCCAGG	TAGTCTTGCCCCACTTACCGGT
	Fibromodulin	X16485	ACAACCAGCTGCAGAAGATCC	TTCATGACATCCACCACGGT
	Fibronectin	K00800	ACTGCCCACTCCTACAACCA	CAAAGGCATGAAGCACTCAA
	Link Protein	U02292	AAGCTGACCTACGACGAAGCG	CGCAACGGTCATATCCCAGA
Matrix Proteases	MMP1	AF290429	GGACTGTCCGGAATGAGGATCT	TTGGAATGCTCAAGGCCCA
	MMP3	AF135232	CACTCAACCGAACGTGAAGCT	CGTACAGGAACTGAATGCCGT
	MMP9	AF135234	TCCCTTCCTTGTCAAGAGCAA	TACTTGGCGCCCAGAGAAGAA
	MMP13	AF069644	TGGTCCAGGAGATGAAGACC	TGGCATCAAGGGATAAGGAA
	ADAMTS4	AF192770	AACTCGAAGCAATGCACTGGT	TGCCCGAAGCCATTGTCTA
	ADAMTS5	AF192771	CTCCCATGACGATTCCAA	AATGCTGGTGAGGATGGAAG
Anti-Catabolic	TIMP1	AF144763	TCCCTGGAACAGCATGAGTTC	TGTCGCTCTGCAGTTTGCA
	TIMP2	AF144764	CCAGAAGAAGAGCCTGAACCA	TGATGTTCTTCTCCGTGACCC
	TIMP3	AF144765	TTTGGCACGATGGTCTACACC	CCTCAAGCTTAAGGCCACAGA
Transcription Factors	Sox9	AF278703	TGAAGAAGGAGAGCGAGGAG	GTCCAGTCGTAGCCCTTGAG
	c-Fos	AF069515	CTCGAGTTCATCCTAGCGGC	GCCCCCACTCAGATCAAGAG
	c-Jun	AF069514	AGCTGGAGCGCCTAATCATACA	CCTCCTGCTCATCTGTCACGTT
Signaling Molecules	MAPK1	NM175793	TCCAAGGGCTACACCAAGTC	GTGGTTCAGCTGGTCAAGGT
	COX2	AF004944	AAAAGCTGGGAAGCCTTTTC	GCTCTTTCCTCCCTTTCACA
	IL-1β	M37211	CCACCCAGGGATCCTATTCT	TCATTTCGTTGATGGGTTCA
	TNFα	AF011926	CATCAACAGCCCTCTGGTTC	CCTACTGCTTCCATCCCTTG
	TGFβ	M36271	CACGTGGAGCTGTACCAGAA	ACGTCAAAGGACAGCCACTC
Reference	HSP70	L10428	ACCTTCGACGTGTCCATCCT	CTCACCATGCGGTTATCGAA
	ribosomal 6P	BG467315	TCGTGACTCCACGAGTTCTG	TGGCCTCCTTCATTCTCTTG
Housekeeping	18S ribosomal	AF176811	TCGAGGCCCTGTAATTGGAA	GCTATTGGAGCTGGAATTACCG
	G3PDH	AF077815	ATCAAGAAGGTGGTGAAGCAGG	TGAGTGTCGCTGTTGAAGTCG

Table 3.1: Bovine primer sequences for genes examined using real-time PCR. Annealing temperatures ~60°C, length ~ 100 bp.

3.2.4 Clustering & Statistical Analyses

To elucidate the main expression patterns induced by dynamic loading, the expression levels from the inhibitor free, BAPTA treated and Rp-cAMP treated (for dynamic compression only) timecourses were combined into gene expression vectors. To emphasize expression vector shape rather than amplitude, each vector was standardized by the vector standard deviation (see Section 2.5), and clustered using two different clustering techniques. First, principal component analysis was applied to the data matrix that contained all standardized gene vectors from either dynamic compression or shear to determine the main principal components (similar to eigenvectors). The projection of the standardized vectors along the three main principal components was used to create a three dimensional representation of the data which enabled the

number of groups to be determined graphically (see Section 2.5 for more detail). Euclidean distance k means clustering of the three dimensional gene projection coordinates was then performed to group the genes. A second technique applying correlation-based k means clustering to the full-length standardized expression vectors was also used to ensure reliable clustering. Centroids were calculated as the average of the gene expression vectors within a group. To determine if distinct expression patterns had been found, Students t-test between group centroid vectors was performed using the Euclidean distance between the centroid vectors and the variance of each centroid (calculated as the average gene to centroid norm for all genes within a group). To confirm the gene groupings were robust, the top five ranked groupings were examined, as well as varying the number of total groups.

In an effort to further elucidate the effect of mechanical forces on gene transcription, expression vectors containing the inhibitor-free 1, 4, and 24 hour timepoints of 50% static compression expression levels (Figure 2.11 & Figure 2.12) were combined with dynamic compression and shear inhibitor-free time-courses. Clustering analysis was performed as just described. Gene expression levels were compared to the normalized control level of 1; a p-value < 0.05 was considered significant.

3.2.5 Promoter Analysis

The co-expression of a group of genes suggests common regulatory mechanisms [111,112]. The sequences 2000 bp upstream and 200 bp downstream of the start of exon 1, for each gene were obtained using the TOUCAN Java applet [113] and the Ensembl database [114]. Human sequences were chosen as the bovine database was incomplete. Sequences were placed in groups based on the results from clustering the inhibitor-free expression profiles from each loading type. The Toucan sub-applet MotifScanner [113] was used to search the TRANSFAC 6.0 public vertebrate database [115] for transcription factor binding site position weight matrices that were over-expressed in the grouped sequences compared with an Eukaryote Promoter Database 3rd order background model. A prior probability of 0.2 was chosen and for each group transcription factors with positive significance values [113] were considered statistically over-represented.

3.3 Results

3.3.1 Effects of Dynamic Compression

Dynamic compression of cartilage explants generally upregulated many genes in a time dependent manner (expression levels for all genes are shown in Section 3.5, Figure 3.8 & Figure 3.9). Matrix proteins aggrecan and type II collagen (Figure 3.2) responded to long-term dynamic compression with increases of 30-100% after 24hrs. Link protein, type I collagen, fibromodulin and fibronectin responded in a similar way (Figure 3.8). The expression of COX-2 and most matrix proteases increased by 100 to 200% by 24hrs, although MMP3, MMP9, MMP13 and COX-2 were mainly suppressed during earlier timepoints (Figure 3.2, Figure 3.8 & Figure 3.9). Of the TIMPs, only TIMP1 was upregulated by dynamic compression (Figure 3.9). Immediate early genes c-Fos and c-Jun and signaling genes mitogen activated protein kinase-1 (MAPK1), and TNFα were transiently upregulated by 100 to 200% after 1hr, returning to control levels after 8 hrs of loading (Figure 3.2 & Figure 3.8). TGFβ and ribosomal-6 phosphate were unaffected by dynamic compression (Figure 3.9). Sox9, IL-1β and HSP70 were mildly upregulated only at the 4 hour timepoint (Figure 3.2 & Figure 3.9), though HSP70 was scarcely detected even during loading and, hence, was not included in the clustering analysis.

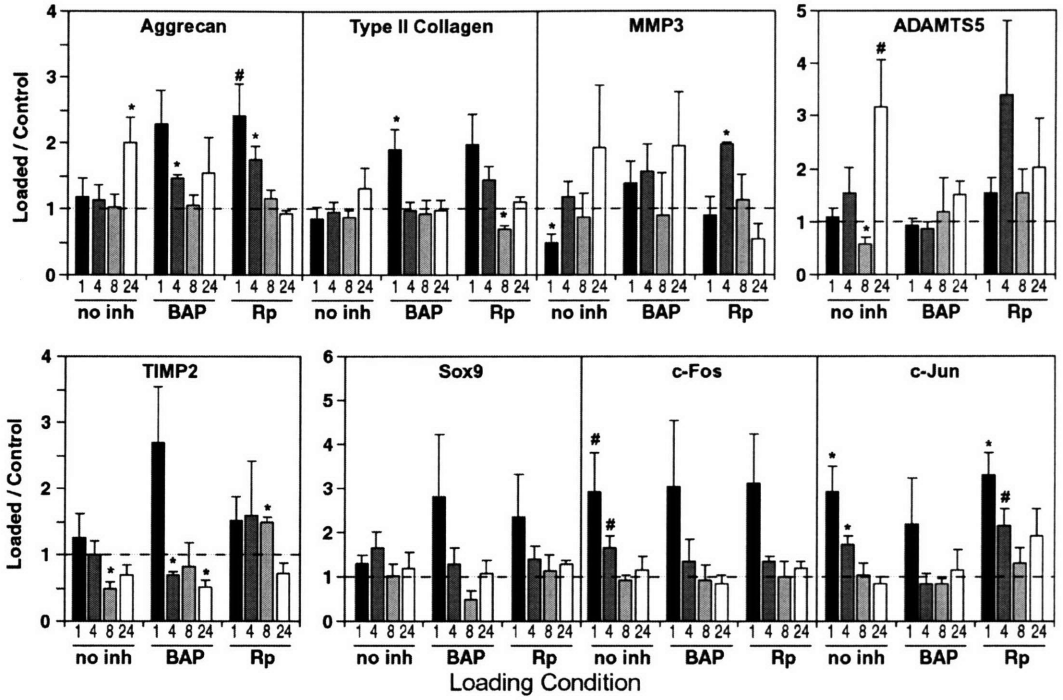

Figure 3.2: Selected gene expression profiles induced by dynamic compression (3% strain, 0.1Hz). Conditions include dynamic compression time-courses from inhibitor-free (no inh, n = 7), BAPTA-AM pre-treatment (BAP, n = 5) or Rp-cAMP pre-treatment (Rp, n = 4). Expression levels are normalized to those of control explants which were compressed to 5% strain (dashed line). ■1hr, ■4hr, ■8hr, □24hr. Mean + SE. *, $p < 0.05$, # $p < 0.07$ only

When the inhibitor-free, BAPTA treated, and Rp-cAMP treated gene expression levels were combined, PCA identified three major principal components that account for over 75% of the variance in the data set. Identical gene groupings were found using either PCA or correlation based clustering techniques producing three statistically distinct and robustly conserved groups (Figure 3.3, Table 3.2). (Prior to clustering HSP70 and MMP9 were removed as PCA analysis identified their gene expression profiles as very different from all other genes). Group C1 contained a number of matrix proteins and was characterized by upregulation after 24hrs of dynamic compression. The presence of BAPTA-AM suppressed the long-term upregulation of Group C1 genes, but enhanced expression only at earlier time points (1 & 4 hrs). Similarly Rp-cAMP treatment suppressed long-term upregulation of Group C1 but enhanced short-term expression. Group C2 was mainly composed of proteases that were suppressed during early timepoints, upregulated by 24 hrs of loading, and generally restrained to controls levels when BAPTA-AM was present (Figure 3.3). Rp-cAMP treatment generally upregulated Group C2 expression, especially COX-2. Group C3 contained transcription factors c-Fos, and c-Jun and other signaling related molecules that exhibited transient upregulation by dynamic compression,

which was partially suppressed by BAPTA-AM and unaffected by Rp-cAMP treatment during loading (Figure 3.3).

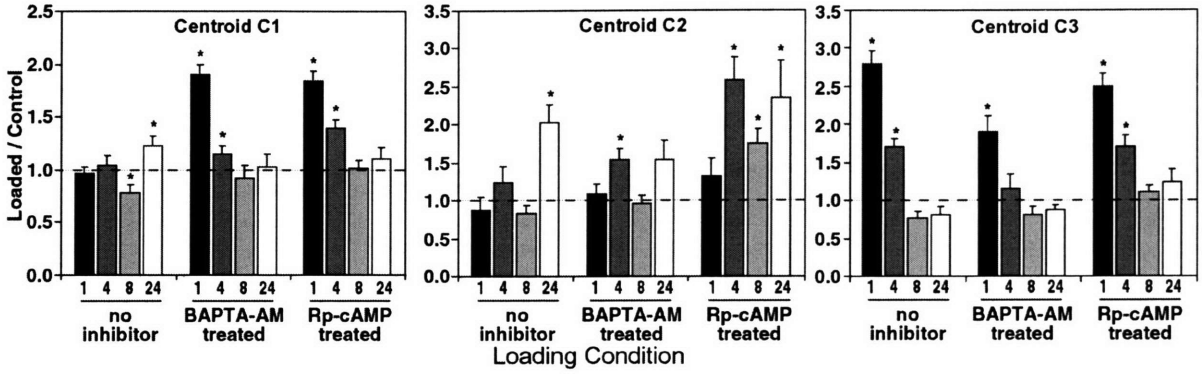

Figure 3.3: Main expression trends induced by dynamic compression (3% strain, 0.1Hz) with and without pre-treatment with inhibitors of the intracellular calcium or cAMP signaling pathways. Centroid expression vectors were calculated by averaging the standardized gene expression vectors in each group. Expression levels are normalized to those of control explants which were compressed to 5% strain (dashed line). Mean + SE (n = number of genes in a group). *, $p < 0.05$

Group	Grouped genes	p values for centroid separation	Centroid C1	Centroid C2
C1	Aggrecan, Type I & II Collagen, Link Protein, Fibromodulin, MMP1, TIMP2, TIMP3, Sox9, IL-1β, TGFβ, Ribosomal 6P	Centroid C1		
C2	Fibronectin, MMP3, MMP13, ADAMTS4, ADAMTS5, TIMP1, COX-2	Centroid C2	0.010	
C3	c-Fos, c-Jun, MAPk1, TNFα	Centoid C3	0.013	0.006

Table 3.2: Main groups found by clustering the gene expression profiles induced by dynamic compression with and without pretreatment with inhibitors of intracellular calcium and cAMP, and statistical comparisons between the group expression profiles. The Euclidean distance between the projection coordinates of pairs of centroids was used in comparison of means Student's *t* tests. The number of genes within each group represented the degrees of freedom. Intra-centroid variance was calculated using the distance between gene projection coordinates and the appropriate centroid (see Section 2.5 Equation 2.13).

3.3.2 Effects of Dynamic Tissue Shear

Dynamic shear had a markedly pro-anabolic effect on gene transcription (all gene expression profiles are shown in Section 3.5, Figure 3.10 & Figure 3.11). In particular, aggrecan, type II collagen, link protein, fibromodulin and fibronectin were all upregulated 1.5 to 5.4 fold by 24 hrs; aggrecan was upregulated almost 100% after 1 hr (Figure 3.4). Interestingly, Sox9 was transiently upregulated by almost 100% after 1 hr (Figure 3.4). Matrix proteases and COX-2 were again upregulated after 24hrs with MMP1 upregulated 4 fold and MMP3 up 1.5 fold (Figure 3.4 & Figure 3.11). The TIMPs were upregulated by 50 to 200% at varying timepoints

(Figure 3.4 & Figure 3.11). Similar to dynamic compression, c-Fos and c-Jun were transiently upregulated by 1-3 fold by 1 hr in response to dynamic shear, and c-Jun remained upregulated by 2 fold after 24hrs (Figure 3.4). TGFβ and IL-1β were mildly transiently upregulated at early timepoints, and ribosomal-6 phosphate was unaffected (Figure 3.11). MAPk1 was upregulated approximately 150% after 1 and 24 hours (Figure 3.11).

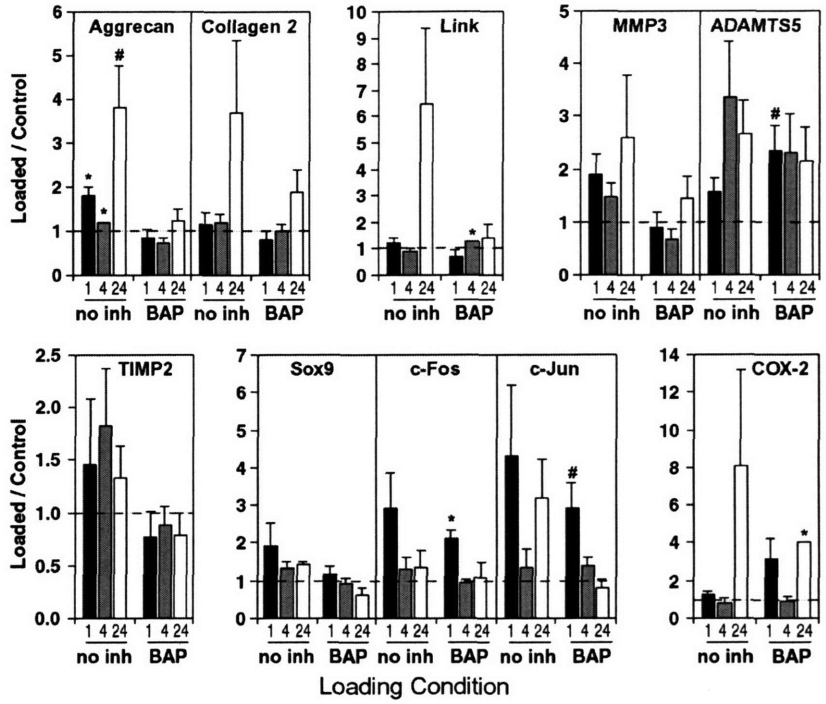

Figure 3.4: Selected gene expression profiles induced by dynamic shear (3% shear strain, 0.1Hz) without (no inh, n = 4) and with BAPTA-AM treatment (BAP, n = 4). Expression levels are normalized to those of control explants which were maintained at cut thickness (dashed line). ■1hr, ■4hr, □24hr. Mean + SE. *, $p < 0.05$, # $p < 0.07$ only

The main three principal components found by PCA of the dynamic shear stimulated inhibitor-free and BAPTA treated expression profiles accounted for 89% of the data variance, and clustering analysis highlighted three distinct and robustly conserved expression patterns (Figure 3.5, Table 3.3). Group S1 contained a majority of the matrix proteins and proteases (Figure 3.5, Table 3.3) that were upregulated by long-term (24 hr) dynamic shear; most of these genes were also upregulated by 24 hrs of dynamic compression (Figure 3.3), though shear led to an even greater effect. In contrast to dynamic compression, the presence of BAPTA-AM suppressed the expression of matrix proteins and proteases during dynamic shear to control levels at all timepoints, with no enhancement after 1 hr. Hence, matrix proteins and proteases grouped together in response to dynamic shear, while matrix proteins and proteases grouped

separately in analysis of dynamic compression. Group S2 contained genes that transiently responded to dynamic shear and were partially suppressed when BAPTA-AM was present, similar to Group C3. Genes in Group S3 had a slower transient response to dynamic shear that was suppressed by the presence of BAPTA-AM. Group S3 had the lowest individual gene to centroid correlations indicating that the genes were only loosely grouped, probably based on their poor correlation to the genes in other groups.

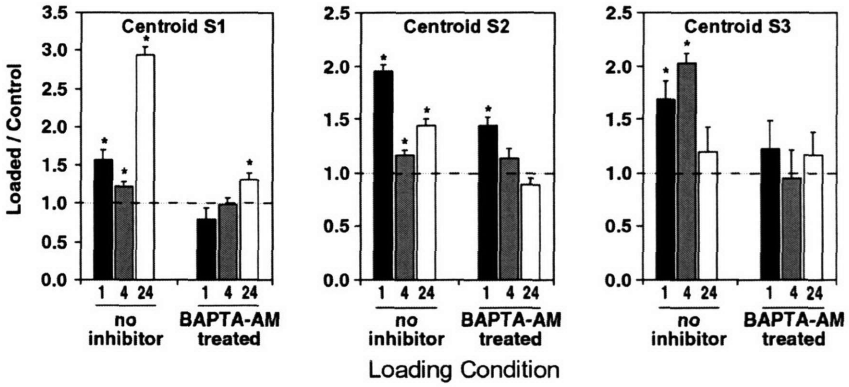

Figure 3.5: Main expression trends induced by dynamic shear (3% shear strain, 0.1Hz) with and without BAPTA-AM pretreatment. Centroid expression vectors were calculated by averaging the standardized gene expression vectors in each group. Expression levels are normalized to those of control explants which were maintained at cut thickness (dashed line). Mean + SE (n = number of genes in a group). *, $p < 0.05$

Group	Grouped genes	p values for centroid separation	Centroid S1	Centroid S2
S1	Aggrecan, Type II Collagen, Link Protein, Fibromodulin, Fibronectin, MMP1, MMP3, MMP13, TIMP3, MAPk1, COX2, Ribosomal 6P	Centroid S1		
S2	Type I Collagen, MMP9 ADAMTS4, Sox9, c-Fos, c-Jun, TNFα, TGFβ	Centroid S2	2×10^{-4}	
S3	ADAMTS5, TIMP1, TIMP2, IL-1β	Centoid S3	0.007	0.049

Table 3.3: Main groups found by clustering the gene expression profiles induced by dynamic shear with and without BAPTA pre-treatment, and statistical comparisons between the group expression profiles. The Euclidean distance between the projection coordinates of pairs of centroids was used in comparison of means Student's *t* tests. The number of genes within each group represented the degrees of freedom. Intra-centroid variance was calculated using the distance between gene projection coordinates and the appropriate centroid (see Section 2.5 Equation 2.13).

3.3.3 Effects of Mechanical Loading Type on Gene Expression

To compare the effects of different mechanical loading regimes on chondrocyte gene expression, the 1, 4, and 24hr inhibitor-free timepoints from the dynamic compression and dynamic shear experiments were combined with data from cartilage explants that were

compressed over a 5 minute interval to a final strain of 50% and held for periods of 1, 4 and 24 hrs. The expression levels for all genes are shown in Section 3.5, Figure 3.12 & Figure 3.13. Clustering analysis revealed that four principal components were necessary to represent the data. The added complexity of the dataset was evidenced by a minimum of four groups being required for the clustering techniques to produce similar results, resulting in identical groupings (Figure 3.6, Table 3.4). All four centroids were found to be significantly separated from each other and statistically more correlated than randomly grouped genes (Figure 3.7, Table 3.4). Group M1 contained aggrecan, type II collagen, link protein, fibromodulin, MMP1, and TIMP3, which were transiently upregulated 50% by static compression but inhibited by 24 hrs (Figure 3.7). Group M1 genes were also upregulated ~50% by 24 hrs of dynamic compression and 3.5 fold by 24 hrs of dynamic shear. Most Group M1 genes were in Groups C1 and S1. Group M2 contained type I collagen, matrix proteases MMP-3,-9-13 and ADAMTS4, as well as TNFα, COX2 and ribosomal 6 phosphate, which were upregulated by long-term loading by all three protocols. Static compression induced the greatest upregulation of Group M2, 3 fold after 24 hrs, and both dynamic compression and dynamic shear induced milder upregulation of ~50% (Figure 3.7). Dynamic shear for 1 hr also upregulated Group M2 genes. c-Fos, and c-Jun formed Group M3 and were characterized by transient upregulation in response to all loading protocols (Figure 3.7). Static compression induced the greatest upregulation in Group M3 (> 6 fold), and which remained partially upregulated after 24 hrs; dynamic compression and dynamic shear produced smaller increases (2 fold) and mainly at the 1 hr timepoint. Group M4 contained genes from Group S3 and were only responsive to dynamic shear (Figure 3.7).

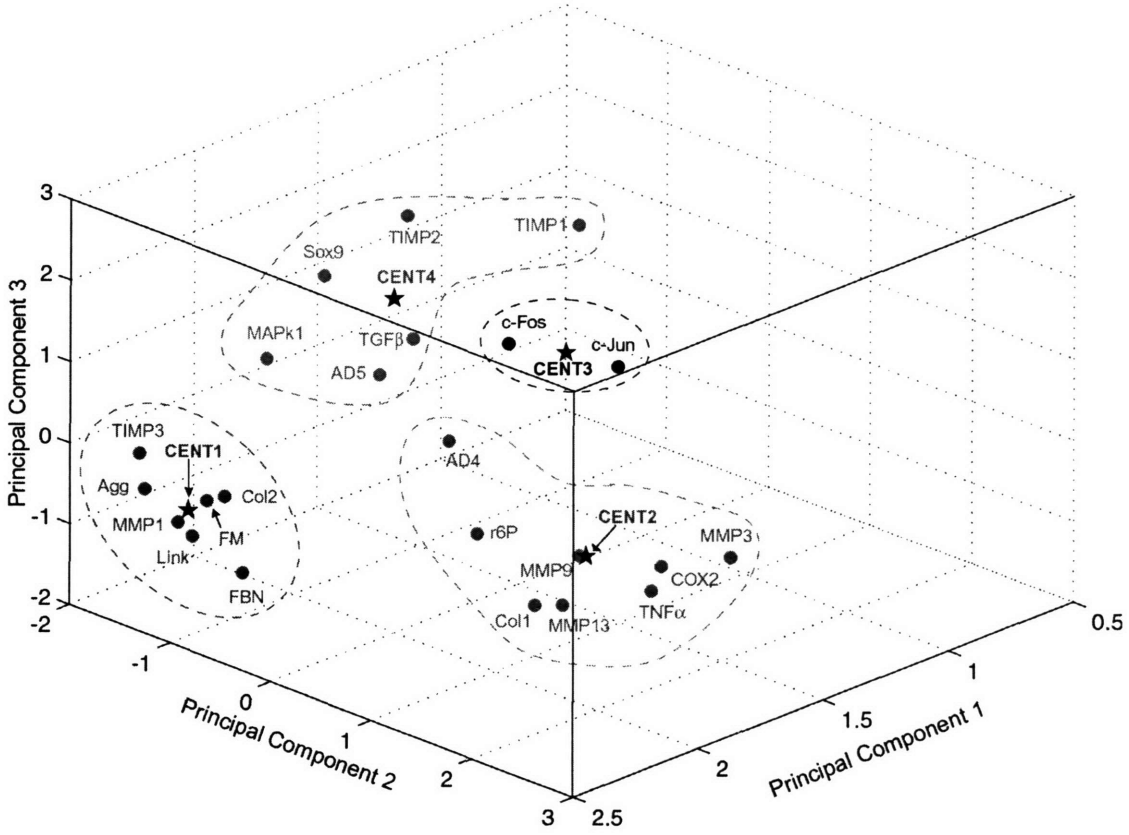

Figure 3.6: Three-dimensional representation of the gene expression profiles induced by static compression, dynamic compression, and dynamic shear. The gene expression profiles induced by inhibitor-free loading protocols were combined and projected onto the three main principal components found by PCA. The resulting weights are the gene projection coordinates. Groups were obtained by clustering the projected coordinates (four principal components were used), and verified by clustering the complete expression vectors. Abbreviations are as follows: *Agg*, aggrecan; *Col1*, type I collagen; *Col2*, type II collagen; *FM*, Fibromodulin; *FBN*, Fibronectin; *AD4*, ADAMTS4; *AD5*, ADAMTS5; *r6P*, ribosomal 6 phosphate; *CENT*, group centroid

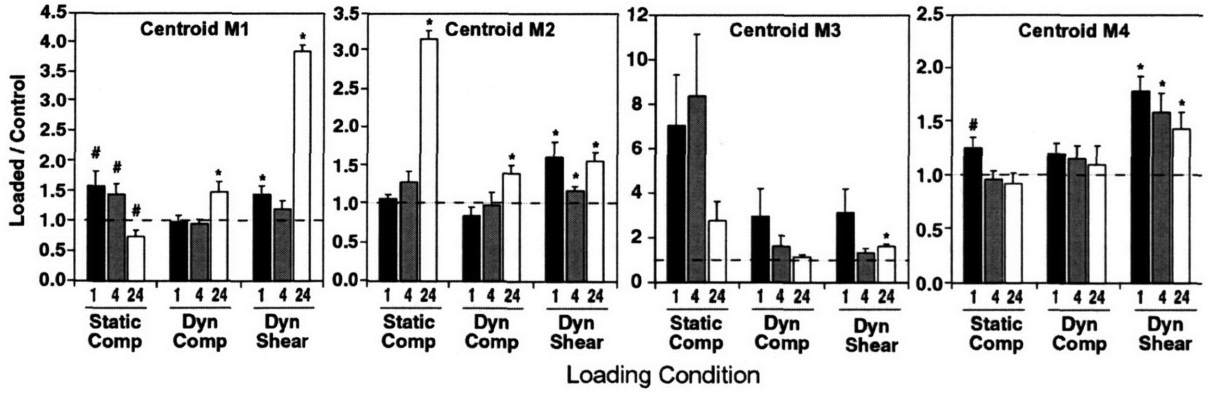

Figure 3.7: Main expression trends induced by static compression, dynamic compression, and dynamic shear. Centroid expression vectors found by averaging the standardized gene expression vectors in each group. Normalized to corresponding control explants (dashed line). Mean + SE (n = number of genes in a group). *, $p < 0.05$. #, $p < 0.07$ only

Group	Grouped genes	p values for centroid separation	Centroid M1	Centroid M2	Centroid M3
M1	Aggrecan, Type II Collagen, Link Protein, Fibromodulin, MMP1, TIMP3	Centroid M1			
M2	Type I Collagen, MMP3, MMP9, MMP13, ADAMTS4, TNFα, COX2, Ribosomal 6P	Centroid M2	4.2×10^{-5}		
M3	c-Fos, c-Jun	Centroid M3	6.7×10^{-3}	6.1×10^{-3}	
M4	ADAMTS5, TIMP1, TIMP2, Sox9, MAPk1, TGFβ	Centroid M4	1.5×10^{-2}	3.5×10^{-3}	3.3×10^{-2}

Table 3.4: Main groups found by clustering the gene expression profiles induced by static compression, dynamic compression, and dynamic shear, and statistical comparisons between the group expression profiles. The Euclidean distance between the projection coordinates of pairs of centroids was used in comparison of means Student's *t* tests. The number of genes within each group represented the degrees of freedom. Intra-centroid variance was calculated using the distance between gene projection coordinates and the appropriate centroid (see Section 2.5 Equation 2.13).

3.3.4 Promoter Analysis of Co-expressed Genes

The promoter sequences of the genes grouped by clustering across inhibitor-free loading type were compared for common transcription factor binding sites. For Group M2 (Table 3.4), which contained mainly catabolic genes, the following transcription factor binding sites were over-represented (except for ribosomal 6 phosphate): pre B-cell Leukemia TF, Fork head Homologous X, Activating protein 1, Octomer binding factor, NFκB, CCAAT/enhancer binding protein and Glucocorticoid receptor α. The diversity of this set of transcription factors suggests they may be common to the genes in Group M2 due to variety of upstream signals (i.e., signals including developmental, metabolic, cytokine, mechanical stimuli). However, it is interesting that a least one TRE AP1 binding site was found in each gene in Group M2 and at least one NFκB binding site was found in type I collagen, MMP3, MMP9 and COX2. Related to Serum Response Factor 4 (RSRF4) was over-represented in the upstream sequences of Group M1. AP2 and Serum Response Factor (SRF) were over-represented in Group M3. SRFs are important mediators of c-Fos induction by extracellular stimuli (reviewed in [116]). Media was exchanged sixteen hours before loading, therefore, if serum related transcription factors are involved the stimulus would be due to mechanical loading induced changes in media environment, perhaps via chondrocyte autocrine/paracrine mechanisms or factors released from the ECM.

3.4 Discussion

Chondrocytes respond to mechanical forces in a frequency dependent manner, by regulating matrix protein biosynthesis [26,33,55,80] and the composition of the ECM [51,52,79]. This study is the first to demonstrate the widespread regulation of genes involved in cartilage homeostasis by time-varying mechanical forces in cartilage explants. We showed that time-varying compression upregulates matrix protein and protease transcription, in contrast to the effects of static mechanical compression (Figure 3.12). Dynamic shear also induced matrix protein transcription in the absence of fluid flow or hydrostatic pressure gradients, highlighting the importance of cyclic matrix deformation in chondrocyte mechanotransduction. Examination of the time-course expression profiles induced by dynamic compression, dynamic shear, and static compression showed that chondrocyte's differentially regulate functional subsets of genes in response to mechanical forces. Furthermore most genes examined required intracellular calcium release in order to respond to mechanical stimuli.

Cartilage experiences a variety of loading forces *in vivo*, including compression and shear, both in a continuous (static) and cyclic manner (i.e. walking). Physiologic loads induced by daily activity range from sudden loads that induce high hydrostatic pressures over short time periods with little strain (15-20MPa, 1-3% strain [93]), to moderate cyclic activity (~2MPa, ~5% strain [117]), to sustained compressive loads for 5-30 minutes that induce from 10% to up to 45% compression [23]. Our study aimed at examining the individual components of *in vivo* mechanical forces by investigating three loading regimes. Applying moderate dynamic compressive loading cyclically deformed the ECM and induced fluid flow and HP gradients. Physiologically-relevant dynamic shear loading only induced matrix deformation with minimal fluid flow or HP gradients. Previous experiments in our laboratory applying up to 50% static compression (physiologically relevant maximum) examined the effects of transiently induced fluid flow and HP gradients, and long-term matrix consolidation (Chapter 2).

In general, dynamic loading is considered an anabolic stimulus for cartilage. Dynamic compression of cartilage explants increases PG and type II collagen synthesis within 4 hours, which is sustained for up to 48 hours [81]. Dynamic compression has also been used to produce stronger tissue engineered implants [54,84]. Dynamic shear also increases matrix biosynthesis, preferentially collagen synthesis [55]. In the present study clustering analysis showed that dynamic compression and dynamic shear upregulated matrix proteins particularly after 24 hours

(Group C1, Figure 3.3 and Group S1, Figure 3.5). Dynamic shear induced the greatest 24 hour increase with most matrix proteins increasing by > 200% compared to the dynamic compression induced increase of around 100% (Figure 3.8 & Figure 3.10). The similarity in matrix protein expression profiles suggests that cyclic matrix deformation is the essential component of mechanical loading that upregulates matrix protein gene transcription. Fehrenbacher et al applied high-amplitude dynamic compression (6MPa, 0.1Hz) to full-thickness juvenile porcine cartilage explants for 50 minutes and after a 2 hour recovery period saw decreased type I and II collagen transcription, but MMPs, TIMPs and aggrecan were unaffected [118]. The loading conditions applied are predicted to induce ~50% strain with insufficient re-swelling time, which suggests that their loading regime may be more similar to a 50% static compression than the moderate amplitude dynamic compression we applied. Our results are in general agreement with cell-based studies showing that cyclic pressure-induced strain increases aggrecan gene expression [58], perhaps through stretching of the cell membrane.

Recently dynamic compression was found to increase normal matrix turnover. Dynamic compression of chondrocyte-seeded fibrin gels [53] or peptide scaffolds [87] resulted in increased GAG loss during long-term culture. Dynamic compression of bone-cartilage explants upregulated MMP2 and MMP9 protein expression and protease activity within 3 hours and was sustained for 24 hours [32]. Although we only saw small changes in MMP9 gene transcription, the expression of other matrix proteases was upregulated, particularly after 24 hours of dynamic compression (Figure 3.2 & Figure 3.8). Interestingly COX-2, a known stimulator of PG degradation via prostaglandin-E2 [102] and activator of matrix proteases [102], always clustered with a majority of the proteases (Figure 3.3, Figure 3.5 & Figure 3.7) and thus may be part of the mechanotransduction signaling pathway. In our experiments long-term dynamic shear also increased matrix proteases and COX-2 transcription (Figure 3.4, Figure 3.10 & Figure 3.11). Therefore, a study into the long-term effects of cyclic loading on matrix protease activity is necessary to confirm the anabolic benefits.

To further interpret the influence of mechanical loading type, we clustered the inhibitor free timecourses of 50% static compression, dynamic compression and dynamic shear into four statistically distinct group expression patterns (Figure 3.7). Interestingly the groups contained functionally related genes (Figure 3.7), suggesting that mechanical forces differentially affect functional subsets of genes. For example, Group M1 contained 5 of the 6 matrix proteins and

therefore may be consider an anabolic or high turnover group. MMP1 and TIMP3 which were also in Group M1 always clustered with the matrix proteins (Figure 3.3, Figure 3.5 & Figure 3.7) and may be the balancing components of this subset. Although dynamic shear and dynamic compression induced similar expression trends in Group M1, static compression induced a remarkably different trend with upregulation following the onset of loading and suppression by 24hrs after matrix consolidation had reached equilibrium (Figure 3.7). This highlights the responsiveness of matrix proteins to the time varying nature of mechanical stimuli. The strong similarity between dynamic compression and dynamic shear induced matrix protein trends further supports the hypothesis that matrix deformation is the key regulator biophysical regulator of matrix proteins during loading.

Group M3 contained c-Fos and c-Jun, and transiently responded to all types of mechanical loading tested (Figure 3.3, Figure 3.5 & Figure 3.7). The milder stimulation of Group M3 in response to the dynamic loading regimes compared to static compression, may actually be related to the amplitude of the initial deformation applied to the cartilage explant. c-Fos and c-Jun are downstream of the mitogen activated protein kinases [116] which have been identified as mechanically sensitive to static compression [65,95]. Extracellular signal-regulated kinases 1 and 2 (ERK1/2) become maximally phosphorylated within 10 minutes of application of a 50% static compression, indicating an immediate response to the changing environmental conditions [65]. The mRNA levels of c-Fos and c-Jun (also known as immediate early genes) have been observed to transiently increase >40-fold after an injury stimulus of 50% compression at a strain rate of 1mm/second [119]. Therefore the onset of mechanical loading, which induces matrix deformation, fluid exudation and increased HP may be the general stimulatory signals for c-Fos and c-Jun. The fact that c-Fos and c-Jun were less affected by long-term cyclical matrix deformation suggests this is an adaptive response; in particular the absence of stimulation by long-term dynamic shear indicates a particular sensitivity to HP.

Group M2 contained most of the matrix proteases, COX-2 and type I collagen. (Type I collagen always clustered with the matrix proteases (Group C2 & Group S1)). Group M2 can be considered a catabolic group and was always upregulated after 24hrs of mechanical loading, in contrast to Group M1. Group M2 had a maximal response to static compression, as did Group M3. Group M3 genes, c-Fos and c-Jun, dimerize to form the activating protein-1 complex (AP-1). AP-1 and NFκB transcription factors had binding sites that were over-represented in

promoter sequences of Group M2 genes and are involved in cytokine induction of matrix proteases in chondrocytes [16,17]. We identified the AP-1 binding site in all genes in Group M2 supporting a connection between the two groups. Therefore, one could speculate that the transient upregulation of transcription factors c-Fos and c-Jun in response to the onset of loading regulates the matrix proteases at later timepoints. A binding site for the glucocorticoid receptor, which suppresses AP-1 activity [120], was also identified in the promoter region of genes in Group M2 possibly serving to counterbalance the regulation of this group.

Fluid shear, pressure-induced strain, and mechanical compression increase intracellular calcium concentration in chondrocytes [41,121,122]. Intracellular calcium release is required for fluid shear induced GAG synthesis [60], pressure-induced strain caused chondrocyte hyperpolarization [38], ultrasound induced PG synthesis [123], and compression induced aggrecan gene transcription [63]. In recent experiments it was found that fluid flow induced intracellular calcium release was not responsible for aggrecan gene upregulation; however, increases in cytosolic calcium by other methods did induce aggrecan gene upregulation [124]. In our experiments chelating intracellular calcium while applying dynamic compression suppressed the transcription of matrix proteins (Group C1), and partially inhibited matrix proteases (Group C2), c-Fos, and c-Jun (Group C3) (Figure 3.3), consistent with our previous observations for static compression (Figure 2.6). The main expression trends induced by dynamic shear were also suppressed by intracellular calcium chelation (Figure 3.5), suggesting that the effects of cyclic matrix deformation are mediated by intracellular calcium release. Therefore, intracellular calcium release is a key element through which a variety of mechanical forces that act on cartilage influence chondrocyte behavior.

Cyclic AMP is an important signaling molecule in a number of cell types. Intermittent hydrostatic pressure applied to chick embryo epiphyseal cartilage cells increased cAMP levels [125]. Static compression induced upregulation of aggrecan transcription was prevented by Rp-cAMP, an inhibitor cAMP activated protein kinase A [56]. When we applied dynamic compression in the presence of Rp-cAMP matrix protein transcription was enhanced during the first 1-4 hrs and suppressed by 24 hrs compared to inhibitor free expression levels; matrix protease expression was generally enhanced, and genes that responded transiently (Group C3), were unaffected (Figure 3.3). Rp-cAMP treatment during static compression was observed to enhance and suppress many matrix proteins and proteases (Figure 2.11). Although cAMP

activation of protein kinase A appears necessary for normal chondrocyte mechanotransduction, blocking this pathway does not abolish mechano-induced transcription. cAMP is known to cross-talk with other signaling pathways, for example, high cAMP levels modulate the response of the mitogen activated protein kinase pathway (reviewed in [126]). Therefore, our observations of gene transcription in response to dynamic compression with Rp-cAMP treatment may represent the effects of blocking cAMP crosstalk within the mechanotransduction pathway.

We have shown that time varying mechanical loads, comparable to those experienced *in vivo*, regulate the transcriptional behavior of chondrocytes. Genes encoding proteins with similar functions responded to the mechanical loading in a coordinated manner, suggesting that mechanical forces differentially regulate functional subsets of genes. It would be interesting to determine if this behavior is present in osteoarthritic cartilage where the chondrocyte mechanotransduction pathway is altered. Degradation of cartilage after injury or during osteoarthritis could modify the process through which forces are transduced into biological responses, altering which sets of genes become upregulated, and thus changing the balance between anabolic and catabolic processes. The effect of cartilage species and age need to be considered as human cartilage and chondrocyte properties change with age [127,128]. There is now substantial evidence of a key role for intracellular calcium release in chondrocyte mechanotransduction. The consistent, transient response of transcription factors c-Fos and c-Jun to mechanical loading requires greater investigation and future work will examine the extent to which the mitogen activated protein kinase pathway is involved in mechano-induced gene expression.

3.5 Supplementary Figures

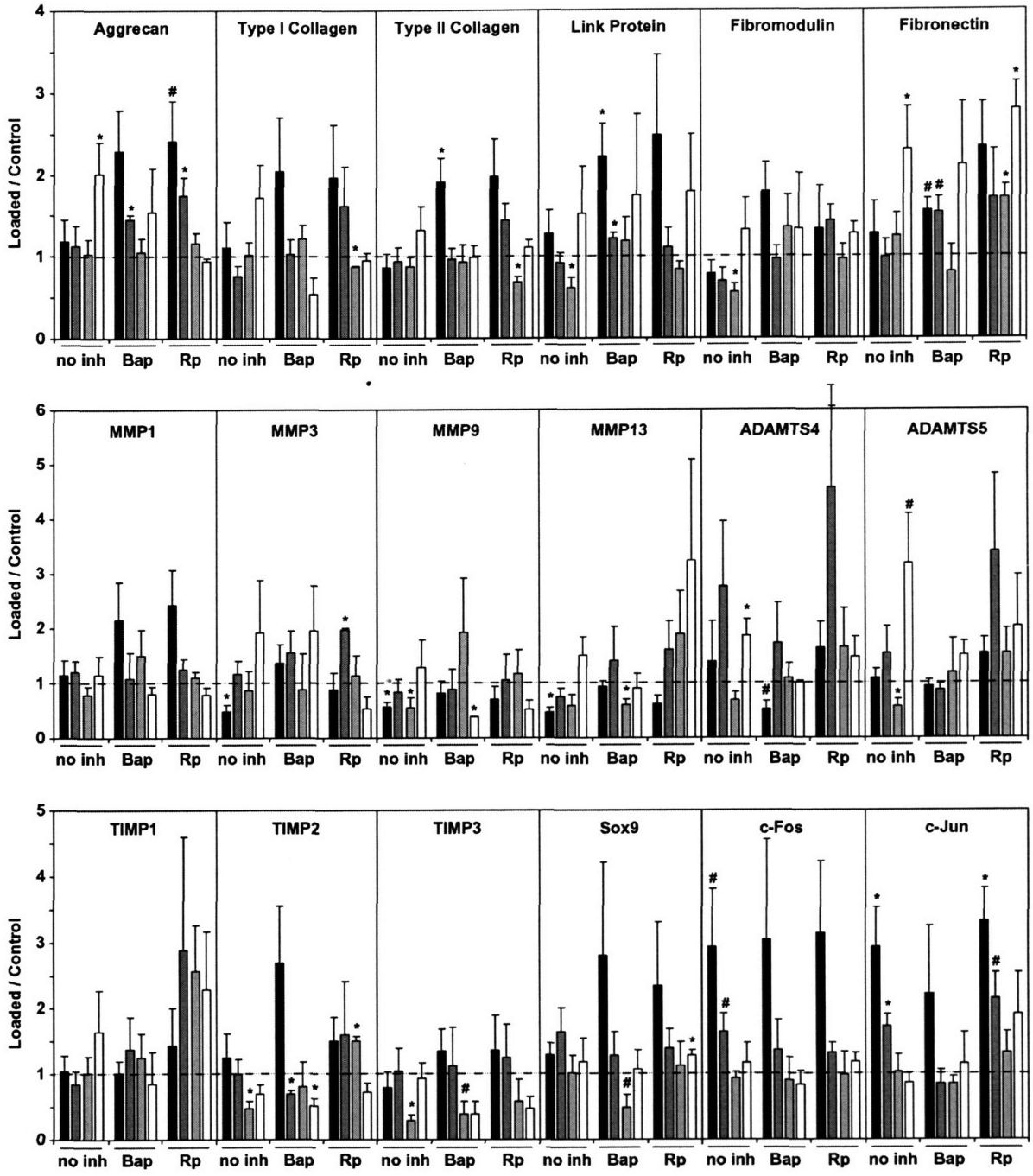

Figure 3.8: Gene expression profiles of matrix proteins, proteases, TIMPs, and transcription factors, induced by dynamic compression (3% strain, 0.1Hz). Conditions include dynamic compression time-courses from inhibitor-free (no inh, n = 7), BAPTA-AM pre-treatment (BAP, n = 5) or Rp-cAMP pre-treatment (Rp, n = 4). Expression levels are normalized to those of control explants which were compressed to 5% strain (dashed line). ■1hr, ■4hr, ■8hr, □24hr. Mean + SE. *, $p < 0.05$, # $p < 0.07$ only

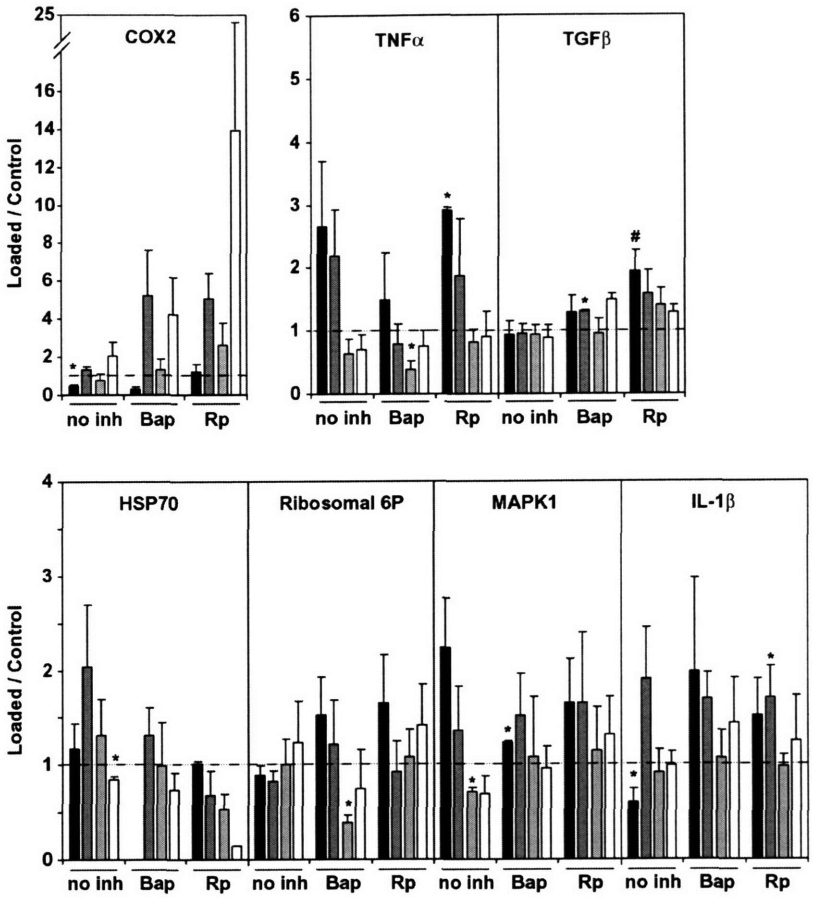

Figure 3.9: Gene expression profiles of signaling molecules induced by dynamic compression (3% strain, 0.1Hz). Conditions include dynamic compression time-courses from inhibitor-free (no inh, n = 7), BAPTA-AM pre-treatment (BAP, n = 5) or Rp-cAMP pre-treatment (Rp, n = 4). Expression levels are normalized to those of control explants which were compressed to 5% strain (dashed line). ■1hr, ■4hr, ■8hr, □24hr. Mean + SE. *, $p < 0.05$, # $p < 0.07$ only

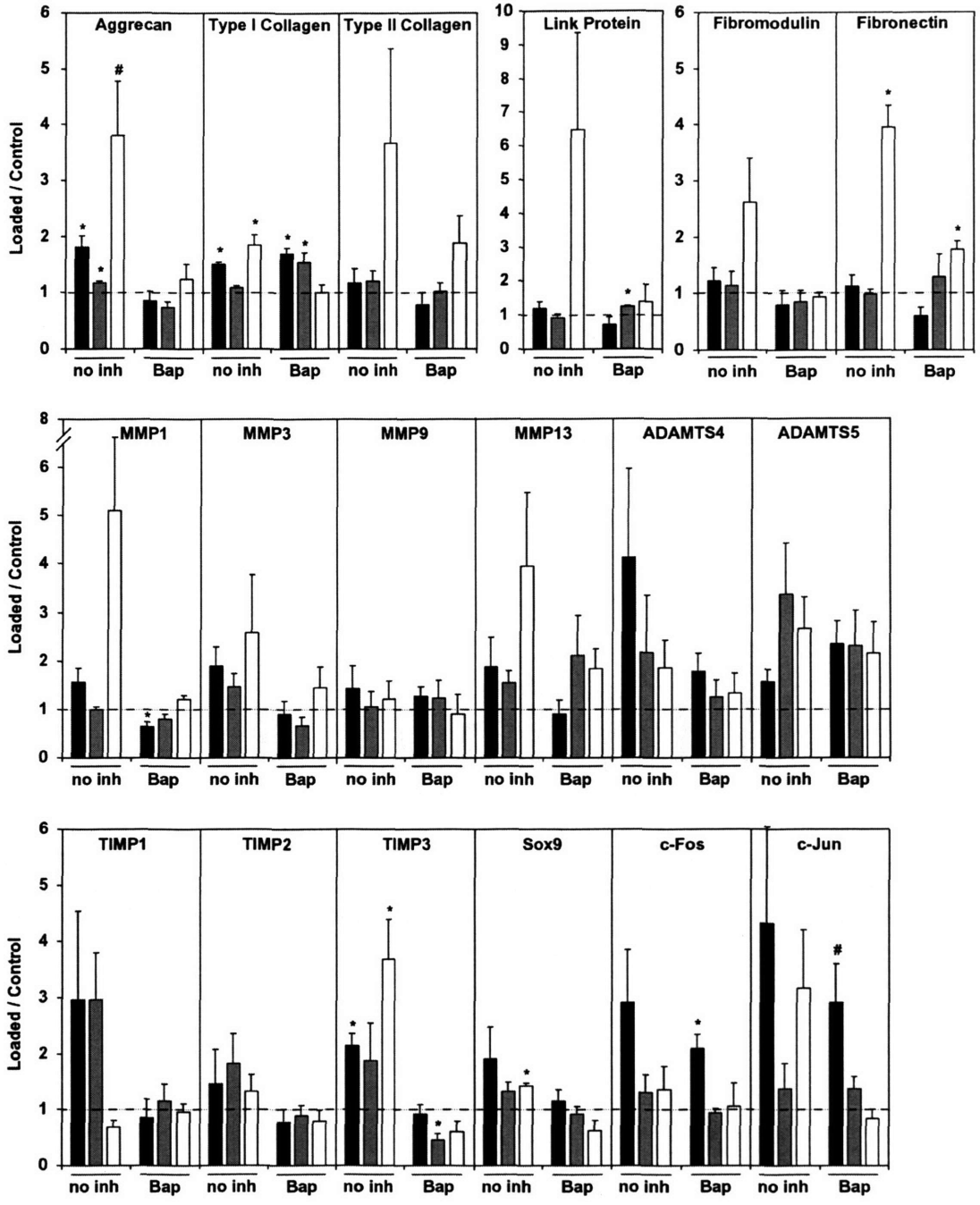

Figure 3.10: Gene expression profiles of matrix proteins, proteases, TIMPs, and transcription factors induced by dynamic shear (3% shear strain, 0.1Hz) without (no inh, n = 4) and with BAPTA-AM treatment (BAP, n = 4). Expression levels are normalized to those of control explants which were maintained at cut thickness (dashed line). ■1hr, ■4hr, □24hr. Mean + SE. *, $p < 0.05$, # $p < 0.07$ only

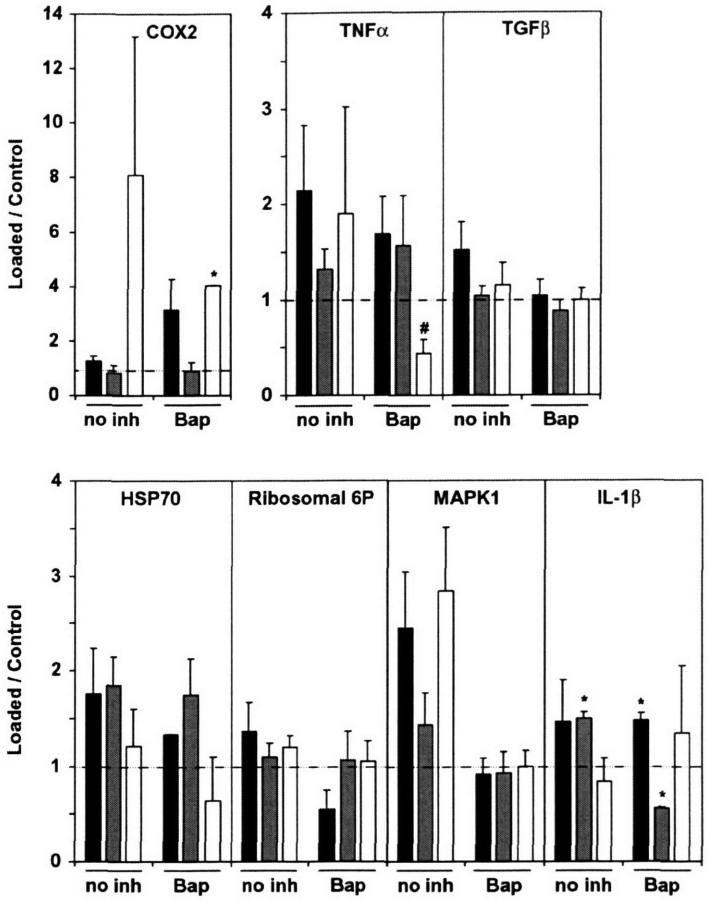

Figure 3.11: Gene expression profiles of signaling molecules induced by dynamic shear (3% shear strain, 0.1Hz) without (no inh, n = 4) and with BAPTA-AM treatment (BAP, n = 4). Expression levels are normalized to those of control explants which were maintained at cut thickness (dashed line). ■1hr, ■4hr, □24hr. Mean + SE. *, $p < 0.05$, # $p < 0.07$ only

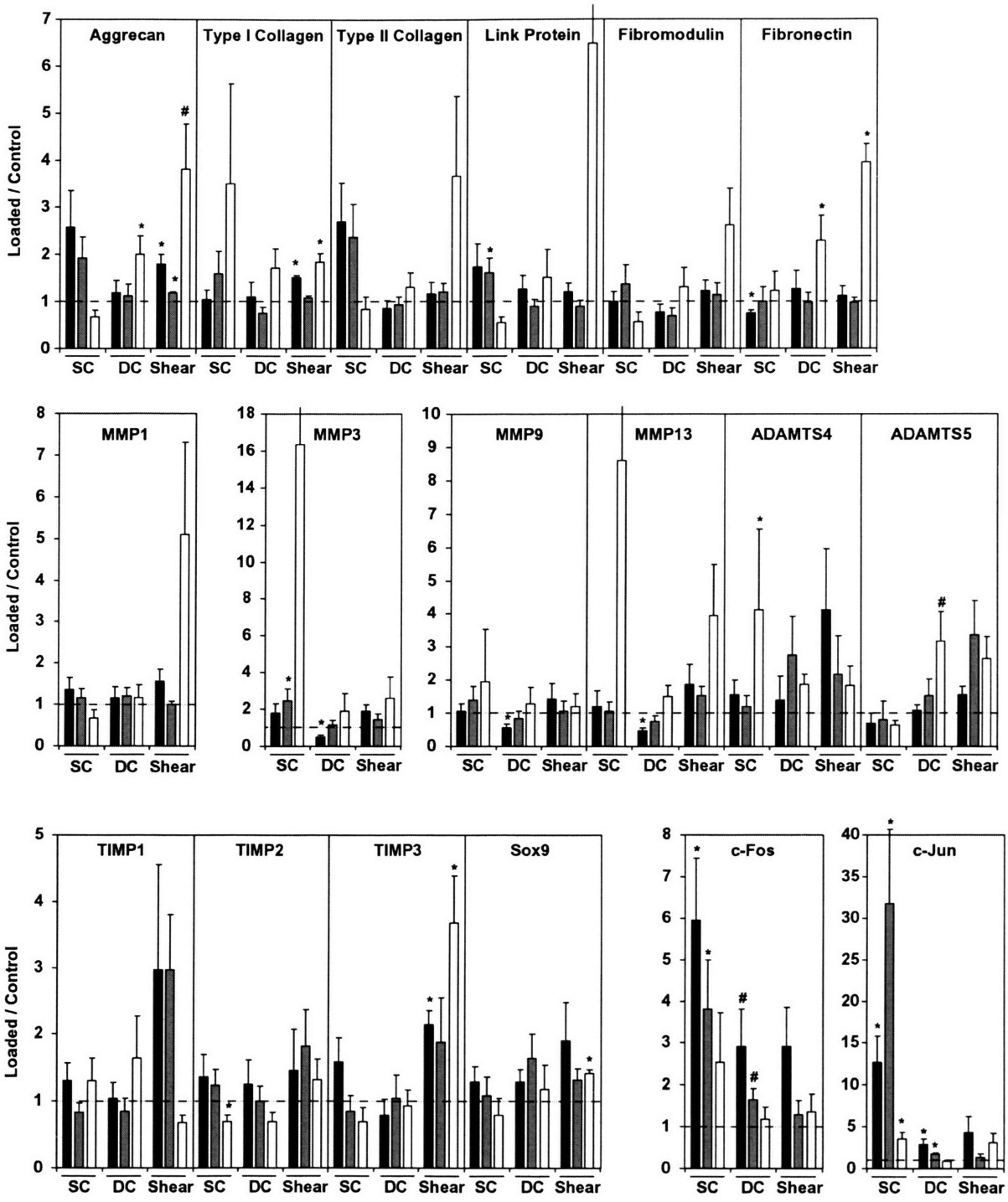

Figure 3.12: Gene expression profiles of matrix proteins, proteases, TIMPs, and transcription factors, induced by static compression (SC), dynamic compression (DC), and dynamic shear (shear). Normalized to corresponding control explants (dashed line). Mean + SE (n = 4-9). *, $p < 0.05$. #, $p < 0.07$ only

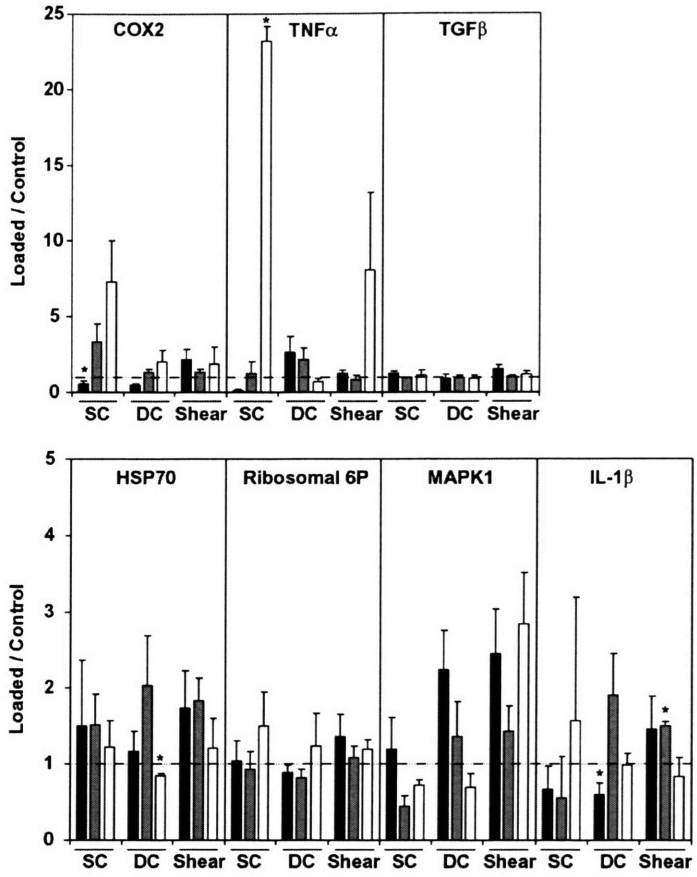

Figure 3.13: Gene expression profiles of signaling molecules induced by static compression (SC), dynamic compression (DC), and dynamic shear (shear). Normalized to corresponding control explants (dashed line). Mean + SE (n = 4-9). *, $p < 0.05$. #, $p < 0.07$ only

Chapter 4

Mitogen-activated Protein Kinase Phosphorylation is necessary for Mechanically-Stimulated Chondrocyte Transcription

4.1 Introduction

Articular cartilage lines the surface of synovial joints allowing smooth lubrication and efficient load absorption. The dense cartilage extracellular matrix (ECM) is composed of a network of proteins, particular proteoglycans (PG) and type II collagen, which produce the structural properties of cartilage. Chondrocytes are responsible for maintaining the ECM via secreting matrix proteins and proteases (enzymes capable of cleaving matrix proteins), and it is known that chondrocyte metabolism is affected by mechanical loads *in vivo* [51,52,79]. Cartilage diseases now afflict greater than 15% of the aging North American population [72]. Rheumatoid arthritis is an auto-immune disease where inflammatory cytokines signal the destruction of the cartilage ECM [129,130]. Osteoarthritis (OA) involves a breakdown in the ability of chondrocytes to maintain a healthy ECM, resulting in thinning of cartilage layers (reviewed in [78,131]). The exact causes of OA are unknown; however, mechanical injury is known to dramatically increase the risk of developing OA [73]. Hence, elucidation of chondrocyte signaling pathways activated in response to external stimuli like mechanical loads and cytokines is of primary importance.

The response of chondrocytes to mechanical loads is known to be dependent on the type, magnitude, and duration of the mechanical stimulus, as well as the presence of an extracellular matrix [22,26,33,44,55,95,132]. In general, the application of static compressive loads to intact cartilage explants for long durations (24 hours) inhibits PG and type II collagen biosynthesis

[21,26,33]. Dynamically compressing [22,29,33,133] or dynamically shearing [55] cartilage explants generally enhances matrix protein biosynthesis. Transcription of matrix proteins and proteases is time-dependently regulated by loading cartilage explants (Figure 3.12)[56,57,118], or by applying hydrostatic pressures [43,44] or pressure-induced strains [58] to chondrocyte cultured in monolayer. Intracellular calcium release and cAMP activation have been identified as signaling pathways regulating mechano-induced transcription (Figure 2.6, Figure 3.3, & Figure 3.5)[56,63,110]. Recently the phosphorylation of extracellular signal-regulated kinases (ERK1/2) have been observed in response to static [65] and dynamic compression [95] of cartilage explants, and fluid induced shear of isolated chondrocyte [67], suggesting that the mitogen-activated protein kinase (MAPK) pathway is also involved in chondrocyte mechanotransduction.

The three MAPKs; ERK1/2, p38, and c-Jun amino terminal protein kinase (JNK), play central roles in chondrocyte responses to extracellular stimuli [97,134]. For example, interleukin-1 (IL-1) and tumor necrosis factor alpha (TNFα), which are major inflammatory cytokines, cause the transient activation of ERK1/2, p38, and JNK in chondrocytes [134-138]. Both TNFα and IL-1 can regulate the transcription and synthesis of a number of metalloproteinases (MMPs) [18,96,139], and there is increasing evidence that these effects require MAPK activation [16,17,140]. In addition, transcription factors that are targets of the MAPKs, such as activating protein-1 (AP1), are present in the promoter regions of MMP1, MMP3, MMP13 [20,97,139]. There is some evidence that the MAPK pathway may also mediate effects of anabolic growth factors [65,69-71,141].

Although there is a wealth of knowledge regarding MAPK signaling in chondrocytes, the role of the MAPK pathway in cartilage mechanotransduction has not been determined. We have previously demonstrated that a number of genes involved in cartilage maintenance are regulated by mechanical forces (Figure 3.7). The aim of this study was to utilize real-time PCR and gene clustering techniques (Section 2.5)[90-92] to determine if MAPK phosphorylation in response to mechanical loading was necessary for mechano-induced gene regulation. Furthermore we applied dynamic tissue shear to cartilage explants to determine if fluid flow-independent cyclic matrix deformation also phosphorylates the MAPKs. We found that ERK1/2 and p38 phosphorylation are induced by dynamic shear and are necessary for the induction of many genes in response to all loading regimes tested in this study.

4.2 Methods

4.2.1 Cartilage Extraction & Mechanical Loading

Cartilage explants were harvested from the patello-femoral groove of 1-2 week old calves as previously described [22]. Cylindrical explant disks (3mm diameter, 1mm thick) were taken from the middle zone layer, washed with phospho-buffered saline, and equilibrated for 2 to 5 days in Dulbecco's modified essential medium (supplemented with 10% FBS, 10mM Hepes Buffer, 0.1mM nonessential amino acids, 20μg/ml ascorbate, 100U/ml penicillin, 100μg/ml streptomycin and 0.25μg/ml amphotericin B). Media was changed every second day and 16 hours before loading commenced. Anatomically matched explants were placed in 12 well polysulphone loading chambers to allow multiple explants to receive identical loading. One of three types of mechanical loading was then applied (Figure 4.1). Static compression loading protocols involved applying a 50% strain (0.5mm compression) over a period of 5-10 minutes and compression was maintained for the indicated durations (Figure 4.1A). Explants maintained in free swelling conditions were used as controls for static compression. Dynamic compression loading protocols involved slowly compressing explants to an offset compression of 5% and then applying a continuous 3% 0.1Hz sinusoidal displacement-controlled compression for the indicated durations (Figure 4.1B). Explants statically compressed to a 5% offset were used as controls for dynamic compression. Dynamic shear protocols involved maintaining explants at cut thickness and applying a continuous 3% shear strain at 0.1Hz for the indicated durations (Figure 4.1C,E), except in the shear-dose response experiments (Figure 4.1D). Explants maintained at cut thickness were used as controls. Upon loading completion explants that received identical loading and inhibitor treatments were pooled and flash frozen using liquid nitrogen.

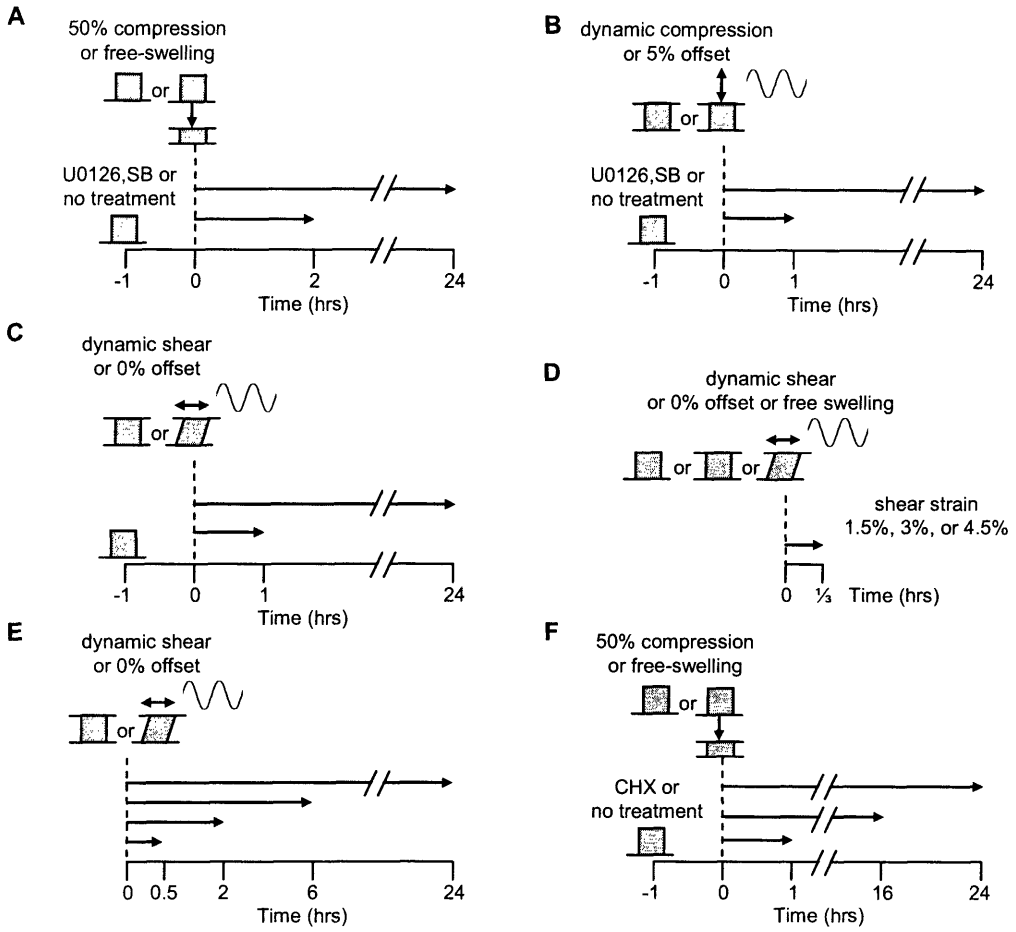

Figure 4.1: Loading protocols for MAPK inhibitor studies (ABC), MAPK phosphorylation studies (DE) and cycloheximide studies (F). A) Static compression of 50% strain was applied for 2 or 24 hours with inhibitors for MEK/ERK (25μM U0126) or p38 (20μM SB203580) added 1 hour prior to loading. Free-swelling explants were used as controls. B) Dynamic compression of 3% strain at 0.1Hz was applied for 1 or 24 hours on top of a 5% static offset, with U0126 or SB203580 added 1 hour prior to loading. Cartilage explants compressed to 5% strain were used as controls. C) Dynamic shear of 3% shear strain at 0.1Hz was applied for 1 or 24 hours on top of a 0% offset, with U0126 or SB203580 added 1 hour prior to loading. Cartilage explants compressed to cut thickness (0% offset) were used as controls. D) ERK1/2 phosphorylation shear-dose response. Dynamic shear was applied for 1.5, 3 or 4.5% shear strain for 20 minutes. Free-swelling explants and explants compressed to cut thickness were used as controls. E) ERK1/2 and p38 phosphorylation time course. Dynamic shear of 3% shear strain at 0.1Hz was applied for 0.5, 2, 6 or 24 hours. In separate experiments static compression of 50% strain was applied for 2 or 24 hours. Explants maintained at 0% offset were used as controls. F) Static compression of 50% strain was applied for 1, 16 or 24 hours with cycloheximide added 1 hour before loading. Free-swelling cartilage explants were used as controls.

4.2.2 Immunobloting for Shear Dose & Duration Responses

For shear dose response experiments, anatomically matched cartilage explants were subjected to a shear strain of 1.5% to 4.5% at 0.1Hz for 20 minutes or to static control or free swelling conditions (Figure 4.1D, 8-10 explants per condition). Three experiments involving five

different animals were performed. Time-course experiments were performed at 3% shear strain 0.1Hz as this stimulus produced the largest activation of ERK1/2.12 cartilage explants were subjected to 3% shear strain at 0.1Hz for 0.5, 2, 6, or 24 hours (Figure 4.1E). In simultaneous experiments a 50% static compression was applied for 2 or 24 hours (see Figure 4.1A no treatment). Cartilage explants were pooled flash frozen and analyzed for ERK1/2 and p38 activation. After loading, samples were frozen in liquid nitrogen and pulverized. Tissues were homogenized in NP-40 type homogenization buffer with protease inhibitors (20mM Tris pH 7.6, 120mM NaCl, 10mM EDTA, 10% glycerol, 1% NP-40, 100mM NaF, 10mM sodium pyrophosphate, 1mM PMSF, 2mM Na_3VO_4, 40μg/ml leupeptin) in the ratio of 100μl/10mg of tissue. Then the homogenates were extracted by rotating at 4°C for 1 hour and centrifuged at 13,000 g for 1 hour. Total protein concentration of each supernatant was quantified by the bicinchoninc acid (BCA) method. Aliquots containing 20μg of protein were suspended in Laemmli-SDS buffer and resolved by SDS-PAGE (10% resolving gel). Then the resolving gel was transferred to a nitrocellulose membrane (Schleicher & Schuell). After the transfer, membranes were blocked with 5% BSA in TBST (10mM Tris pH 7.6, 150mM NaCl, 0.1% Tween 20) for 2 hours at 37°C. Membranes were incubated in phospho-specific anti-ERK1/2 or anti-p38 polyclonal antibody-containing solutions (Cell Signaling Technology Inc, MA) overnight at 4°C. Membranes were washed in TBST (5x10min), incubated with HRP-conjugated secondary antibody (goat anti-rabbit, Jackson ImmunoResearch Laboratories Inc, West Grove, PA) for 1 hour at room temperature, and again washed in TBST. Phospho-proteins were visualized using enhanced chemiluminescence (Renaissance™ ECL, NEN Life Science Products, Boston, MA) and the quantified using densitometry.

4.2.3 Inhibitor Treatment & Loading

To investigate the role of MAPK activation small molecule inhibitors were added to media 1 hour before commencement of a loading protocol. U0126 is a highly potent MEK(ERK) inhibitor (Sigma), and was used at 25μM, a concentration equal to or greater than previously shown to inhibit ERK induced effects in chondrocytes [16,68,138,141]. SB203580 was used to block p38 kinase (Sigma) and was used at 20μM, a concentration equal to or greater than previously shown to inhibit the effects of p38 activation in chondrocytes [140,142,143]. Four U0126 treated explants, four SB203580 treated explants and four inhibitor free explants were

placed in a 12 well chamber and subjected to identical loading. To compare with previous results (Chapter 2 & Chapter 3) static compression was applied for 2 or 24 hours (n = 3-5, Figure 4.1A), or dynamic compression was applied for 1 or 24 hours (n = 4-5, Figure 4.1B), or dynamic shear was applied for 1 or 24 hours (n = 4, Figure 4.1C). Control explants were subjected to the same inhibitor treatments.

To assess the impact of synthesis of signaling factors during mechanical loading, separate experiments were performed where explants were pretreated for 1 hour with the protein translation blocker cycloheximide (100μg/ml, Sigma). A 50% static compression was then applied for 1, 16 or 24 hours to examine the effects of blocking protein synthesis on short and long-term transcription (n = 3, Figure 4.1F). Explants not treated with cycloheximide were placed in the same loading chambers, and free swelling control explants were subjected to the same inhibitors treatments.

4.2.4 Real-time PCR for Inhibitor Studies

RNA was extracted from pooled, frozen cartilage explants by first disrupting in a liquid nitrogen cooled pulverizer. Smashed explants were lysed by blade homogenization (BioSpec Products Inc) in Trizol reagent (Invitrogen), and the lysate was separated using phase-gel spin columns (Eppendorf). RNA was purified using the QIAGEN RNAeasy Mini columns with the DNase digest according to the manufacturer's instructions. Reverse transcription of approximately 1-2μg total RNA was performed using Applied Biosystems reagents on an Eppendorf Mastercycler. Previously designed primers were used for 17 genes involved in cartilage metabolism. Real-time PCR was performed on a MJ Research Opticon2 using Applied Biosystems SybrGreen reagents and protocols. Housekeeping genes (18S & G3PDH) and control samples were run on every plate for normalization purposes. Cycle threshold levels were converted to relative copy numbers using primer specific standard curves. Expression levels from loaded samples were normalized to the average of the housekeeping genes and also to similarly treated control samples.

4.2.5 Clustering & Statistical Analyses

Our previously described clustering technique was used to place genes with similar expression patterns into a predefined number of groups (Section 2.5). In brief, the average expression levels of each gene from each loading condition, duration, and MAPK inhibitor

treatment were combined into expression vectors forming a data matrix of 17 genes by 18 conditions. Each gene expression vector was normalized by the vector standard deviation to emphasize the pattern of expression rather than overall magnitude. Principal component analysis was then used to reduce dimensionality and visualize the similarity between genes in a three dimensional space, so that the number of distinct groups could be estimated. The three-dimensional gene coordinates were then clustered by minimizing a Euclidean distance metric. A second technique, applying *k*-means clustering to the entire gene expression vectors, maximized a correlation-based metric. The optimal grouping was chosen based on both Euclidean distance and correlation metrics, and the group centroid was calculated as the average expression profile from the genes within a group. The top five suboptimal groupings were compared to the optimal grouping to ensure that the trends were robust. Distinct separation between group profiles was tested using the three dimensional space and Student's t-test (See Section 2.5).

Comparisons between inhibitor treated and non-treated mechanically-induced gene expression levels were performed by two-tailed Student's t-test. Expression levels from Group centroids were similarly compared. Statistical significance was attributed for $p < 0.05$.

4.3 Results

4.3.1 ERK Phosphorylation Shear-Dose Response

Phosphorylated ERK1/2 levels in free swelling culture, 0% static control, and 1.5%-4.5% shear at 0.1Hz frequency for 20 min loading were detected using Western blot. A total of three experiments were performed and one of the typical images in shown in Figure 4.2. The increase in the phosphorylated ERK1/2 level reached a maximum value at 3% shear strain and slightly decreased at 4.5% shear strain. Interestingly, there was a dramatic increase in the phosphorylated ERK1/2 level at 0% compression over the free swelling condition (Figure 4.2). The gradual increase in phosphorylated ERK1/2 level with increasing shear stain was observed in two separate experiments.

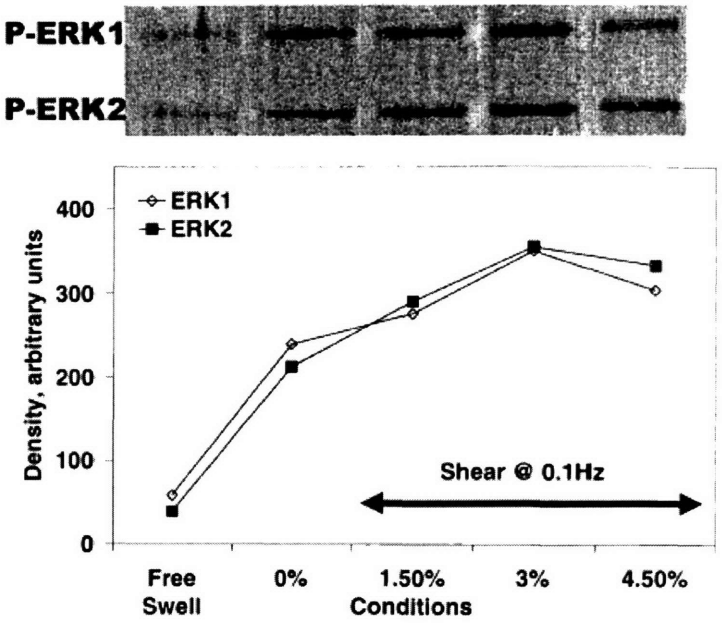

Figure 4.2: Phosphorylated ERK1/2 levels were quantified for free swelling, 0% control, and 1.5-4.5% shear strain at 0.1Hz (20 minutes loading). Performed by Dr Moonsoo Jin.

4.3.2 Time-dependent MAPK Phosphorylation

Applying a 50% static compression for 2 or 24 hours resulted in early activation of ERK1/2, decaying to a sustained 2-fold activation by 24 hours (Figure 4.3A), similar to our previous findings [65]. In contrast, 3% dynamic shear induced a consistent 25% increase in ERK1/2 activation over the entire 0.5 – 24 hour period, with peak activation of 50% after 6 hours of loading (Figure 4.3A). In comparison, ERK1/2 was activated 50-66% after 20 minutes of 3% shear strain (Figure 4.2). Static compression increased p38 phosphorylation 3-fold within 2 hours, and remained elevated by almost 100% after 24 hours (Figure 4.3B), similar to our previous findings [65]. In contrast to the ERK1/2 response to dynamic shear, p38 phosphorylation was delayed and increased with shear duration during the first 6 hours (up to 150%) and remained elevated by 100% after 24 hours (Figure 4.3B).

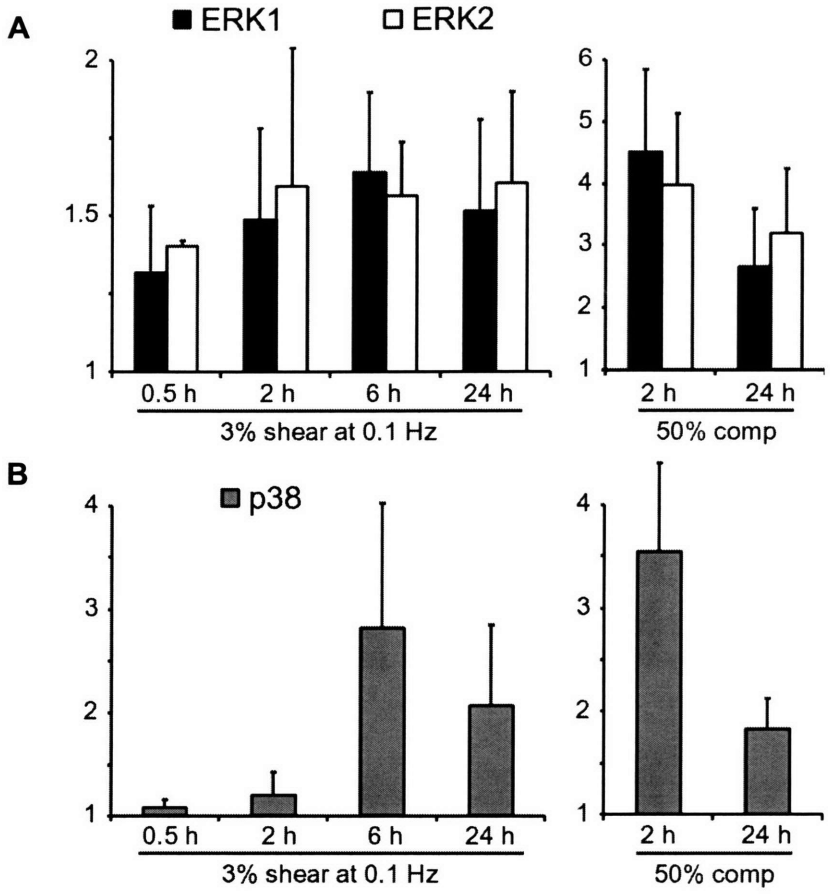

Figure 4.3: ERK and p38 phosphorylation levels were quantified for dynamic shear and static compression time courses. Mean + SE. (ERK n = 3, p38 n = 2). Performed by Dr Moonsoo Jin.

4.3.3 MAPK Inhibition Alters Mechanically Regulated Gene Expression

Validation experiments were performed to test the effectiveness of the MAPK inhibitors in cartilage explants. 50% static compression was applied for 1 hour with inhibitors added to media 1 hour before loading. The experiment was performed in triplicate and western blotting was performed for ERK1/2 and p38. A typical plot is shown in Figure 4.4. No basal phosphorylated ERK1/2 or p38 was detected in free-swelling control samples. 25μM of U0126 completely blocked MEK from phosphorylating ERK1/2 in response to static compression. SB203580 prevents p38 activity not activation, hence, there was no effect of 20μM of SB203580 on p38 phosphorylation induced by static compression. U0126 and SB203580 were added at similar concentration, have similar molecular weights, and potencies, and both affected chondrocyte gene transcription (shown later), therefore it is reasonable to conclude that SB203580 blocked p38 activation in the cartilage explants. Addition of MAPK inhibitors had

marginal effects on free swelling gene expression (data not shown). Matrix proteins were upregulated 10-200% after 2 hours of U0126 or SB203580 treatment, but no effect was observed under U0126 treatment after 24 hours; 24 hours of SB203580 treatment decreased free swelling expression by 50%. Matrix metallo-proteases were upregulated 0-50% after 2 hours of U0126 or SB203580 treatment but were generally not affected after 24 hours. In comparison basal expression levels of transcription factors c-Fos and c-Jun were not affected by U0126 or SB203580 treatment.

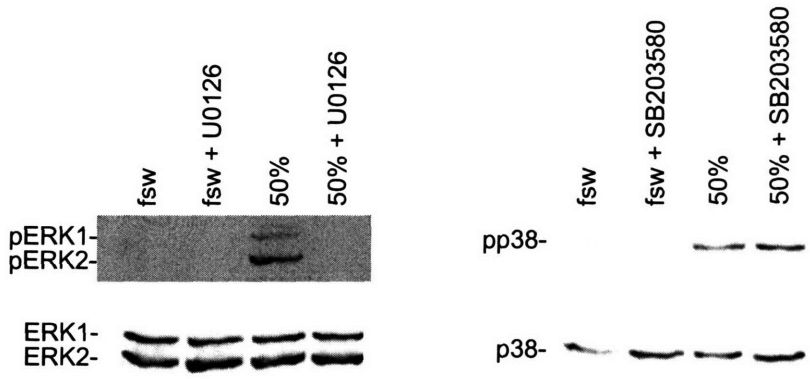

Figure 4.4: Effect of MAPK inhibitors on MAPK phosphorylation in cartilage explants induced by static compression. Inhibitors were added 1 hour before loading at concentrations of 25μM U0126 (MEK blocker) or 20μM SB203580 (p38 blocker). fsw = free-swelling control explants. 50% = 1 hour of 50% compression. Western Blots were performed with the assistance of Diana Chai and Aaron Baker.

Mechanically-induced matrix protein gene expression was affected by MAPK inhibitor pre-treatment (Figure 4.5). Aggrecan transcription was suppressed to control levels in the presence of U0126 or SB203580 for all three loading regimes tested, and for both short (1-2 hour) and long (24 hour) durations, expect after 24 hours of static compression. Type II collagen and link protein were inhibited by U0126 during all types of loading; however, SB203580 did not suppress transcription induced by static compression or 24 hours of dynamic loading suggesting differing roles for ERK1/2 and p38. Mechano-induced transcription of type I collagen and fibronectin was suppressed by U0126 and Sb203580 during most loading conditions, except for 24 hours of dynamic compression. The down regulation of type I and II collagen, fibromodulin and fibronectin by 24 hours of static compression was partially reversed by the addition of U0126 or SB203580.

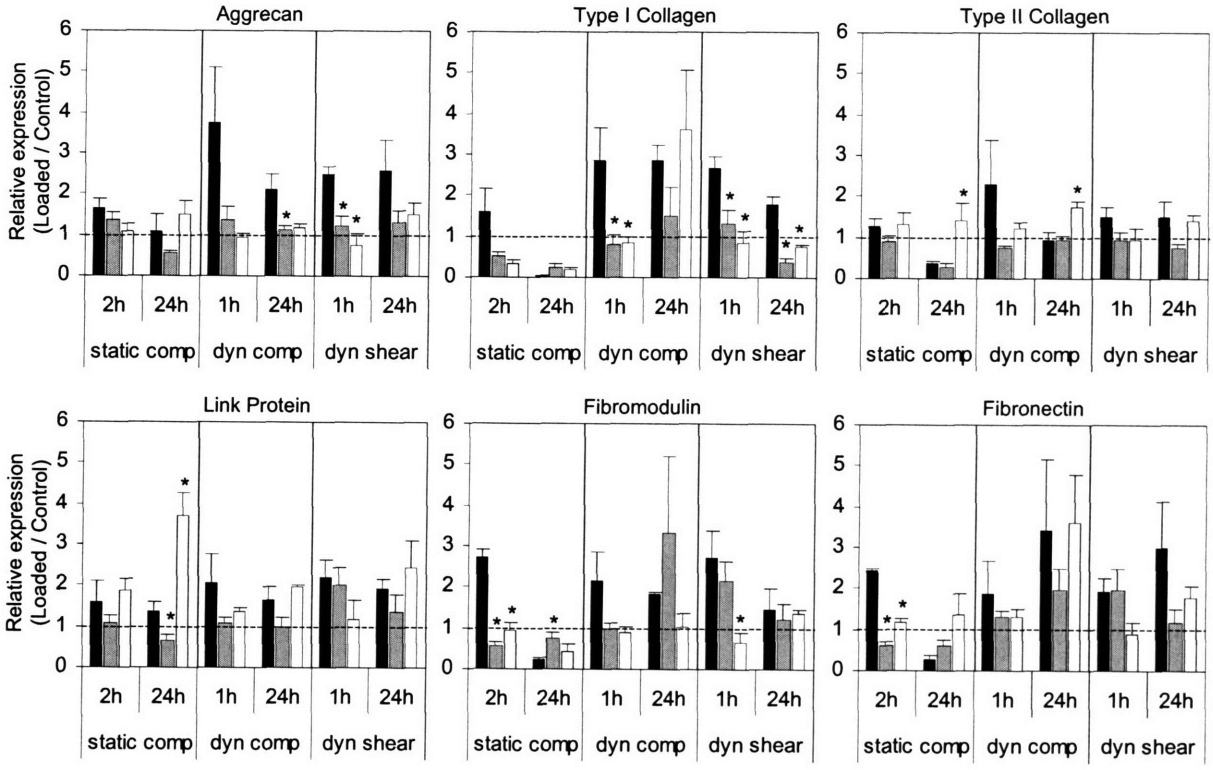

Figure 4.5: Expression of matrix proteins after loading and MAPK inhibitor treatment. ■ no inhibitor, ■ 25μM U0126, □ 20μM SB203580. Mean + SE (n = 4). * $p < 0.05$ between no inhibitor and U0126 or SB203580 normalized expression levels.

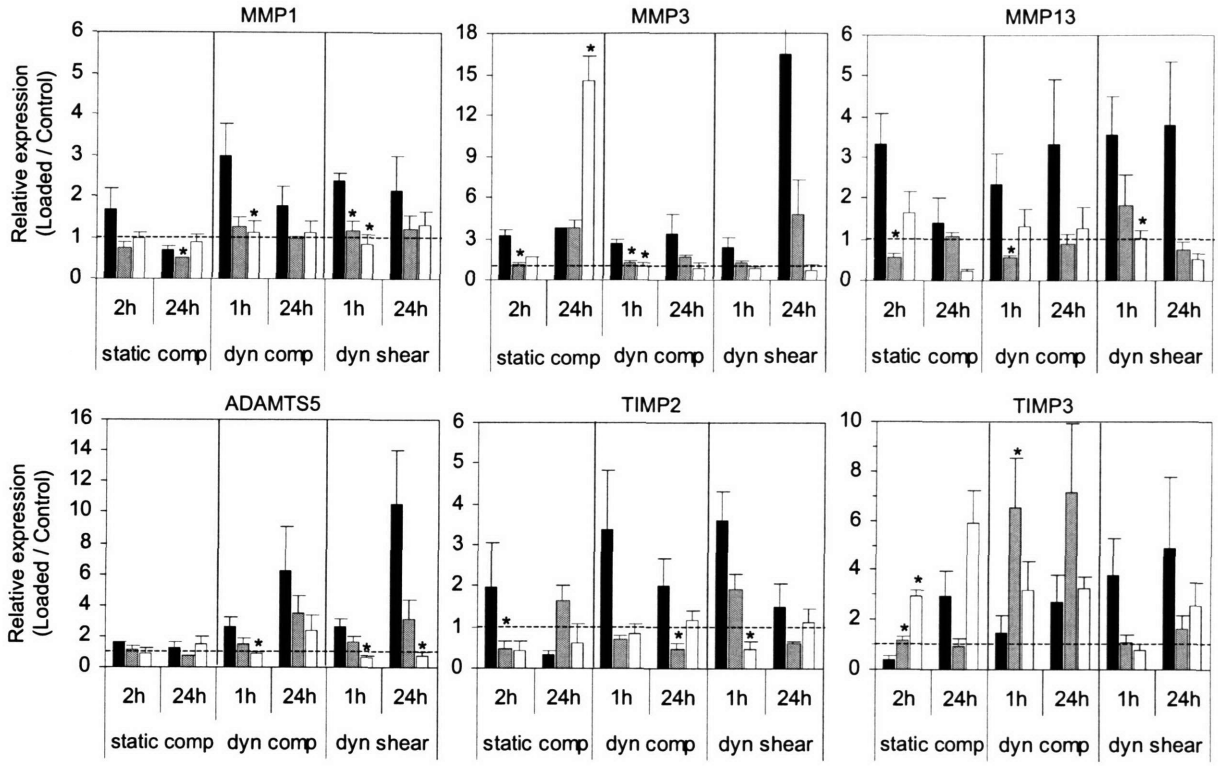

Figure 4.6: Expression of matrix proteases & TIMPs after loading and MAPK inhibitor treatment. ■ no inhibitor, ■ 25μM U0126. □ 20μM SB203580. Mean + SE (n = 4). * $p < 0.05$ between no inhibitor and U0126 or SB203580 normalized expression levels.

After short-term loading, matrix protease transcription was suppressed to control levels by U0126 and SB203580 under all loading regimes (Figure 4.6). U0126 was more suppressive on short-term protease transcription except for MMP13. After 24 hours of each loading regime MMP1, MMP13, and ADAMTS5 expression levels were suppressed to control levels by U0126 and SB203580, even during the 3 to 10 fold upregulation induced by dynamic compression and dynamic shear loading. MMP3 transcription was enhanced by SB203580 under static compression by 24 hours, but dramatically suppressed after both 24 hour dynamic loading regimes. U0126 had no effect on MMP3 transcription after 24 hours of static compression; however, U0126 partially suppressed transcription during both dynamic loading regimes, further suggesting that ERK1/2 and p38 have load-specific regulatory roles.

TIMP2 mechano-induced transcription was generally suppressed by MAPK inhibitors; however, the down regulation of TIMP2 after 24 hours of static compression was reversed by U0126 (Figure 4.6), suggesting the role of ERK pathway may be dependent on the direction of regulation that is induced. TIMP3 mechano-induced transcription was actually enhanced by U0126 and SB203580 during most timepoints of static and dynamic compression; however, both MAPK inhibitors clearly suppressed transcription during dynamic shear (Figure 4.6).

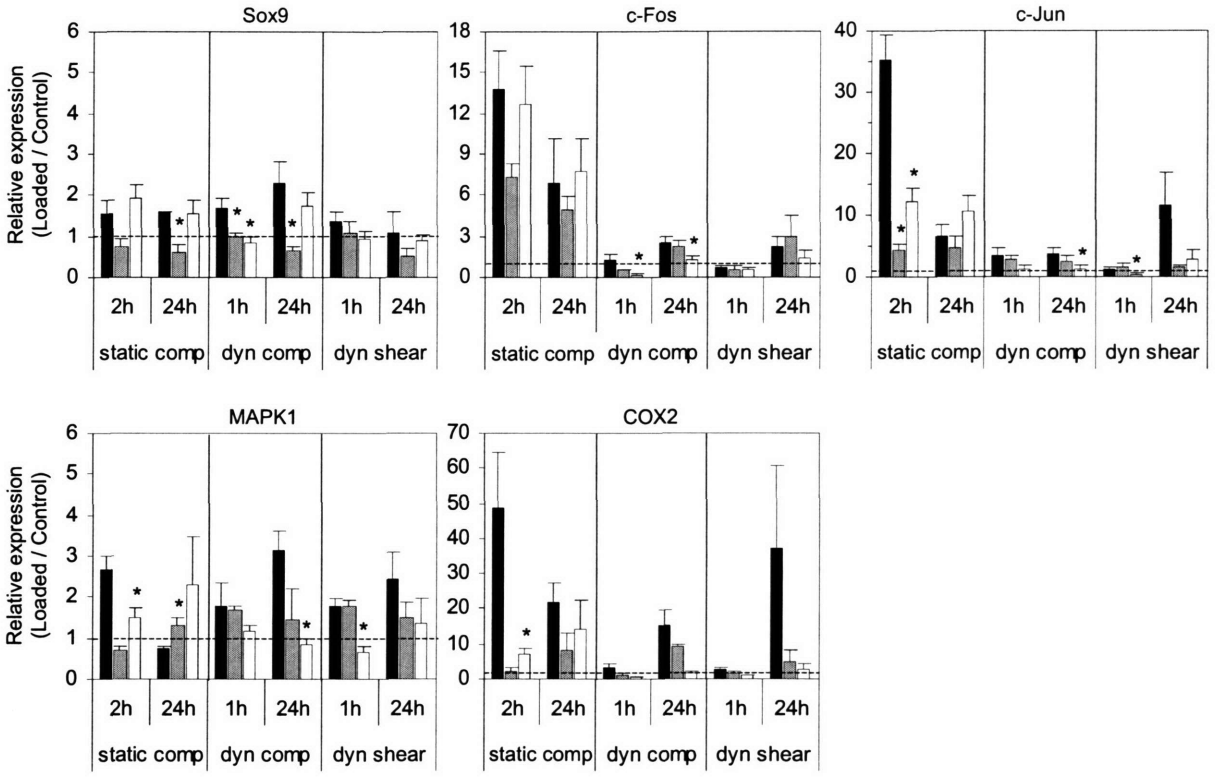

Figure 4.7: Expression of transcription factors & signaling molecules after loading and MAPK inhibitor treatment. ■ no inhibitor, ■ 25μM U0126, □ 20μM SB203580. Mean + SE (n = 4). * $p < 0.05$ between no inhibitor and U0126 or SB203580 normalized expression levels.

The mechano-induced upregulation of transcription factors c-Fos and c-Jun was partially suppressed by U0126 under all loading conditions (Figure 4.7). SB203580 had a suppressive effect on c-Fos and c-Jun transcription during dynamic loading, but either slightly suppressed transcription or even enhanced transcription during static compression. Similarly Sox9 transcription was suppressed by U0126 across load and duration, however, was unaffected by SB203580 except after 1 hour dynamic compression and shear (Figure 4.7). Mechano-induced

transcription of COX2 was generally suppressed by MAPK inactivation (Figure 4.7). MAPK1 response to loading with MAPK inhibitors was load and time dependent (Figure 4.7).

4.3.4 Gene Clustering Analysis

Gene clustering was performed to determine the overall effects of U0126 and SB203580 on genes that responded similarly to mechanical loading. Four statistically distinct groups were found ($p < 0.02$ for separation between each group) (Figure 4.8). The upregulation induced by all types and durations of mechanical loading for matrix proteins and proteases in Group 1 was suppressed by treatment with U0126 or SB203580 (Figure 4.8). However, Group 1 genes were down regulated by 24 hour static compression and treatment with MAPK inhibitors partially returned expression to control levels. Group 2 contained genes that were upregulated to a greater extent after 24 hours of dynamic loading, which was suppressed by U0126 and SB203580. During static compression Group 2 expression levels were suppressed by U0126, however, SB203580 had a mixed effect. Link protein, MMP3, and TIMP3 (Group 3) exhibited distinct transcription profiles in response to loading and MAPK inhibitor treatment. Although Group 3 was upregulated 100% in response to dynamic compression, neither U0126 nor SB203580 had an effect on link protein or TIMP3 expression. U0126 suppressed Group 3 after static compression; however, SB203580 enhanced expression of Group 3 genes after 24 hours of static compression. Group 4 contained transcription factors c-Fos and c-Jun as well as COX2 and exhibited the largest response to static compression, which was partially suppressed by SB203580 and to a greater extent by U0126. Both MAPK inhibitors suppressed the mechano-regulation of Group 4 in response to dynamic loading with SB203580 being more effective.

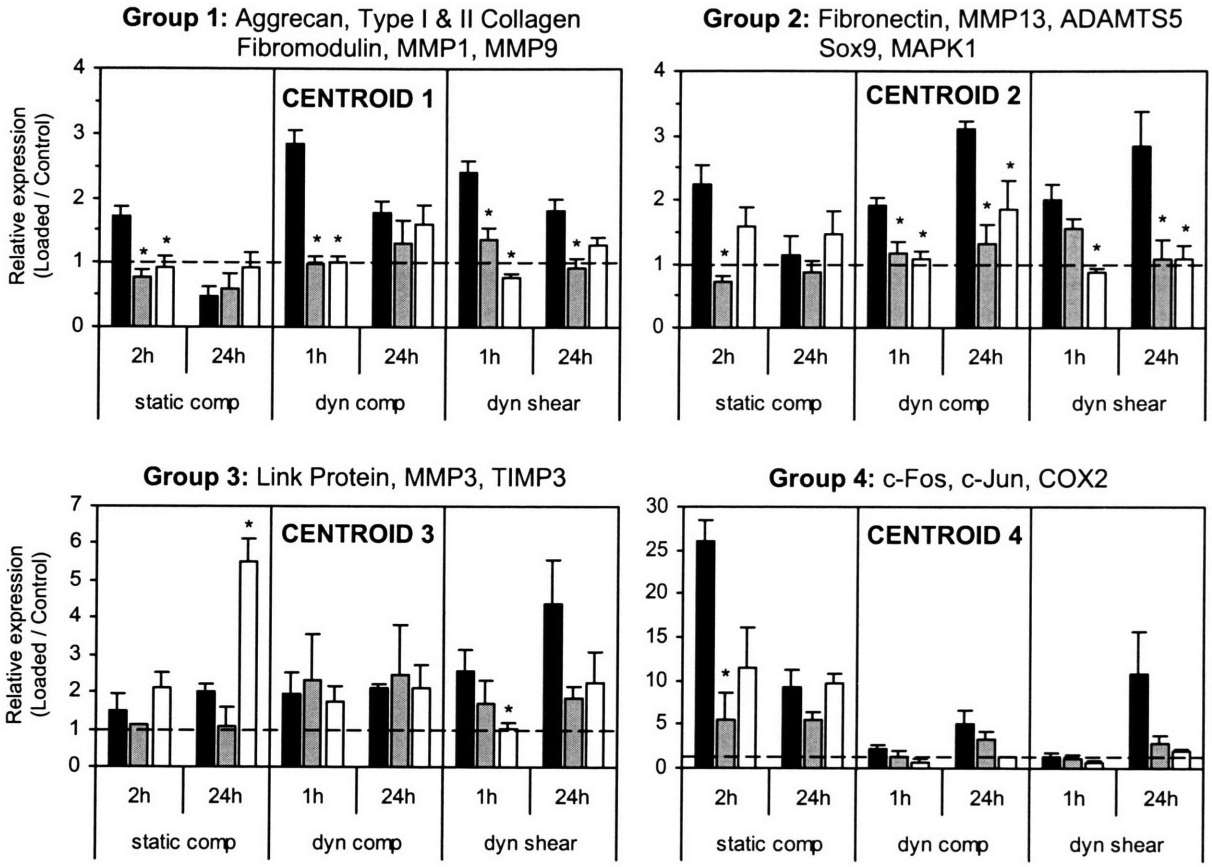

Figure 4.8: Group expression profiles after loading and MAPK inhibitor treatment. Normalized to control levels (dashed line). ■ no inhibitor, ▪ 25μM U0126, □ 20μM SB203580. Mean + SE (n = 4). * $p < 0.05$ between no inhibitor and U0126 or SB203580 treated normalized expression levels.

4.3.5 Effect of Cycloheximide Treatment

The inhibition of protein synthesis with cycloheximide greatly affected a number of genes that responded to 50% static compression (Figure 4.9). Static compression transiently induced the upregulation aggrecan, type II collagen and link protein which was altered with cycloheximide treatment to become a delayed upregulation with increasing compression duration (Figure 4.9), however, fibromodulin and fibronectin were unaffected (data not shown). MMP3 (Figure 4.9), and ADAMTS5 were greatly suppressed by cycloheximide particularly at later timepoints; upregulation of MMP1 and ADAMTS4 were partly suppressed; however, MMP9 and MMP13 were unaffected (data not shown). TIMP3 upregulation was suppressed by cycloheximide during compression at all timepoints; however, TIMP2 was only affected by cycloheximide treatment during longer compression durations (data not shown). Sox9

transcription was suppressed below control levels by CHX treatment during loading (Figure 4.9). The large upregulation of c-Fos and c-Jun by static compression was completely blocked by cycloheximide treatment (Figure 4.9), as was the upregulation of COX2 at later timepoints (data not shown). The invasive effect of blocking protein synthesis with cycloheximide did affect gene expression in free-swelling control samples (data not shown). In particular, the transcripts for Sox9, c-Fos, and c-Jun increased dramatically which complicates interpretation of these results.

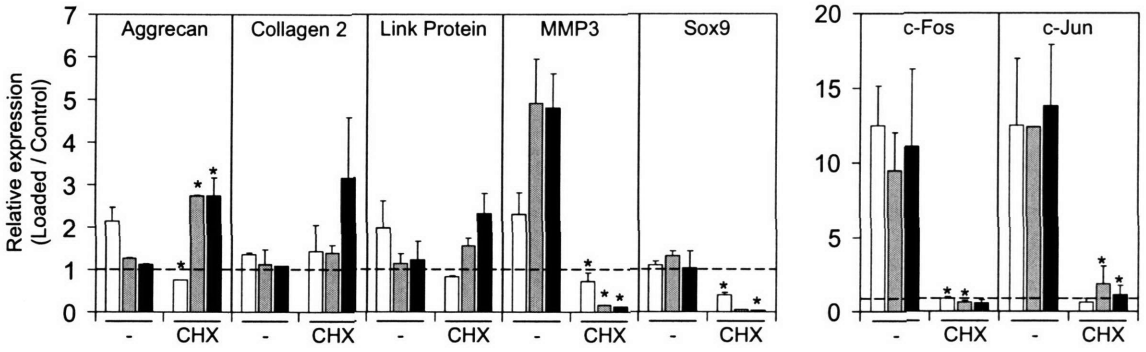

Figure 4.9: Role of protein synthesis in static compression induced gene transcription. Cartilage explants were treated with 100μg/ml of cycloheximide 1 hour prior to 50% static compression for □1, ▒16 or ■24 hours. Expression was normalized to free swelling control levels (dashed line). Mean + SE (n = 3). * $p < 0.05$ between cycloheximide (CHX) and no inhibitor (-) expression levels.

4.4 Discussion

The MAPKs are important signaling molecules for transducing mitogen and stress-related signals into nuclear responses, affecting a number of transcription factors in a variety of cell types ([64] for review). The unique mechanical environment of cartilage has been shown to cause MAPK activation [65,95]. This study is the first to demonstrate the sustained activation of ERK1/2 and p38 pathways in response to dynamic shear loading of cartilage explants. Utilizing real-time PCR we observed that gene transcription, induced by a variety of mechanical loading conditions, was suppressed by MAPK inhibitors, suggesting a role for MAPK signaling in the chondrocyte mechanotransduction pathway.

We observed a modest but dose dependent increase in ERK1/2 activity in response to dynamic shear (Figure 4.2 & Figure 4.3). ERK1/2 activation has also been demonstrated in response to continuous static compression of cartilage explants, where the time course consisted of an increase within 10 minutes that decayed to a sustained 3-fold activation level by 24 hours [65]. Dynamic compression induced a > 2 fold sustained increase in ERK1/2 activation [95].

Both static and dynamic compression induce transient and sinusoidal fluid flows and pressures [33,34,109], whereas dynamic shear induces primarily cyclic matrix deformation with minimal fluid flow and hydrostatic pressures [55]. The small effect of dynamic shear on ERK1/2 phosphorylation suggests that the ERK1/2 phosphorylation time course is sensitive to hydrostatic pressures and fluid flows. Static compression caused a transient activation of p38 (Figure 4.3)[65]. In contrast, p38 phosphorylation increased with dynamic shear loading duration during the first 6 hrs (Figure 4.3), suggesting that cyclic matrix deformation mediates p38 signaling in this system, though the effects of dynamic compression on p38 are unknown. All three loading regimes regulate PG and type II collagen synthesis [22,26,33,55], however, only the dynamic loading regimes enhance synthesis [22,33,55]. Therefore, the long-term effects of mechanical loading are associated with long-term upregulation of specific MAPKs, however, the directional regulation of protein synthesis must involve additional signaling factors.

The sustained activation of ERK1/2 and p38 kinases by dynamic shear (Figure 4.3), and the transient activation in response to static compression [65], occur over much longer time scales than typical MAPK responses to cytokine treatment. In chondrocyte cultured in monolayer, IL-1 activates ERK1/2 within 15 minutes, with ERK1/2 phosphorylation returning to basal levels within 1-4 hours [17,136,138]. Similar transient effects have been shown for IL-1 [17,136,137] and TNFα [137] treatment on p38 and JNK phosphorylation. The different temporal responses of MAPKs to mechanical loading and cytokine treatment suggests the differential regulation of a common receptor or that distinct mechano-receptors exist. The surrounding ECM may also modulate MAPK responses in chondrocytes. Li et al observed that IL-1 treatment of chondrocytes monolayer exhibited transient ERK phosphorylation; however, IL-1 treatment of cartilage explants resulted in sustained phosphorylation for over 16 hours [95]. Chondrocytes cultured on the surface of cartilage explants for 4 days also responded to IL-1 with sustained ERK activation [95]. Therefore, the adaptive response of chondrocytes to external signals may be dependent on the presence of an ECM, and suggests that mechano-receptors are integrated with the ECM.

Using clustering techniques we have shown that ERK1/2 & p38 kinases have a role in regulating a variety of temporal gene expression patterns (Figure 4.8). Inhibition of ERK activation with U0126 during static compression suppressed gene regulation in all four groups suggesting a role for the large, biphasic ERK activation seen in our current (Figure 4.3) and

previous experiments [65]. p38 inhibition with SB203580 partially suppressed static compression induced gene transcription in Groups 1,2 and 4 consistent with the transient p38 activation seen in our current (Figure 4.3) and previous experiments [65]. p38 inhibition completely suppressed all group expression levels induced during dynamic shear, suggesting a role for the 3 fold activation of p38 during long-term dynamic shear. Interestingly inhibiting ERK also had a general suppressive effect on dynamic shear induced gene transcription even though only mild ERK1/2 activation was observed. The common regulatory effects of p38 and ERK suggest some overlap or cooperation of downstream transcription factors is involved, which may explain the complete suppressive effects with either inhibitor for certain genes. Suppression of dynamic compression induced ERK activation [95], or of p38 during dynamic compression decreased gene expression in all groups except for Group 3, which suggests that additional signaling factors are involved. The widespread inhibition of gene transcription by ERK or p38 suppression is similar to our observations regarding intracellular calcium release and cAMP activation (Figure 2.6, Figure 3.3, & Figure 3.5). In particular p38 phosphorylation (Figure 4.8), and intracellular calcium release (Figure 3.5) are essential for gene transcription to be induced by dynamic shear. Therefore, there may be some crosstalk or hierarchy in the transduction of mechanical signals through the intracellular calcium, cAMP, ERK1/2 and p38 signaling pathways in cartilage explants. However, Hung et al have shown that fluid induced shear activation of ERK was calcium independent in isolated chondrocytes [67].

In general, ERK1/2 are thought to regulate cell growth and proliferation, whereas p38 and JNK are thought to respond to stresses (reviewed in [64,126,144]). In chondrocytes, the ERK and p38 pathways have been associated with catabolic signals [17,97,134,136-138,143]. Hence, the suppression of matrix protein transcription, particularly aggrecan, during loading with ERK inhibitors was an unexpected result (Figure 4.5). However, there is some evidence suggesting that the MAPKs transduce anabolic signals in chondrocyte metabolism. Pro-anabolic growth factor TGFβ, induced ERK1/2 and p38 phosphorylation in ATDC5 chondrogenic cells, which was required for enhanced aggrecan transcription [68]. p38 phosphorylation was also found to be a contributing factor towards TGFβ stimulated PG synthesis and chondrocyte proliferation [70,71]. Insulin like growth factor-1 (IGF1), promotes anabolic chondrocyte behavior, and transiently upregulates ERK phosphorylation [65,69]. The widespread involvement of MAPKs in mechanically induced transcription of matrix proteins, proteases, and TIMPs (Figure 4.6)

strongly suggests that the MAPK pathway may be a central conduit through which mechanical signals regulate chondrocyte homeostasis.

Our results showing that mechanically-induced matrix protease transcription was regulated partly via MAPK phosphorylation (Figure 4.6), are similar to experiments that demonstrate cytokine regulation of matrix proteases via MAPKs [16,17,140,142]. This similarity may indicate that mechanical loading and cytokines share common receptor and intracellular mechanisms, or that release and/or synthesis of signaling factors is a downstream component of mechanically loading, as is postulated in a chondrocyte monolayer model of mechanotransduction [38]. By treating cartilage explants with cycloheximide during static compression we demonstrated that protein synthesis was necessary for normal mechano-induced transcription (Figure 4.9). Interestingly the effect was not limited to matrix proteases as matrix proteins were also dramatically affected (Figure 4.9). Blocking proteins synthesis has also been shown to prevent TGFβ induced aggrecan transcription in ATDC5 chondrogenic cells [68]. However, certain genes were suppressed within 1 hour which may be too fast for cytokine/growth factor effects and more likely indicates the synthesis of transcription factors. Transcription factors c-Fos and c-Jun are downstream targets of the MAPKs (reviewed in [64]), were largely upregulated under multiple loading conditions, and were partially suppressed by MAPK inhibition (Figure 4.7). Therefore, c-Fos and c-Jun are prime candidates for common mechano-induced and cytokine activated transcription factors [20]. The delayed upregulation of aggrecan and type II collagen during cycloheximide treated static compression is unexpected and further work is required to elucidate a mechanism.

We observed some gene-specific responses to MAPK inhibitors during loading. MMP3, link protein, and TIMP3 transcription was enhanced by SB203580 during 24 hours of static compression (Group 3, Figure 4.8). Type II collagen, link protein, and TIMP3 were also relatively unaffected by SB203580 under a number of loading conditions (Figure 4.5 & Figure 4.6). These specific responses may indicate that additional transcription factors and regulatory pathways are involved in the transduction of mechanical signals. It has been proposed that SB203580 may also affect JNK phosphorylation [145,146]. Identifying additional signaling pathways and mechano-induced transcription factors will be the focus of future work.

We have demonstrated that ERK and p38 MAPKs are activated in response to mechanical loads, in particular, dynamic shear time-dependently regulated p38 phosphorylation.

However, the activation of MAPKs occurred in response to all three loading regimes, and therefore was not responsible for determining the direction of matrix synthesis in response to load. We demonstrated that ERK1/2 and p38 phosphorylation are involved in the time-dependent mechano-regulation of matrix protein and protease gene transcription, confirming a role for MAPK signaling in the cartilage mechanotransduction pathway. Observing the response of the MAPK pathway to injurious loading, mechanical loading of osteoarthritic tissue, and during tissue engineering protocols, will help establish the anabolic and catabolic roles of MAPK signaling in cartilage mechanotransduction.

Chapter 5

Radial Dependence of Mechanically-induced Gene Transcription

5.1 Introduction

The cartilage extracellular matrix (ECM) is subjected to a variety of mechanical loads during daily activity. Joint exercise is considered more beneficial for cartilage than inactivity [51,52]; however, joint over-loading [10,75] and the wear and tear of aging, lead to degradation of the cartilage matrix and impaired mechanical properties (for review see [78]). Chondrocytes, the cells responsible for maintaining the cartilage ECM, have limited reparative capacity (for review see [131]), and it is now estimated that 1 in 6 North Americans have the cartilage disease osteoarthritis [72]. Therefore, it is very important to understand how chondrocytes respond to mechanical forces and regulate the composition of the ECM.

The biological effects of physical activity on cartilage have been replicated *in vitro* by apply precisely-controlled mechanical forces to intact cartilage explants. In general, static compressive loads suppress the synthesis of the major ECM matrix proteins, aggrecan, and type II collagen [22,26], whereas dynamic compressive [27,33,45], and dynamic shear loading [55] increase matrix protein synthesis. Hence, dynamic loading protocols are being incorporated into tissue engineering strategies [53,54,84]. The transcription of matrix proteins, matrix proteases (the enzymes responsible for turnover the ECM), and endogenous protease inhibitors are regulated by static compression [56], dynamic compression, and dynamic shear loading in cartilage explants (see Figure 3.12). Analytic models applying poroelastic [34,35] and biphasic theory [31] have been used to predict the spatial profiles for the hydrostatic pressure gradients, fluid flow velocities, streaming currents, and radial strains generated by compressing cartilage

(see Figure 5.1), which is a charged, poroelastic tissue (for review see [1]). The spatial distribution of aggrecan and type II collagen synthesis induced by mechanical loading have been mapped using autoradiographic techniques [34,55,147,148]; however, there is no information regarding the spatial distribution of genes induced by mechanical loading.

Monolayer cultures are used to determine the effects of isolated physical forces on chondrocyte behavior. The application of cyclical or intermittent hydrostatic pressures (HP) to chondrocytes increases proteogylcan synthesis [42,60], as well as aggrecan and type II collagen transcription [43], whereas high magnitude static HP decreases aggrecan transcription [42], similar to results of compressing cartilage explants. Constant velocity, fluid flow-induced, membrane shear increases aggrecan promoter activity [67], and proteogylcan synthesis [61]. Deformation of cell culture plates by cyclic pressure-induced strain deforms chondrocytes in the absence of fluid flow, and transiently increases the transcription of aggrecan [58]. The ability of chondrocytes to respond to these isolated physical stimuli suggests that the response *in vivo,* and in the explant system, is a complex combination of biophysical factors.

We have previously characterized the time-dependent responses of a number of genes involved in cartilage metabolism to continuous static compression, dynamic compression, and dynamic shear loading (Figure 3.7). In an effort to further elucidate the physical forces responsible for the observed gene induction we compared the mRNA levels in central versus peripheral sections of cartilage explants after 24 hours of each loading type. We observed relative changes in gene expression between the central and peripheral regions that were gene-specific and dependent on the type of loading applied. In particular, matrix protein transcription was greater in the peripheral regions in response to static and dynamic compression and but reduced in response to dynamic shear.

5.2 Methods

5.2.1 Cartilage Harvest

Articular cartilage/bone cores were drilled from the femoropatellar groove of 1-2 week old calves. During the harvesting process the cartilage was kept moist with phospho-buffered saline supplemented with antibiotics: 100U/ml penicillin, 100μg/ml streptomycin and 0.25μg/ml amphotericin B. Cartilage/bone cores were cut into 1mm thick cartilage slices using a microtome, and four 3mm diameter, 1mm thick explant disks were punched out of each slice

using a dermal punch. Cartilage explants were incubated in low glucose Dulbecco's modified essential medium supplemented with 10% FBS, 10mM Hepes Buffer, 0.1mM nonessential amino acids, 20μg/ml ascorbate, 100U/ml penicillin, 100μg/ml streptomycin and 0.25μg/ml amphotericin B, for 2 days to allow equilibration. Medium was changed 16 hours prior to mechanical loading, with 6mls of medium for each group of 12 explants in a 6 well plate (500μl per explant). During medium exchange cartilage explants were divided amongst the loading conditions such that explants from each slice were distributed evenly between control and loaded groups.

5.2.2 Mechanical Loading

For each loading condition twelve cartilage explants were placed into a polysulphone loading chamber and positioned inside an incubator-housed loading apparatus [25]. Explants subjected to static compression were compressed to a 50% strain over 5-10 minutes and maintained at 50% strain for 24 hours. Explants that were dynamically compressed were first compressed to cut thickness (0% compression slowly applied over 10 minutes to minimize the transient effects due to the onset of loading), and then 3% strain at 0.1Hz was applied for 24 hours. Explants subjected to dynamic shear were first compressed to cut thickness (0% compression slowly over 10 minutes) and then 3% shear strain at 0.1Hz was applied for 24 hours. In contrast to previous experiments, control explants from all three loading protocols were subjected to 0% compression for 24 hours. Separate controls for each loading condition were still performed. Each loading protocol was performed six times using different animals.

Upon loading completion, explants were removed from chambers, dried using sterile gauss, and a biopsy punch (Premier Medical Supplies, PA) was used to excise a 1.5mm diameter cylindrical core of tissue from each explant. The twelve cores were pooled and flash frozen in liquid nitrogen as were the twelve rings which contained the peripheral sections of the explant. The excision of the core regions increased the time between loading completion and freezing by 3-4 minutes and was considered too short to permit significant changes in gene expression. A circle of radius 0.75mm was chosen as the boundary as previous experiments measuring radiolabel incorporation in response to dynamic compression, both at the whole explant and micron scale, identified differences between central and peripheral regions, using boundaries of 0.6-1.0mm (see Figure 5.1)[33,34].

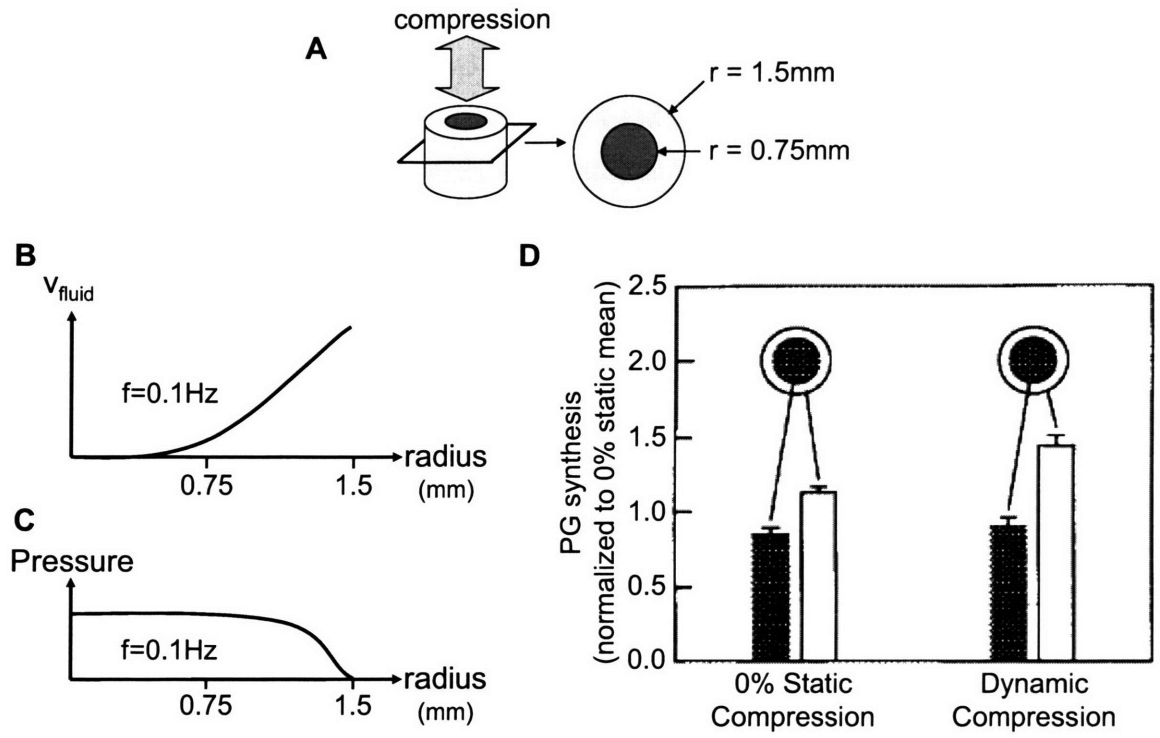

Figure 5.1: Unconfined compression of cartilage explants (A) induces radially varying physical stimuli. Dynamic compression at 0.1Hz induces higher fluid velocities at the explant periphery (B), with greater hydrostatic pressures in the explant center (C, see [34]). Radial variations in proteoglycan biosynthesis have been observed in response to static compression and 3% strain, 0.1Hz dynamic compression (D, taken from [33]).

5.2.3 RNA Extraction & PCR

Twelve cartilage explants were used for each sample as twelve 1.5mm diameter central core samples contained the equivalent mass of four cartilage explants. Tissue samples were disrupted using a liquid nitrogen cooled pulverizer. Pulverized *Center samples* produced only a thin crisp of pulverized cartilage, compared to *Ring samples*. Smashed samples were lysed by blade homogenization (BioSpec Products Inc) in Trizol reagent (Invitrogen), and Center samples appeared to be completely homogenized. The homogenized lysate was separated using phase-gel spin columns (Eppendorf), and excess high weight material was noted below the phase-gel in the Ring samples. RNA was purified using the QIAGEN RNAeasy Mini columns with the DNase digest according to the manufacturer's instructions. Reverse transcription of approximately 1-2μg total RNA was performed using Applied Biosystems reagents on an Eppendorf Mastercycler.

Previously designed primers were used for 18 genes involved in cartilage metabolism. Real-time PCR was performed on a MJ Research Opticon2 using Applied Biosystems SybrGreen reagents and protocols. Housekeeping genes, 18S and G3PDH, and control samples were run on every plate for normalization purposes. Cycle threshold levels were converted to relative copy numbers using gene specific standard curves. Housekeeping gene expression levels were comparable to those measured on previous plates indicating that the Center samples contained a sufficient yield of RNA, and were probably extracted with a higher efficiency. Expression levels from loaded samples were normalized to the average of the housekeeping genes and also to similarly treated control samples.

5.2.4 Data Analysis

The relative expression of the Ring samples was further normalized to the relative expression of the Center samples. Expression levels were averaged from repeated experiments and values three standard deviations from the mean were considered outliers and removed. Data are represented as mean + standard error (n = 6). To highlight differences between gene induction in the Ring and Center samples across the three loading types, a clustering analysis was performed. For each gene the Ring (loaded/control) / Center (loaded/control) average from each loading condition was combined into an expression profile. As the gene expression profiles contained three data points direct visualization was possible and principal component analysis was not necessary. The number of clusters was identified from the three dimensional plot and Euclidean distance based *k*-means clustering of the gene expression coordinates was performed to confirm the six clusters. Group expression profiles were calculated as the averaged expression of the genes in a group. Standard errors of the group expression profiles were calculated for each loading condition using the expression levels of genes in a group and the number genes in that group. The Euclidean distance between two groups and the intra-group variance were used to determine if the group expression profiles were statistically distinct patterns (see Section 2.5).

5.3 Results

5.3.1 Individual Expression Profiles

The ratio of the mechano-induced expression in the ring versus the center for each gene in response to each loading condition is shown in Figure 5.2. Many genes showed differential

responses between the ring and center, which was dependent on the type of loading applied. In response to static compression aggrecan and type II collagen mRNA levels were greater in the ring region by 60-100% compared with the center region (Figure 5.2); however, overall expression levels were suppressed below control levels consistent with previous results (Figure 2.2)[56,57]. The synthesis rate of aggrecan during 50% static compression also increases in the explant periphery relative to the center by approximately 30-40%, with overall synthesis below that of free-swelling cartilage [33,34,147]. Dynamic compression preferentially increased transcription of aggrecan and type II collagen in the explant periphery (~30% greater than the center, Figure 5.2), similar to previous biosynthesis studies [33,34]. Aggrecan transcription was greater in the center region in response to dynamic shear by 20% (Figure 5.2), which has been shown in micron-scale autoradiographic studies [55], although no differences were seen in overall explant measures. Type II collagen also showed greater transcription in the center region in response to dynamic shear (Figure 5.2), however, no radial dependence was observed in biosynthesis studies [55]. Link protein transcription exhibited a strong preference for the explant periphery in response to static compression (150%), dynamic compression (100%), and a minor center preference in response to dynamic shear (15%)(Figure 5.2). Expression of fibronectin was similar to aggrecan and type II collagen, and fibromodulin showed differential mechano-induction towards the peripheral regions particularly in response to dynamic compression (Figure 5.2).

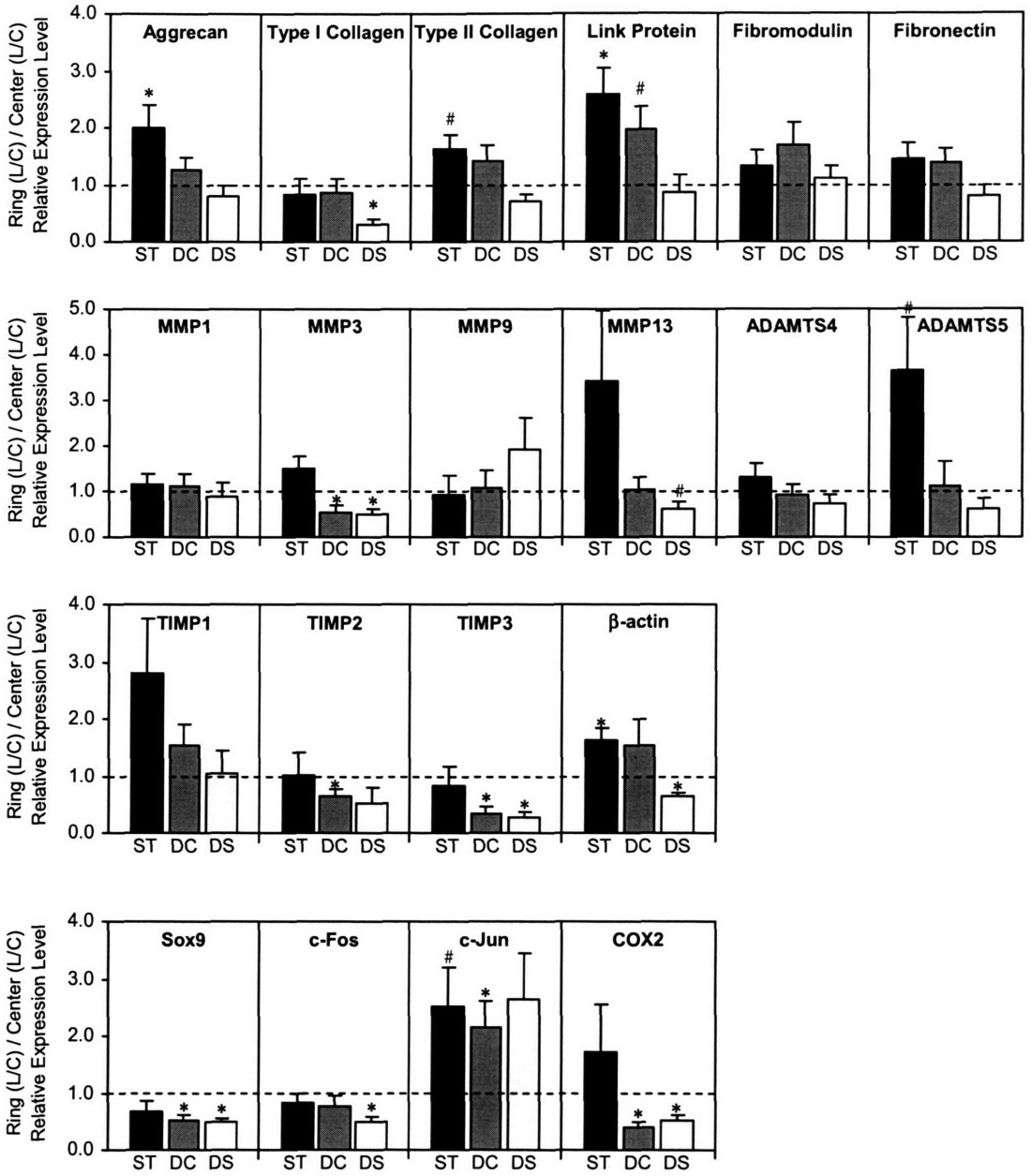

Figure 5.2: Comparison of mechanically induced gene expression levels in the peripheral ring and central core regions of cartilage explants. ST = 50% static compression for 24 hours. DC = 3% strain, 0.1Hz dynamic compression for 24 hours. DS = 3% shear strain, 0.1Hz dynamic shear for 24 hours. L = loaded, C = control. Mean + SE (n = 6). * $p < 0.05$, # $p < 0.07$ only, compared to center = ring expression (dashed line).

Matrix proteases exhibited a range of radius-dependent responses to mechanical loading (Figure 5.2). MMP3 was one of the only genes to demonstrate a reversed differential response between static compression (increased in ring by 50%) and dynamic compression (increased in center by 50%)(Figure 5.2). MMP3 also showed a statistically significant 50% increase in

transcription in the central region compared with the ring in response to dynamic shear, which is remarkable as the stresses and strains induced by dynamic shear are uniform throughout the radial direction of the explant [55]. In response to static compression the expression of MMP13 and ADAMTS5 increased in the ring relative to the center by 250%, however, there was no radial dependence in response to dynamic compression, and a smaller center preference of 40% in response to dynamic shear (Figure 5.2). ADAMTS4 and MMP1 showed only minor differences between ring and center expression (Figure 5.2). The expression of MMP9 was unlike any other gene with a relative 90% increase in expression in the explant periphery compared with the center only for dynamic shear (Figure 5.2).

For both dynamic compression and dynamic shear, TIMP2 and TIMP3 expression levels in the explant periphery were only 30-60% of the center region expression levels (Figure 5.2). In contrast, TIMP1 expression was greatest in the explant periphery by almost 200% in response to static compression, and 50% in response to dynamic compression (Figure 5.2). β-actin transcription was greatest in the explant periphery by 50% in response to static or dynamic compression and greatest in the central region by 35% in response to dynamic shear (Figure 5.2), suggesting β-actin should not be used as a housekeeping gene. Transcription factors Sox9 and c-Fos were greatest in the central region by 20-50% in response to all three loading types (Figure 5.2). c-Jun showed the opposite response being increased in the explant periphery by greater than 100% during all three loading types (Figure 5.2). COX2 expression mirrored that of MMP3, with a relatively increased expression in the explant periphery during static compression, but increased expression in the center region during dynamic compression and dynamic shear (Figure 5.2).

5.3.2 Clustering Analysis

To determine the similarity between gene responses, the relative transcription levels in Figure 5.2 are displayed together in the three dimensional plot in Figure 5.3. Each coordinate is the ratio of the relative mechano-induced expression in the ring compared with the explant center. The expression profiles of MMP9 and c-Jun appeared distinct from all other genes, being increased in the ring in response to dynamic shear. Four groups of genes were obvious from Figure 5.3, and Euclidean distance based *k*-means clustering was used to confirm the groupings

and calculate group centroids (Figure 5.4). Each group was statistically distinct from all other groups ($p = 5x10^{-7}$ to 0.032).

Group 1 contained genes that showed increased expression in the ring versus the center in response to static and dynamic compression (~50%), with reduced expression in the ring by 18% in response to dynamic shear (Figure 5.4). Most matrix proteins were in Group 1, as well as β-actin and MMP1 (MMP1 actually showed no radial dependence). The radius dependent expression pattern of Group 2 was very similar to Group 1, except that the expression in the ring was much greater during static compression compared with the dynamic compression (Figure 5.4). Group 2 contained the remaining matrix protein (link protein), and also TIMP1. The common trend of genes in Group 3 was preferential expression in the center region in response to both dynamic loading regimes (Figure 5.4). Group 3 genes had a mixed response to static compression which averaged out to no radius dependence. Group 3 contained genes with a variety of functions; the proteases MMP3 and ADAMTS4, catabolic signaling molecule COX2, two of the TIMPs (TIMP2 and TIMP3), a matrix protein not typically found in cartilage (type I collagen) and transcription factors Sox9 and c-Fos. Group 4 contained MMP13 and ADAMTS5 which like Group 2, showed a large differential expression in the ring versus center in response to static compression; however, Group 4 showed no radial preference in response to dynamic compression, and showed reduced expression in the ring (by 40%) in response to dynamic shear, similar to Group 3.

Figure 5.3: (next page) Three dimensional plot of the ring versus center gene expression levels in response to three loading regimes. Also shown for just static and dynamic compression. Agg = aggrecan, Col1 = type I collagen, Col2 = type II collagen, FM = fibromodulin, FBN = fibronectin, AD = ADAMTS.

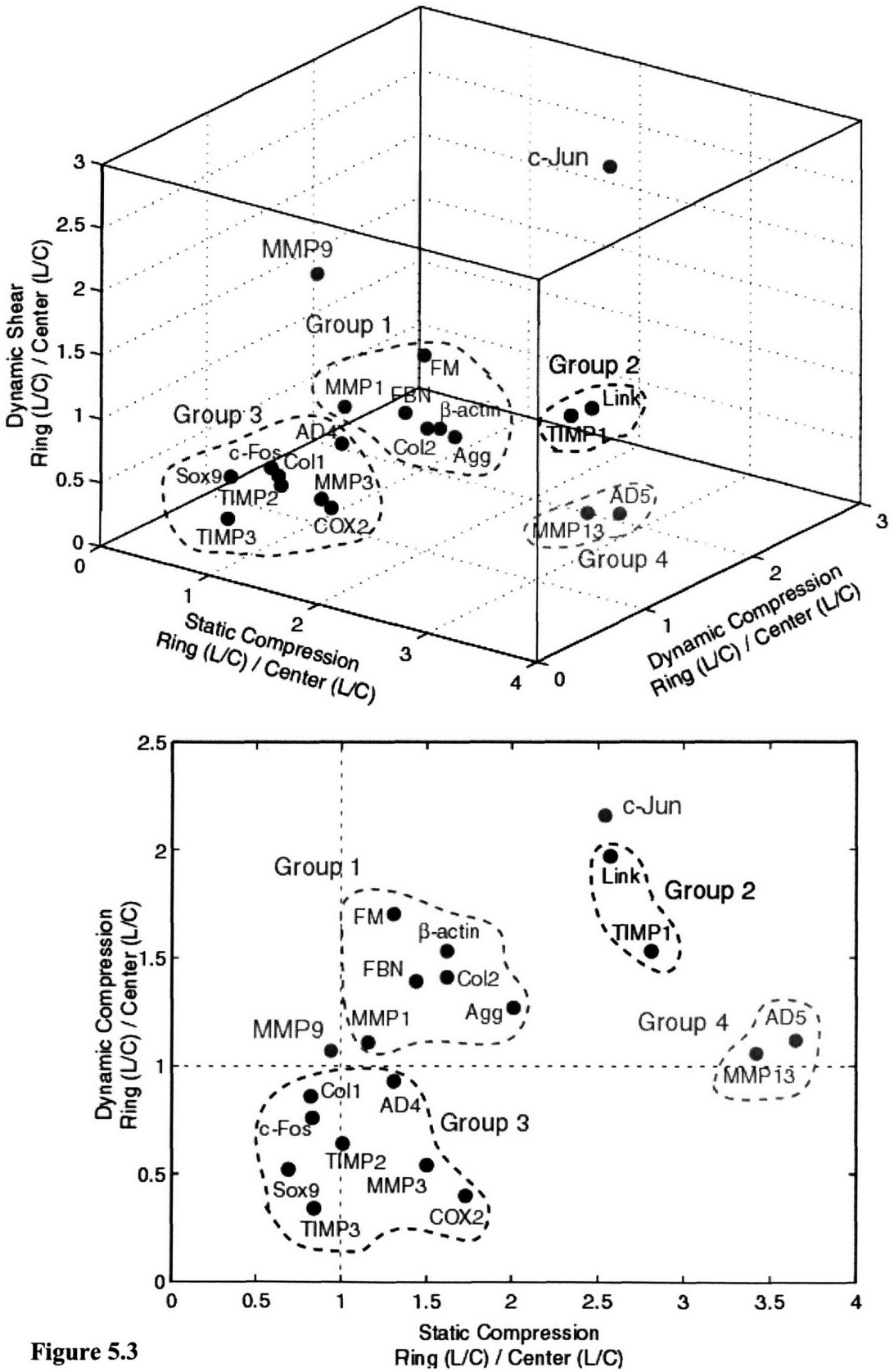
c-Jun
MMP9
Group 1
FM
MMP1
FBN
β-actin
Group 2
Link
TIMP1
Group 3
AD4
c-Fos
Col1
Col2
Agg
Sox9
MMP3
TIMP2
AD5
COX2
MMP13
TIMP3
Group 4
Dynamic Shear
Ring (L/C) / Center (L/C)
Static Compression
Ring (L/C) / Center (L/C)
Dynamic Compression
Ring (L/C) / Center (L/C)
Dynamic Compression
Ring (L/C) / Center (L/C)
Static Compression
Ring (L/C) / Center (L/C)

Figure 5.3

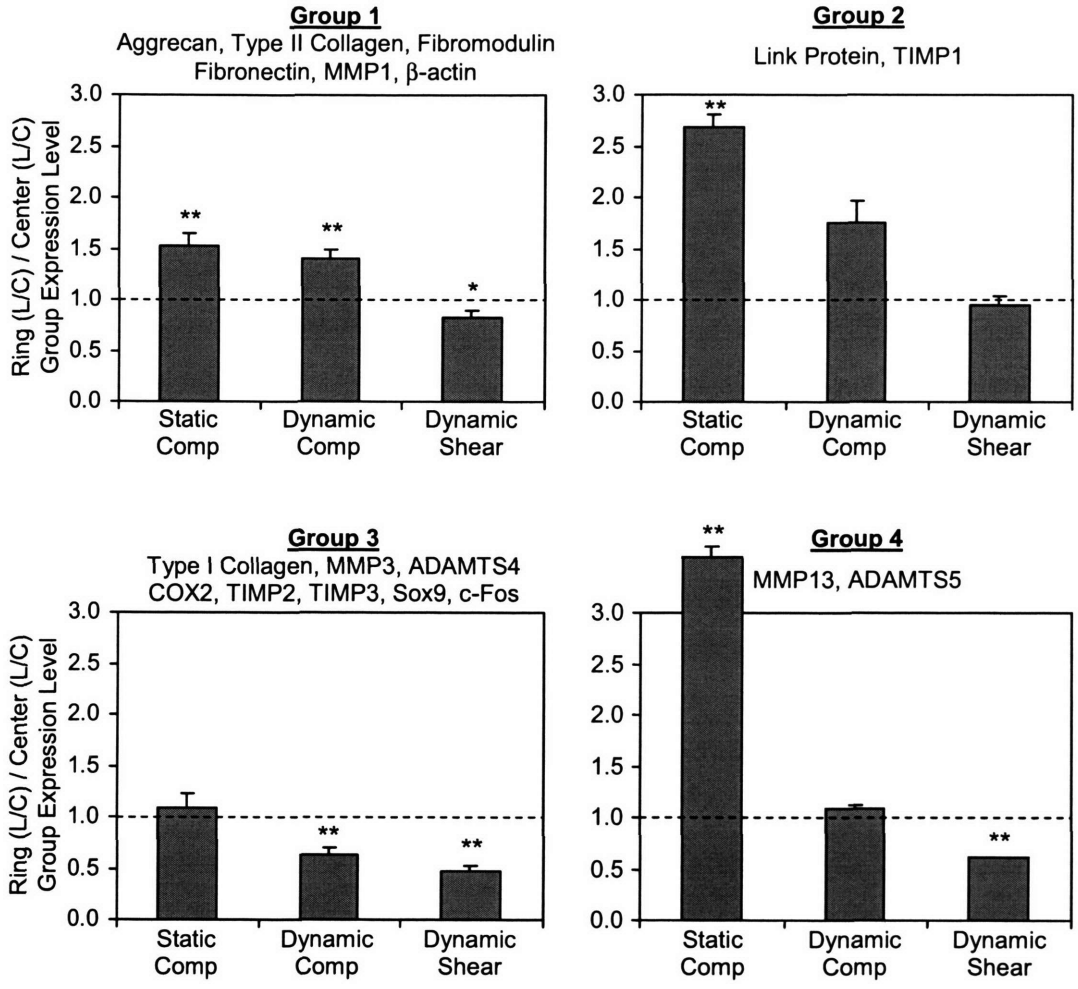

Figure 5.4: Main ring versus center gene expression trends in response to static compression, dynamic compression and dynamic shear. * $p < 0.05$ only, ** $p < 0.001$

5.4 Discussion

We and others have previously shown that chondrocytes regulate gene expression and biosynthesis in cartilage explants in response to a variety of mechanical stimuli (Figure 3.7)[22,26-28,31,33,55-57]. Here we have examined the effects of three mechanical loading regimes by comparing mechano-induced gene expression in both the periphery and central regions of cartilage explants. We found that many genes exhibited regulation that was radius dependent and was also specific to the type of loading applied. Using clustering analysis we showed that the radius dependence of matrix proteins in response to compression was distinct from that of matrix proteases, with matrix proteins preferentially expressed in the periphery of the explant and matrix proteases preferentially expressed in the explant center.

The mechanical environment experienced by a chondrocyte *in vivo* is a complex combination of transient and static, stresses and strains. Researchers model these physical forces by using defined explant geometries and feedback controlled precision loading devices [25,29,48,56]. The static compression model applies a ramp displacement which is held throughout the compression timecourse in a radially unconfined geometry [22]. The strain is usually applied over the course of 5–10 minutes, in contrast to injury experiments where 50% compression is applied in 0.5 seconds [22,24]. The imposed strain results in immediate tissue pressurization (highest in the explant center), followed by radially-directed fluid flow (greatest at the explant periphery). These phenomena last for about 15-30 minutes [22], after which the explant returns to the original tissue pressure and is described as a consolidated equilibrium (reviewed in [1]). Although the physical effects of the initial compression are transient it is postulated that the biological effects may last much longer. A 50% static compression is known to induce a transient increase in matrix protein gene expression, lasting about 4 hours, before decaying to the suppressed equilibrium levels characteristic of biosynthesis responses (Figure 2.2)[56,57]. The same compression mode also activates ERK1/2 and p38 phosphorylation within 10 minutes, an affect that takes greater than 24 hours to return to original levels [65]. In our current experiments aggrecan and type II collagen mRNA levels, although suppressed by static compression, were preferentially expressed in the peripheral region of the explant (Figure 5.2). Similar results have been observed for aggrecan biosynthesis [33,34,147]. Taken together these results suggest that the transient hydrostatic pressures and radial fluid flows induced by static compression may differentially regulate matrix protein transcription.

The dynamic compression loading regime is used to imitate walking and exercise with compression usually applied at a frequency between 0.1-1Hz [27,29,33]. Within this frequency range cartilage behaves as a poroelastic tissue becoming stiffer with frequency [149], hence only small strains (1-5%) are applied on top of a constant strain offset (to ensure contact throughout the compression cycle). Models describing the stresses and strains induced by dynamic compression predict that the hydrostatic pressures and radial strains are greatest in the explant center, and that fluid flow velocity non-linearly increases towards the explant periphery [34,35]. At very low frequencies, 0.01Hz, there is less radial variation in fluid flow velocity or aggrecan biosynthesis [33,34]. Buschmann et al hypothesized that there was a threshold radial fluid flow velocity required to upregulate aggrecan biosynthesis [34]. We found increased transcription of

matrix proteins at the explant periphery in response to dynamic compression (Groups 1 & 2, Figure 5.4), particularly for aggrecan and type II collagen (Figure 5.2), which suggests that there might exist a threshold radial fluid flow velocity required to enhance matrix protein transcription. Combining the observations from static and dynamic compression it appears that hydrostatic pressures might inhibit matrix protein gene transcription and/or that radial fluid flow might enhance transcription. Our previous results showing similar expression profiles of matrix protein transcription and biosynthesis between dynamic compression and dynamic shear (Figure 3.7)[33,55,81] suggests that matrix deformation is the dominant physical factor regulating transcription.

The roles of hydrostatic pressure, radial fluid flow, and radial strain in the explant system can be further delineated by examining the group profile responses to static and dynamic compression. In isolated chondrocytes, aggrecan transcription, synthesis or promoter activity, is known to increase in response to transient pressure-induced-strain [58], fluid flow induced shear [61,67], and cyclic hydrostatic pressure [42-44]. However, in our explant model transcription of aggrecan and other matrix proteins (Group 1, Figure 5.4), was greatest in the peripheral area of the explant where only the fluid flow velocity induced by compression is greatest. This suggests that hydrostatic pressure, fluid flow and matrix strains may have different capabilities for influencing matrix protein gene expression within cartilage explants, and/or that the relative magnitude of the strains, pressures and fluid velocities within an explant dictates the overall response. Furthermore the effects of these factors may be gene specific. Link protein and TIMP1 (Group 2, Figure 5.4) exhibited a much stronger radial dependence in response to static compression (compared to dynamic compression), perhaps due to larger strains, pressures and fluid flows that would be transiently generated. Similarly matrix proteases MMP13 and ADAMTS4 (Group 4, Figure 5.4), had radius-dependent responses only to static compression, and not dynamic compression indicating that the time varying nature of the physical factors is important. In isolated chondrocytes MMP3 transcription has been shown to decrease in response to transient cyclic pressure-induced-strain [58]; however, in our experiments dynamic compression promoted MMP3 in central regions where the radial strains and hydrostatic pressures were greatest. In contrast MMP3 was greatest in the periphery in response to static compression. In general there were many genes (Group 3, Figure 5.4) that were expressed higher in the central region of the explant in response to dynamic compression and this may indicate

sensitivity to hydrostatic pressure gradients. These gene-specific radius-dependent responses to mechanical loading suggest that hydrostatic pressures, fluid flows, and matrix deformation are all detected by the chondrocyte. Therefore, it must be that intracellular signaling processes convert and combine these factors into complex biological responses.

An unexpected result of our study was the radial dependence of dynamic shear induced transcription (Figure 5.4). The dynamic tissue shear applied in this study is a simple shear that should induce minimal fluid flow [55]. There are no induced volume changes and so only minor hydrostatic pressure gradients will occur at the edges of the explant, hence, there should be minimal radially varying physical phenomena [55]. We have demonstrated that although dynamic compression enhances diffusion of macromolecules, such as IGF1, into explants [81], dynamic shear does not enhance diffusion, suggesting minimal fluid flow is occurring [150]. We have previously shown radially-constant biosynthesis of aggrecan and type II collagen when comparing center and peripheral regions, but also observed a small radius-directed decline in aggrecan biosynthesis in autoradiographic studies [55]. However, in our current dynamic shear experiments we observed greater expression in the explant center for Groups 1,2 and 4 (Figure 5.4), and greater expression in the peripheral region for MMP9 and c-Jun (Figure 5.2). Common control conditions were used for all loading types to ensure all genes were being normalized identically between loading conditions. Therefore, we propose that the observed radial dependence induced by dynamic shear may be a result of hindered diffusion of growth factors and cytokines produced by the chondrocytes. The synthesis of growth factors and cytokines (i.e. TNFα, IGF1, IL1, IL4) by chondrocytes within the cartilage explant would generate a chemical gradient with these factors being released into the surrounding media, resulting in relatively higher concentrations being present in the explant center, which could cause a differential transcriptional response. Dynamic shear does not enhance diffusion, hence the gradient would remain throughout loading. Dynamic compression would be expected to enhance diffusion and reduce any such gradients, whereas static compression might also generate autocrine/paracrine diffusion gradients. Hence, isolating the effects of physical forces may be confounded by the presence of chemical gradients.

Using the cartilage explant model we have associated physical stimuli induced by mechanical loading with radius-dependent changes in gene transcription. Our current study has demonstrated that matrix protein gene transcription is regulated by static and dynamic compression, with

greatest expression in the explant periphery, where fluid flow velocities are greater. We have also shown that matrix proteases, TIMPs and transcription factors are differentially expressed in explant regions containing either hydrostatic pressure or radius-directed fluid flow. The identification of roles for isolated physical forces was complicated by suspected chemical gradients and further studies will focus on quantifying the presence and role of such signaling mechanism in intact cartilage.

Chapter 6

Concluding Remarks

Cartilage homeostasis is regulated by mechanical forces and becomes unbalanced following injury and during the progression of osteoarthritis. The objectives of this thesis were to quantify temporal gene expression changes in chondrocytes within their native extracellular matrix, induced by mechanical loading conditions that represent components of *in vivo* loading, and to associate mechanically-induced changes in gene transcription with intracellular signaling pathways.

In Chapter 2 we showed the widespread regulation of chondrocyte gene expression (matrix proteins, proteases, TIMPs, transcription factors, cytokines and growth factors) by static compression using real-time PCR and clustering analysis techniques. Gene expression profiles of matrix proteins were regulated by the magnitude and duration of compression, being transiently upregulated and then suppressed below control levels. Matrix proteases exhibited a distinctly different expression pattern and were upregulated with compression duration. Therefore, in support with previous biosynthesis studies we have shown that catabolic processes dominate over anabolic processes during static compression and that this response is time dependent.

The expression patterns induced by dynamic compression and dynamic shear, discussed in Chapter 3, demonstrated that chondrocyte transcription was load-dependent. Dynamic compression increased the transcription of matrix proteins and proteases with increasing duration, confirming that the time varying components of mechanical loading are also signaling mechanisms. Dynamic shear preferentially increased matrix protein transcription, suggesting that cyclic matrix deformation is an anabolic stimulus for cartilage tissue. In Chapter 5 the roles of hydrostatic pressure gradients and radial fluid flows (in conjunction with matrix deformation), were compared by sectioning cartilage explants into regions where distinct physical stimuli were

occurring. In general, the results from static compression and dynamic compression studies showed that regions with higher fluid flow velocities promote matrix protein transcription, and regions with higher hydrostatic pressures promote matrix protease transcription. Comparison of the expression profiles induced by the three different loading types indicates that the overall direction of transcription is regulated primarily by the type of matrix deformation applied.

The time dependent expression profiles generated from the loading conditions described in Chapters 2 and 3 were used to identify intracellular signaling molecules involved in the mechanotransduction pathway. Chelation of intracellular calcium prevented the upregulation induced in matrix proteins, proteases, TIMPs, and transcription factors in response to static and dynamic compression, and in particular dynamic shear, suggesting that intracellular calcium release is an early step in the pathway that regulates chondrocyte transcription in response to matrix deformation. The activation of protein kinase A by cAMP both suppressed and enhanced certain genes in response to mechanical loading, suggesting that the cAMP pathway may play a modulating role in mechanotransduction. Chapter 4 describes our discovery that the phosphorylation of MAPKs, ERK1/2 and p38, was necessary for the transcriptional regulation of most genes we investigated in response to all three loading types. The similarity in genes regulated through intracellular calcium release and the MAPK pathway suggests a hierarchical relationship.

In addition to signaling cascades activated by mechanical loading we have found evidence suggesting that chondrocytes may respond to mechanical loading by synthesizing signaling factors. We measured the immediate but transient increase in mRNA levels of transcription factors c-Fos and c-Jun in response to all three loading types. It is known that c-Fos and c-Jun (which form activating protein 1) are regulated by the MAPK, and that activating protein-1 binding sites are found in matrix protease and catabolic signaling molecule promoter regions. Furthermore, the transient response of c-Fos and c-Jun was greatest in response to static compression, similar to the long term upregulation of matrix proteases. The prevention of protein synthesis during static compression, greatly suppressed the mechano-regulation of matrix proteins, proteases, and transcription factors (Chapter 4), suggesting that signaling molecules are synthesized by chondrocytes in response to mechanical forces.

Our observations are described pictorially in Figure 6.1. A surprising discovery of this thesis was that matrix proteins and proteases were regulated by the same intracellular signaling

pathways. Future experiments will hopefully identify signaling molecules that are responsible for the distinct expression trends induced by mechanical loading. In addition, the intracellular signaling pathways activated by static compression were also utilized by dynamic compression and dynamic shear; therefore, it remains for future researchers to identify force-specific receptors and signaling events. Our dynamic shear experiments induced radius-specific gene expression patterns which was unexpected and suggests that future models of cartilage mechanotransduction will need to incorporate spatial gradients of autocrine/paracrine signaling factors in addition to physical stimuli.

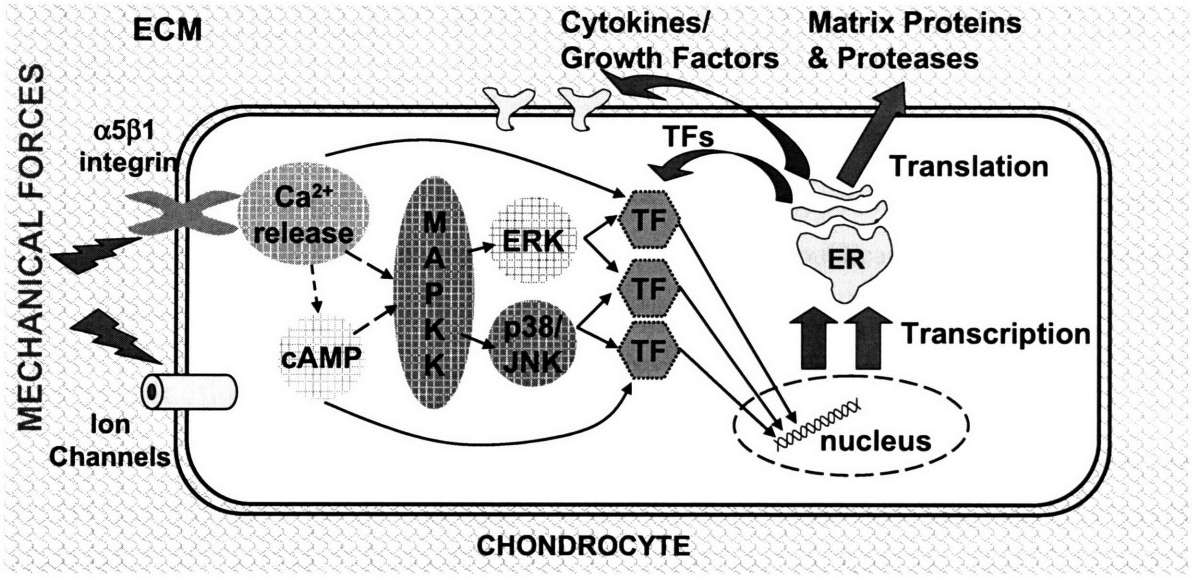

Figure 6.1: Schematic of the chondrocyte mechanotransduction pathway. TF = transcription factors, ECM = extracellular matrix. α5β1 integrin, stretch activated ion channels and protein synthesis were included based on pre-existing literature. Dashed lines indicate speculated relationships. Red arrows indicate fast feedback signaling mechanisms. Blue arrows indicate anabolic and catabolic metabolic outputs.

Appendix A

Effect of Injurious Loading and Co-culture on Chondrocyte Gene Expression

The following section describes the clustering analysis for the injury and co-culture experiments performed by Jenny Lee. (Adapted from [119], and accepted for publication in part in *Arthritis & Rheumatism*).

A.1 Introduction

Acute joint injury increases the risk of developing osteoarthritis [73-75]; however, the mechanisms leading to cartilage degradation are not fully understood. Injurious mechanical compression of cartilage explants is known to damage the extracellular matrix, leading to increased water content [24,151,152], decreased mechanical stiffness [24,152], and increased hydraulic permeability [24,83,152-156]. In the days following mechanical injury GAG and collagen fragments are released into culture medium [24,82,83,153,155,156]. Clinical studies have shown elevated levels of MMP3 and TIMP1 from 1 day to 20 years following a joint injury [157,158], and inflammatory cytokines TNFα and IL-1β are upregulated during the first week of an injury and decrease to levels seen in chronic arthritis after three weeks [15]. However, it is still not clear through which pathways a mechanical injury is transduced into a complicated biological response such as osteoarthritis (OA).

After acute joint injuries the synovial fluid within the knee joint contains increased levels of matrix proteases [9] and inflammatory cytokines [15], however the origin of these factors is unknown. The synovium is known to express matrix proteases, MMP3 and ADAMTS5, and IL-

1β [159,160]. Co-culturing cartilage with synovium decreases matrix biosynthesis [161,162], with synergistic decreases following joint injury [162]. Therefore, the synovium may play an active role in signaling cartilage degradation following injury.

There is little knowledge regarding the changes in gene transcription induced immediately after an acute joint injury. The objectives of this study were (1) to quantify the effects of *in vitro* mechanical injury on 21 genes central to cartilage maintenance, including genes encoding macromolecules of the extracellular matrix (ECM), proteases that can cleave ECM proteins and their natural inhibitors, transcription factors, and cytokines known to affect cartilage metabolism; (2) to determine if co-culture of cartilage with joint capsule tissue including synovium can selectively affect chondrocyte gene expression; (3) to determine the effects of injurious compression on gene expression in co-cultured cartilage.

A.2 Methods

A.2.1 Tissue Harvest

Articular cartilage explants were harvested from the femoropatellar grooves of 1-2 week old calves using previously developed methods [22]. In brief, 9 mm diameter cartilage-bone cylinders were drilled perpendicular to the cartilage surface. These cylinders were then placed in a microtome holder and the most superficial ~200 μm layer was removed to obtain a level surface. Up to three sequential 1 mm slices were cut from each cylinder, and 4 explant disks (1 mm thick, 3 mm diameter) were cored from each slice using a dermal punch, producing 48 explants in total from each joint. Joint capsule tissue was cut from the medial side of the joint immediately proximal to the articular cartilage. Full thickness samples consist of fibrous tissue with a single layer of synovial tissue on the cartilage facing side. Joint capsule tissue was cut into 36 pieces ~5 mm square using a razor. Cartilage explant disks and joint capsule samples were then equilibrated separately in culture medium for 2 days (low glucose DMEM supplemented with 10% fetal bovine serum, 10mM HEPES buffer, 0.1mM nonessential amino acids, 0.4mM proline, 20μg/ml ascorbic acid, 100U/ml penicillin G, 100μg/ml streptomycin, and 0.25μg/ml amphotericin B).

A.2.2 Injurious Compression & Co-culture Treatment

Injurious compression was performed using a custom-designed incubator-housed loading apparatus [25] to injuriously compress cartilage explants as described previously [24,83,156]. The injury protocol consisted of a single unconfined compression displacement ramp to a final strain of 50% at a velocity of 1 mm/s (strain rate 100%/s under displacement control), followed by immediate removal of the displacement at the same rate. Application of this strain resulted in an average peak stress of ~20 MPa and has been shown previously to result in cell death and tissue matrix damage when applied to similar bovine cartilage explants [24,83,152,154,156]. Injured explants were immediately returned to culture medium and incubated for up to 24 hours, with or without joint capsule present. For co-culture samples, cartilage tissue (injured or non-injured) was cultured in the same well of a tissue culture plate with a piece of joint capsule tissue for the duration of the experiment. The two pieces of tissue were not in direct contact during culture. Cartilage maintained in free swelling culture without joint capsule tissue served as controls for each experiment.

Groups of 6 cartilage explants from an experimental treatment group were removed from culture at 1, 2, 4, 6, 12, and 24 hours, flash frozen in liquid nitrogen, and stored at -80°C. Groups of 6 free swelling explants were frozen at 4 and 24 hours to serve as controls. For each experiment, explants in each treatment or control group were purposely matched across depth and location along the joint surface to prevent bias based on location; as a result, each experimental condition represents an average of specimens within the femoropatellar groove.

A.2.3 RNA Extraction & Real-time PCR

RNA was extracted from the 6 pooled cartilage explants by first pulverizing the tissue and then homogenizing in Trizol reagent (Invitrogen, CA) to lyse the cells. Extracts were then transferred to Phase Gel Tubes (Eppendorf AG, Germany) with 10% v/v chloroform and spun at 13,000g for 10 min. The clear liquid was removed from above the phase gel and RNA was isolated from the sample using the RNeasy Mini Kit (Qiagen, CA). Genomic DNA was removed by a DNase digestion step (Qiagen, CA) during purification. Absorbance measurements were read at 260 nm and 280 nm to determine the concentration of RNA extracted from the tissue and the purity of the extract. The average 260/280 ratio of absorbencies was 1.91±0.10. Reverse

transcription (RT) of equal quantities of RNA (25 ng per µl RT volume) from each sample was performed using the Amplitaq-Gold RT kit (Applied Biosystems, CA).

Real-time PCR was performed using the MJ Research Opticon 2 instrument and SYBR Green Master Mix (Applied Biosystems, CA). Primers were designed for matrix molecules (collagen II, aggrecan, link protein, fibronectin, fibromodulin, and collagen I), proteases (MMP-1, MMP-3, MMP-9, MMP-13, ADAMTS-4, ADAMTS-5), protease inhibitors (TIMP-1, TIMP-2), cytokines (TNF-α, IL-1β), housekeeping (β-actin, GAPDH), transcription factors (c-Fos, c-Jun), and growth factor (TGF-β) using Primer Express software (Applied Biosystems, CA). Standard curves for amplification using these primers were generated; all primers demonstrated approximately equal efficiency, with standard curve slopes ~1 indicating a doubling in cDNA quantity each cycle.

In each experiment, expression levels measured in treated sample groups (co-culture with joint capsule or injurious compression followed by co-culture) were normalized to those of free swelling control groups for each gene; expression data are presented as the average of three replicate experiments (+ SE).

A.2.4 Clustering Analysis

To distinguish the main expression trends, a *k*-means clustering algorithm [77,89,90,163] was applied to the combined data set of time course data for expression following injurious compression, co-culture with joint capsule, and injurious compression followed by co-culture. Each gene vector was standardized to emphasize the pattern of expression, as described previously (see Section 2.5). Principal Component Analysis (PCA) was used to visualize the similarity between gene expression profiles in three dimensions. Genes were clustered using two iterative methods: (1) to minimize the Euclidean distance between gene and group center in three dimensional space, or (2) to maximize the correlation between the gene and group profiles using the full length expression vectors. Group profiles were calculated as the average of the expression profiles of the genes in each group. The clustering algorithm was initialized by randomly choosing starting genes and deterministically converged to a final grouping. To ensure that an optimal clustering solution for the twenty-one genes was found, the algorithm was re-run sufficient times to cover every deterministic ending solution. The optimal solution was chosen as the grouping that scored highest under each clustering technique (see Section 2.5 for details).

From inspection of the three dimensional representation the number of groups was varied from three to six, and six groups were chosen to best represent the trends.

A.3 Results

The expression trends induced by injury were remarkably different than those produced by non-injurious loads (Figure A.1 & Figure A.2). Expression of matrix proteases increased dramatically during the 24 hours following injury, for example, MMP3 increased ~ 250 fold and ADAMTS5 increased > 40 fold. c-Fos and c-Jun, which were shown to transiently respond to static and dynamic loading (Figure 3.12), also responded to injury but with a much larger transient increase (40-100 fold within 1 hour). In contrast, transcription of matrix proteins and TIMPs did not significantly change following injury. Injury increased the expression of housekeeping genes GAPDH and β-actin, hence, expression levels were normalized using total RNA absorbance measurements. The presence of joint capsule with or without injury treatment also upregulated matrix proteases MMP3, ADAMTS5, and ADAMTS4 by greater than 10-fold. To highlight the trends induced by injurious loading, and to determine the effects of co-culture with joint capsule tissue, clustering techniques were employed that were described in Section 2.5.

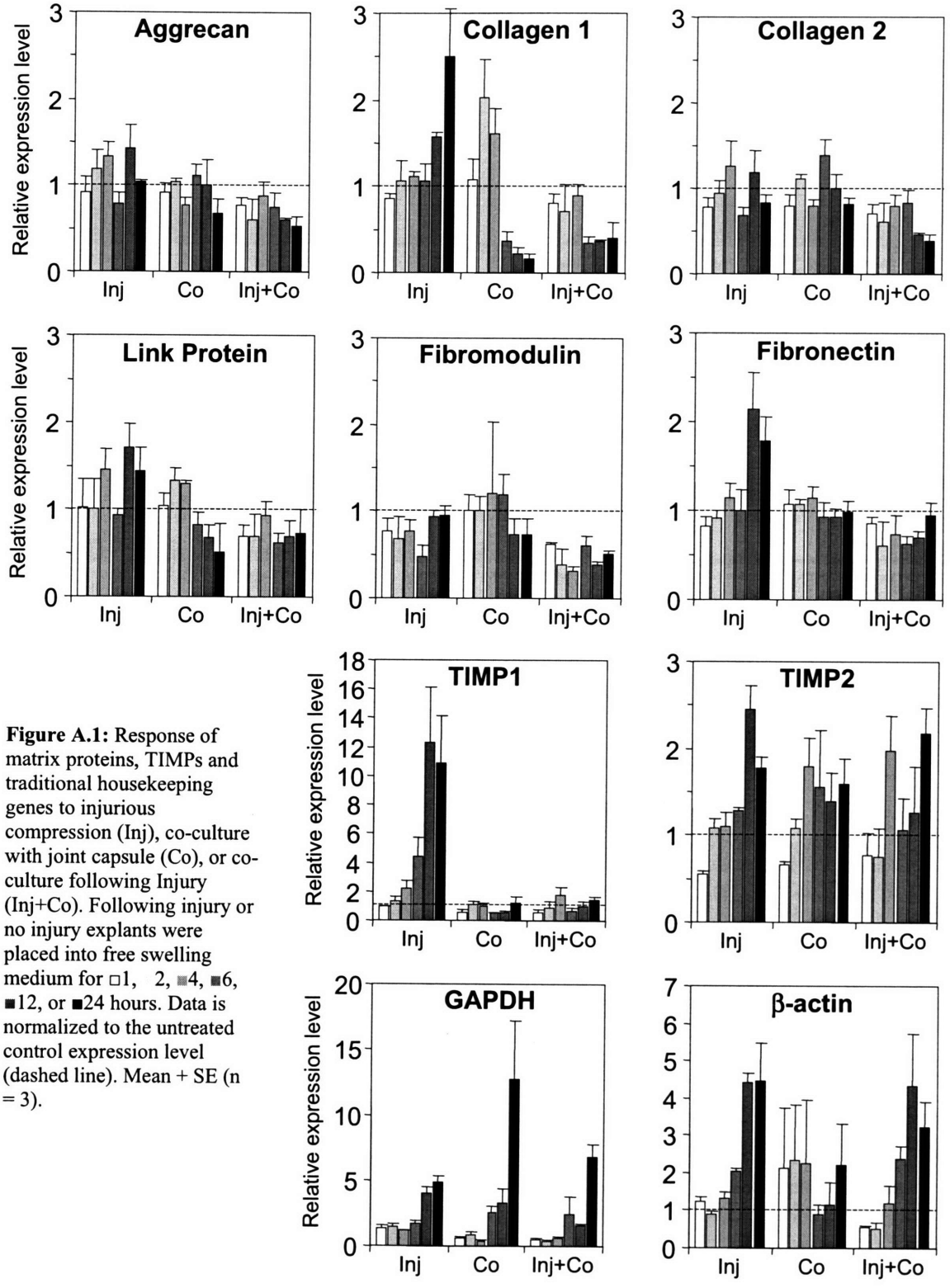

Figure A.1: Response of matrix proteins, TIMPs and traditional housekeeping genes to injurious compression (Inj), co-culture with joint capsule (Co), or co-culture following Injury (Inj+Co). Following injury or no injury explants were placed into free swelling medium for □1, 2, ■4, ■6, ■12, or ■24 hours. Data is normalized to the untreated control expression level (dashed line). Mean + SE (n = 3).

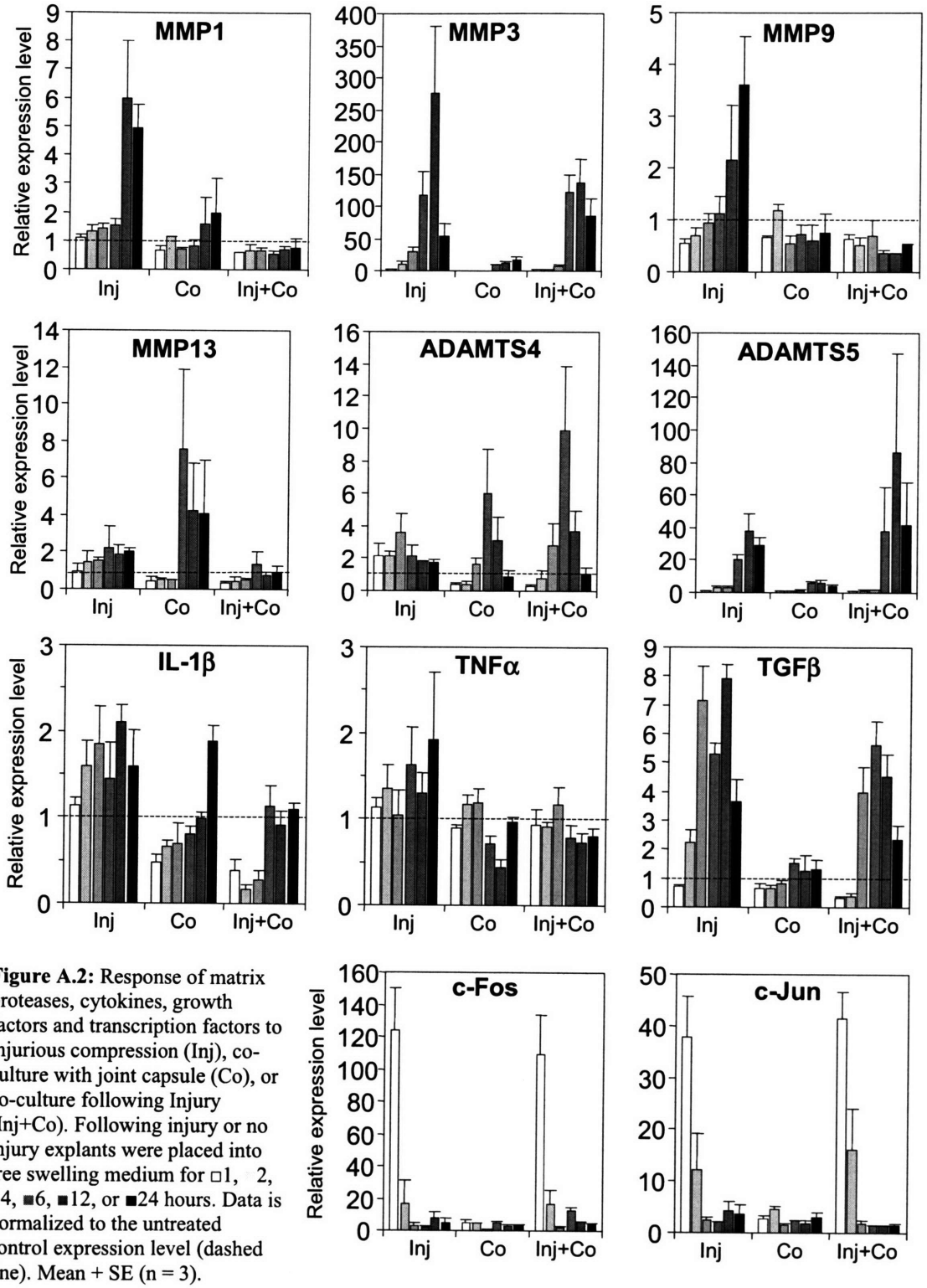

Figure A.2: Response of matrix proteases, cytokines, growth factors and transcription factors to injurious compression (Inj), co-culture with joint capsule (Co), or co-culture following Injury (Inj+Co). Following injury or no injury explants were placed into free swelling medium for □1, ▒2, ▒4, ■6, ■12, or ■24 hours. Data is normalized to the untreated control expression level (dashed line). Mean + SE (n = 3).

A.3.1 Clustering Analysis of Injury & Co-culture Treatments

Principal component analysis of the standardized injury, co-culture, and injury + co-culture data matrix highlighted three principal components which accounted for 72% of the variance (structure) of the data (Figure A.3). The remaining principal components individually accounted for < 8% of the variance each. Principal component 1 (PC1) contained variation due to injury, PC2 contained variation due to injury + co-culture, and PC3 contained early variation due to injury with and without co-culture and late variation due to co-culture alone. The direction of regulation contributed by a principal component depends on the sign of the projection coordinate for each gene.

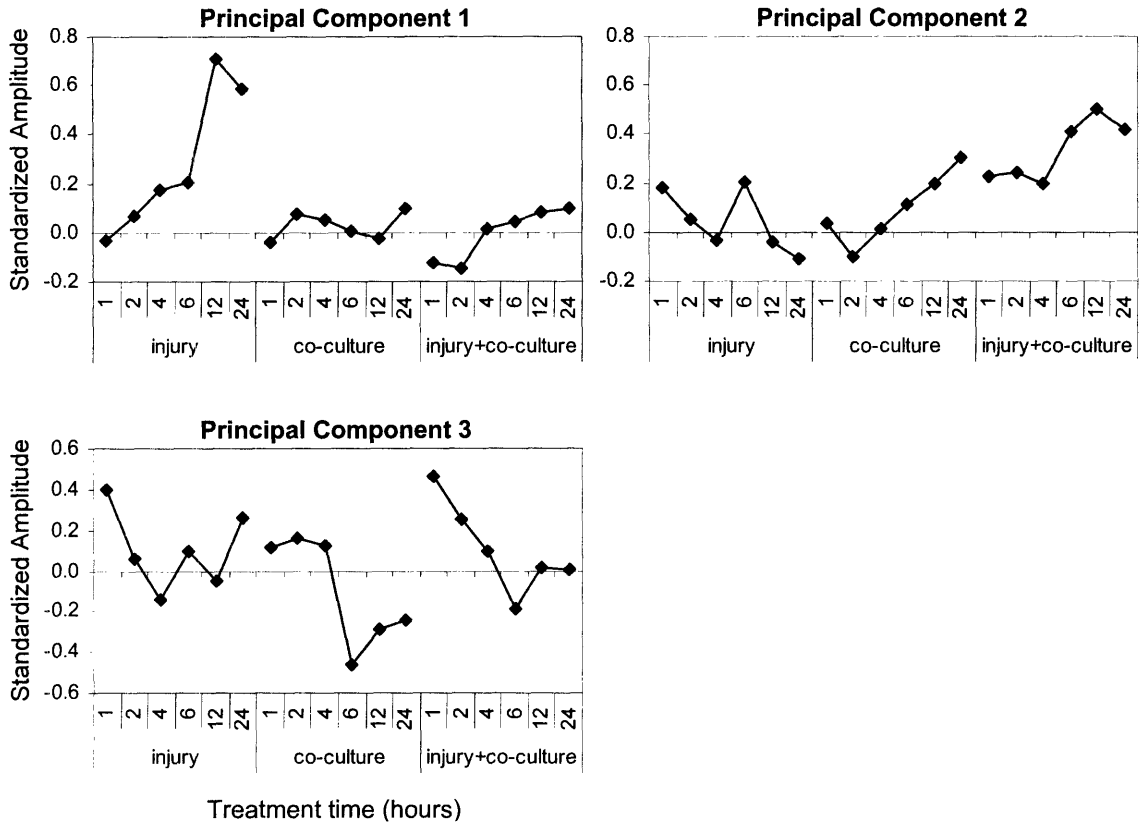

Figure A.3: The three main principal components of the injury, co-culture and injury + co-culture data set. Principal components 1, 2, and 3 account for 35%, 25%, and 12% of the variance in the data respectively. PCA was applied to the entire standardized data set, hence zero on the Y-axis is equivalent to the control level. X-axis is treatment time in hours.

Representation of the gene vectors by projecting along the three main principal components highlighted the trends in expression (Figure A.4). Three distinct groups could be visually isolated (Groups 1, 2, & 3, Figure A.4B). The remaining genes formed a plane that transitioned from large, time-dependent responses to injury with and without co-culture (left side, Figure A.4A), to milder responses to injury without co-culture (right side, Figure A.4A). Applying Euclidean-based, projection-coordinate clustering or correlation-based expression vector clustering produced identical, robust groupings with significantly separated group centroids ($p < 0.02$, Figure A.5).

Group 1 contained matrix proteins aggrecan, type II collagen and fibromodulin, which did not increase in response to injury or co-culture treatment (Figure A.5). Group 2 contained c-Fos and c-Jun which immediately and transiently responded to injury with or without co-culture, with a relatively mild, constant, increase during co-culture alone. Group 3 contained three loosely grouped genes, proteases (ADAMTS4 and MMP13) and GAPDH, which increased with treatment duration. Group 4 contained two matrix proteases (MMP3, ADAMTS5) as well as TIMP2, TGFβ and β-actin, which exhibited a large, delayed increase following injury with and without co-culture. Group 5 contained fibronectin, MMP, TIMP1 and IL-1β, and responded mildly 12 and 24 hours after injury alone. Group 6 contained type I collagen, link protein, MMP9, and TNFα, and exhibited a small response 12 and 24 hours after injury alone. Group 6 genes were also significantly down regulated when placed in co-culture after injury. Reducing the number of groups to 5 combined groups 5 and 6 and also represents the trends well.

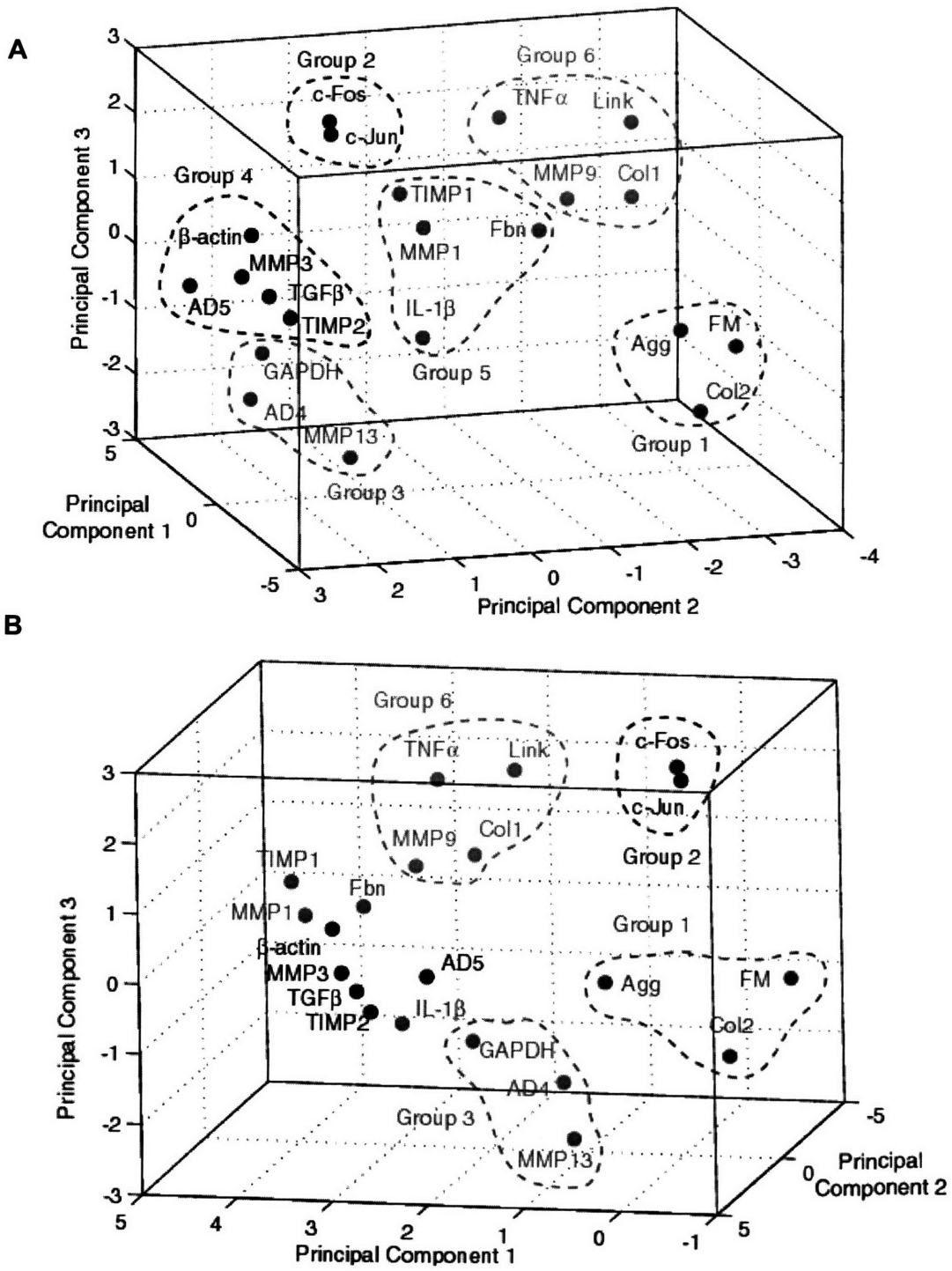

Figure A.4: 3D representation of the injury, co-culture & injury + co-culture data set. Each gene projection coordinates was found by projecting the gene expression vector onto the 3 main principal components found by PCA. Two views are shown to add depth to the 3D plot (i.e. clustering of c-Fos & c-Jun). The axes represent the weighting of each principal component. Abbreviations Agg, aggrecan; Col, collagen; link, link protein; FM, fibromodulin; Fbn, fibronectin; AD, ADAMTS

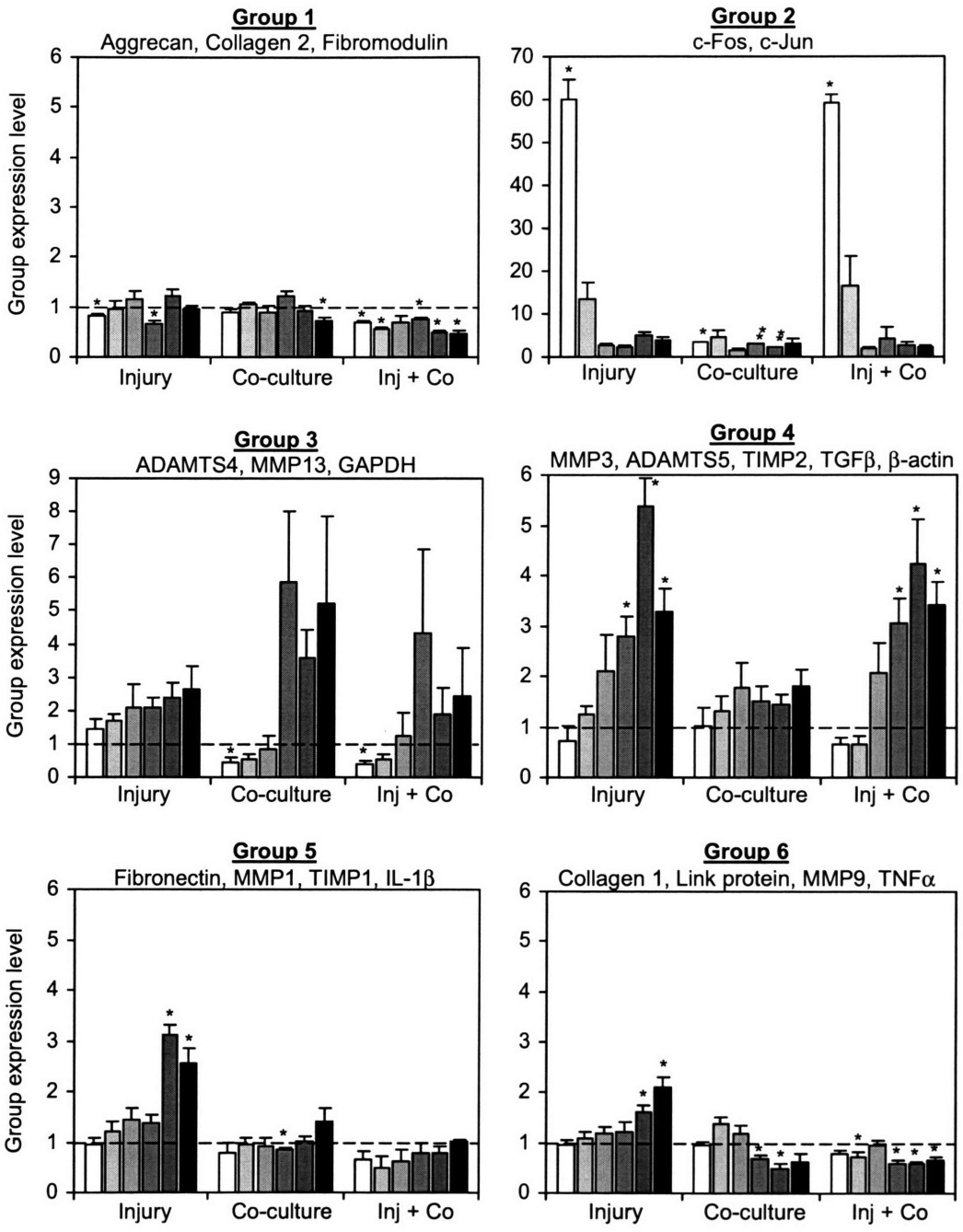

Figure A.5: Main expression trends induced by injury with and without co-culture. Genes were clustered using two separate *k*-means clustering algorithms, either minimizing the Euclidean distance between gene and group center projection coordinates, or maximizing the correlation between gene and group expression vectors. Following injury or no injury disks were placed into free swelling medium for □1, ▒2, ▒4, ■6, ■12, or ■24 hours. Group expression profiles are the average of the gene expression profiles in each group. Normalized to free swelling expression level (dashed line). Mean + SE (n = the number of genes in a group).

A.4 Discussion

A single injurious compression of cartilage decreases extracellular matrix biosynthesis rates, compromises mechanical properties, and reduces chondrocyte viability [24,83,152,155,156]. Co-culture of cartilage tissue explants with joint capsule or synovial tissue has been shown previously to result in decreased chondrocyte biosynthesis rates and loss of type II collagen and aggrecan from the tissue extracellular matrix [161,162,164]. We undertook this study to determine if mechanical injury, or co-culture in joint capsule tissue, or the combination, resulted in changes in gene expression levels in chondrocytes. Real-time PCR analysis was used to measure the gene expression of 21 molecules involved in both cartilage production and degradation at six time points over the course of 24 hours. Using clustering analysis we identified significant changes in responses to each of the different injury models for several molecules.

A.4.1 Effects of Injury & Co-culture on ECM Proteins

Aggrecan and type II collagen (Group 1) were unaffected by injurious mechanical loading. In fact all matrix proteins were located in groups that had no (Group 1) or marginal (Groups 5 & 6) responses to injury. This is in stark contrast to the effects of static and dynamic loading on matrix protein gene transcription (Chapter 2 & Chapter 3), and may indicate that stimuli of longer duration are required to activate anabolic gene transcription, or that enhanced matrix production is a delayed response (which is characteristic of OA). Furthermore immediate decreases in ECM biosynthesis that may result from mechanical injury [24], are unlikely to be related to events at the level of matrix gene transcription (i.e. chondrocyte viability).

Co-culture with synovium resulted in decreased proteoglycan biosynthesis rates in cartilage (measured by $^{35}SO_4$ incorporation), when cultured in contact or at a distance from synovium for 8 days. Cartilage biosynthesis was shown to recover after 4 days cultured in isolation following 8 days of co-culture [161]. Mechanical compression injury followed by 6 days of co-culture caused further decrease in incorporation rates of $^{35}SO_4$ and ^{3}H-proline (measure of collagen synthesis), compared to 6 days of co-culture alone [162]. Within the first 24 hours of co-culture with joint capsule tissue, we did not measure a significant decrease in expression levels of collagen II or aggrecan. It remains possible that expression of these molecules is reduced during longer incubation periods. Consistent with a more substantial

reduction in biosynthesis rates during co-culture with joint capsule that followed injurious compression [162], expression of type II collagen and aggrecan were reduced to ~50% of control levels within 24 hours (Group1). In addition, compression injury was found previously to increase fibronectin protein synthesis [151], and the compression injury used here caused an increase in fibronectin gene expression (Figure A.1).

A.4.2 Catabolic Effects of Injury & Co-culture

The matrix proteases produced a range of responses to injury and co-culture treatment and it is interesting to contrast the responses of MMP3 and ADAMTS5 (Group 4) with those of ADAMTS4 and MMP13 (Group 3). The large increase associated with MMP3 in response to injury, compared with MMP13 (Figure A.2) is similar to trends reported previously using Northern analysis of similar cartilage explants subjected to the same injury protocol, suggesting differential regulation of MMP3 and MMP13 [83]. *In vivo* studies of OA progression following joint injury have also reported differential changes in MMP gene expression levels. In contrast, Le Graverand et al. used a lapine ACL transaction model of OA and found 2-3 fold increased chondrocyte expression of MMP3 and 10-30 fold increased expression of MMP13 [165]. In our *in vitro* models of joint injury, the magnitude of the change in expression measured for aggrecanases, ADAMTS-4 and ADAMTS-5, were quite different with large increases measured for ADAMTS-5 expression compared to that measured for ADAMTS-4 (Figure A.2). Interestingly, ADAMTS-5 was recently identified as the primary aggrecanase responsible for cartilage degradation in murine models of OA [166]. Furthermore, Bau et al. [167] compared chondrocytes isolated from patients with normal articular cartilage to chondrocytes from patients with early and late stage OA. MMP13 and ADAMTS4 expression increased in late stage OA, while MMP3 expression was the highest of the genes tested and was downregulated in OA [167]. Lohmander et al analyzed human synovial fluid after ACL or meniscus injury and found increases in MMP3 and TIMP1 protein levels within 1 day after injury that persisted for 20 years [158]. Similarly, increased chondrocyte mRNA levels of MMP3 and TIMP1 were found in our study after cartilage injury (Figure A.1 & Figure A.2) and in the lapine ACL transection model [165]. Therefore, the high levels of MMP3 and ADAMTS5 found here are consistent with the early stages of OA, and the relative absence of a MMP13 or ADAMTS4 transcripts may indicate their role is primarily in later stages of OA.

Early studies have shown breakdown of the extracellular matrix of cartilage when co-cultured with minced synovial tissue. Co-culture resulted in near complete depletion of type II collagen and proteoglycan from the cartilage by 14 days [164]. Here, we measured increased expression of specific matrix proteases in the chondrocytes activated by co-culture with joint capsule tissue (MMP-3, MMP-13, ADAMTS-4, ADAMTS-5) as well as an additional factor activated by co-culture following mechanical injury (TGF-β). These factors may play a role in degrading both collagen and proteoglycan components of the extracellular matrix in these models. The presence of joint capsule following injury did not have a synergistic effect on the expression of Groups 3 & 4 (except perhaps Group 3, 6hrs). This may indicate that both injury and co-culture utilize or saturate the same signaling pathways. In contrast, expression levels of Groups 5 and 6 were suppressed by the presence of joint capsule during injury.

A.4.3 Effect of Injury & Co-culture on Transcription Factors

The dramatic 40-120 fold early increases in c-Fos and c-Jun transcription were much larger than observed under other loading regimes. We have previously shown that 3% strain dynamic compression and dynamic shear mildly and transiently upregulated c-Fos and c-Jun ~ 4-fold and that gradually applied, 50% strain static compression upregulates c-Fos and c-Jun 10-40 fold (Figure 3.12). Taken together these experiments suggest that the magnitude of c-Fos and c-Jun upregulation is related to the magnitude of the initial stress applied to the tissue, more so than the overall strain or cyclic matrix deformation. Matrix proteases also showed increased transcript levels at later timepoints in response to static compression, have milder responses to dynamic compression and dynamic shear (Figure 3.12), and respond with the largest increases to injurious loading. This evidence suggests a role for c-Fos and c-Jun in chondrocyte mechanotransduction and perhaps as a trigger for cartilage degradation towards OA. Furthermore the binding site for activating protein 1 (c-Fos/c-Jun heterodimer) is known to be present in the promoter region of a number of matrix proteases [97,139]. c-Fos and c-Jun (and certain matrix proteases) were also mildly upregulated with joint capsule treatment, with a ~3-fold continued upregulation, suggesting sensitivity to a factor released into the medium. However, c-Fos and c-Jun response to injury with co-culture treatment was very similar to injury alone suggesting a particular sensitivity to injurious mechanical loading.

A.4.4 Conclusion

In summary, injurious compression caused time dependent changes in the transcription of specific catabolic enzymes that can regulate matrix remodeling and turnover, while many extracellular matrix molecules were unaffected. Our study demonstrates specific changes in chondrocyte transcription occur during co-culture with joint capsule tissue. These changes are altered by inclusion of mechanical injurious compression of cartilage before co-culture. It may be possible to separate the effects of soluble factors released from joint capsule tissue from effects of mechanical loading using these *in vitro* model systems. Future studies are planned to measure cartilage degradation and protein levels of specific matrix proteases that respond to mechanical injury and to examine the longer term effects on gene transcription.

Appendix B

Protocols and Procedures

B.1 Accurate Quantification of Mechano-Regulated Gene Transcription

An objective of this thesis was to accurately measure changes in gene transcription for an intermediate sized set of genes. The real-time PCR technique was chosen as initial experiments using standard PCR identified serious limitations.

B.1.1 Quantitative Capacity of Standard PCR

Variability in measurements of gene expression may stem from inter-tissue differences, variations in mechanical loading parameters, RT and PCR enzyme efficiency, as well as pipette volume variations during PCR. The latter are especially problematic considering PCR logarithmically amplifies low copy numbers of cDNA and the following experiments were designed to determine the amount of noise present in the RT and PCR steps. RT and PCR reactions were performed using a two-step protocol and AmpliTaq-Gold reagents (Applied Biosystems, CA) with a standard thermocycler (Mastercycler, Eppendorf). After gel electrophoresis with SybrGold nucleic dye, densitometry was performed using ScionImage Software (NIH). All experiments were performed using genes abundant in cartilage; aggrecan, type II collagen and G3PDH. In order to ascertain the level of variability in the RT-PCR stages, three aliquots from a common RNA pool were reverse transcribed and amplified. Care was taken to ensure that PCR amplification did not extend into the saturation region. The coefficient of variance (CoV) for the three replicates was ~10%, which should allow discovery of mechanically induced changes in gene expression that are greater than 50%.

To accurately measure transcriptional changes it was necessary to calibrate changes in SybrGold band intensity following PCR with the starting amount of cDNA. Aliquots containing

0.25, 0.50 or 0.75μg of total RNA, were reverse transcribed and amplified. This procedure was performed in duplicate, from separate RNA stocks. Band intensity was normalized by the total intensity of the three dilutions for each gene so that the slopes from different genes and samples could be compared. A linear trend of normalized band intensity versus starting RNA content was observed for all genes and samples (Figure B.1AB). The slope in Figure B.1C is less than unity indicating that changes in band intensity underestimate true changes in mRNA level. The observed offset in Figure B.1C is actually a visual artifact due to the logarithmic nature of PCR, hence, the data is better represented on a log-linear plot in Figure B.1D. Both representations have correlation coefficients ~0.98, and average standard deviations of ~6.5%, demonstrating that band intensity and starting RNA transcript numbers are strongly linearly related.

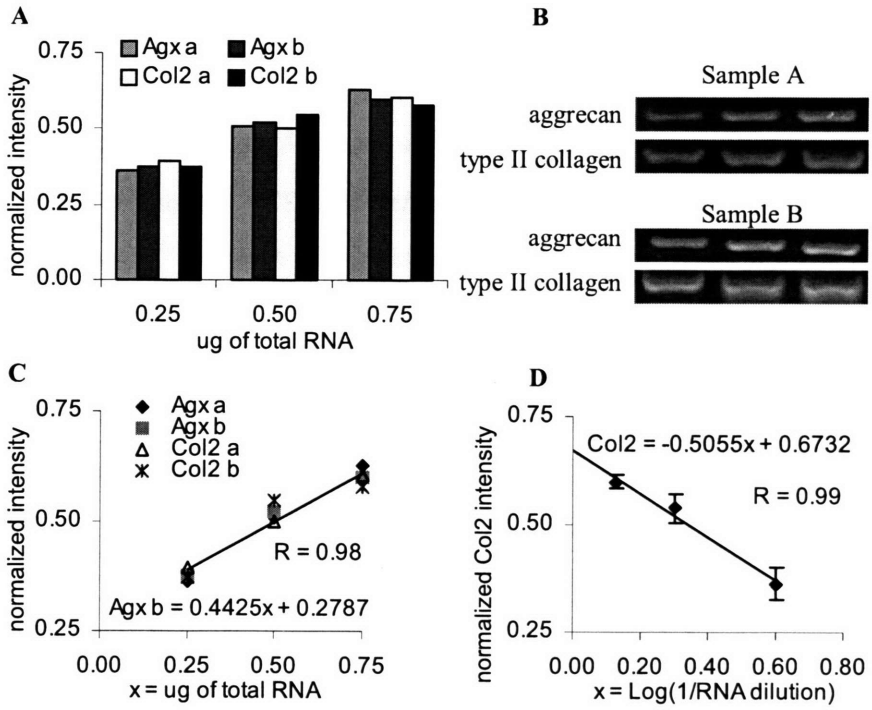

Figure B.1: Comparison between changes in band intensity and starting amount of RNA. The band intensity for each gene was normalized first by dividing by the summed intensity of the three dilutions. A) densitometry values of electrophoresis gels for two genes from two RNA stocks, B) SybrGold electrophoresis gels, C) linear plot of band intensities versus RNA content, D) average type II collagen band intensity plotted against the log of the ratio of 1μg/(μg's of total RNA added).

B.1.2 Normalization Techniques

UV absorbance measurements at 260nm were used to estimate the total RNA content of the two samples in Figure B.1 so that appropriate volumes could be added for the 0.25, 0.50, and

0.75ug aliquots. However, Figure B.1B clearly shows that the aggrecan and type II collagen band intensities were significantly brighter in sample B compared with sample A (similar results were found for G3PDH). Thus the pre-RT-PCR normalization step based on absorbance measurements was inaccurate. This was observed in a number of experiments and it was concluded that absorbance measurements are unreliable for assessing total RNA content in cartilage. This may be attributed to the negatively charged proteoglycans in the ECM, which may also bind to the positively charged silica membrane during RNA isolation (Cynthia Lee, private communication). Alternatively inaccuracies may be due to the small amount of RNA (<5μg) extracted from the tissue. Use of a more sensitive spectrophotometer, or increasing the number of cartilage explants pooled together, may improve the total RNA normalization method. Normalization to housekeeping genes amplified by PCR was selected as a more appropriate normalization method.

B.1.3 Detection of Type II Collagen Mechano-induction using Standard PCR

To determine if standard PCR was sufficiently sensitive to detect mechanically-induced gene expression changes, cartilage explants were compressed by 25% for 2 hours. The experiment was performed in triplicate. Control explants (0% compression) were used to create standard curves containing 0.08, 0.16, 0.24 and 0.32μg of total RNA. Normalization of type II collagen band intensity with housekeeping gene G3PDH band intensity reduced overall sample intensity variation from 25% to 10%, except at the lowest concentration of RNA (0.08μg, x_{axis} = 1.07).

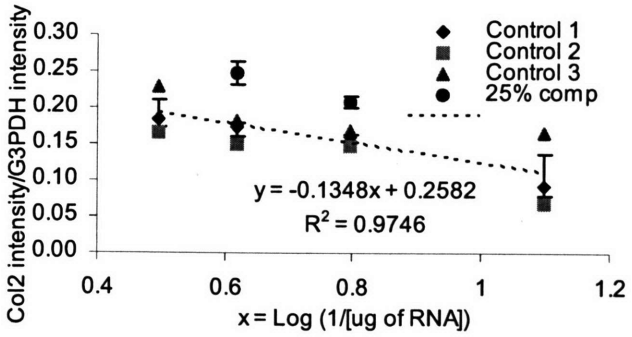

Figure B.2: Regulation of type II collagen after 2hrs of 25% compression measured using standard PCR. Control samples were used to create a standard curve containing 0.08, 0.16, 0.24, 0.32μg aliquots of total RNA (x = 1.1, 0.8, 0.6, 0.5 respectively). 0.16, and 0.24μg aliquots of total RNA of compressed samples were used for comparison. Type II collagen band intensity was normalized against overall G3PDH band intensities.

Although precise estimates of type II collagen transcript level could not be obtained as values were outside the range of the standard curve in Figure B.2, the increase in relative band intensity of ~40% previously associated with 2 hours of static compression was clearly observed. Therefore standard PCR could detect mechano-induced changes in chondrocyte gene expression in cartilage explants.

B.1.4 Improvements using Real-time PCR

Although compression-induced changes in gene expression could be detected using standard PCR, the difficulties encountered during this preliminary study suggested that this technique was not scalable to high throughput analysis. In particular, the less than proportional relationship between band intensity and RNA content limited the range of observable changes and suggested that the CoV was twice that originally measured (20%). Furthermore, ensuring that genes with a range of abundances were not in the saturated region of amplification would be too difficult using standard PCR.

An initial study examining whether real-time PCR could avoid the underestimation observed with standard gel densitometry was performed. In contrast to PCR-gel electrophoresis, real-time PCR machines measure fluorescence at the end of every cycle bypassing cycle optimization and densitometry issues. The threshold cycle number (C_T) is measured as the cycle at which a threshold intensity is reached (see Section B.4.4) and is related to the starting copy number by using appropriate standards for each gene. Primers for a number of genes were redesigned to produce ~100 bp products suitable for real-time PCR. Purified PCR products were used to create five serially diluted standards for which real-time PCR was performed. cDNA obtained from previous samples was amplified as a measure of basal gene expression levels. Appropriate dilutions were then performed to create standard curves centered at basal cDNA levels. The ΔC_T slopes for the standard curves were ~ 1, and indicated primer product doubling in quantity with each cycle, demonstrating the improved sensitivity of real-time PCR. The CoV for repeat measures was ~10%, half the effective coefficient of variance of standard PCR. However, the CoV did increase as the initial transcript abundance decreased. To ensure accurate measurements it is recommended to that only genes which produce C_T values less than 30 cycles are examined.

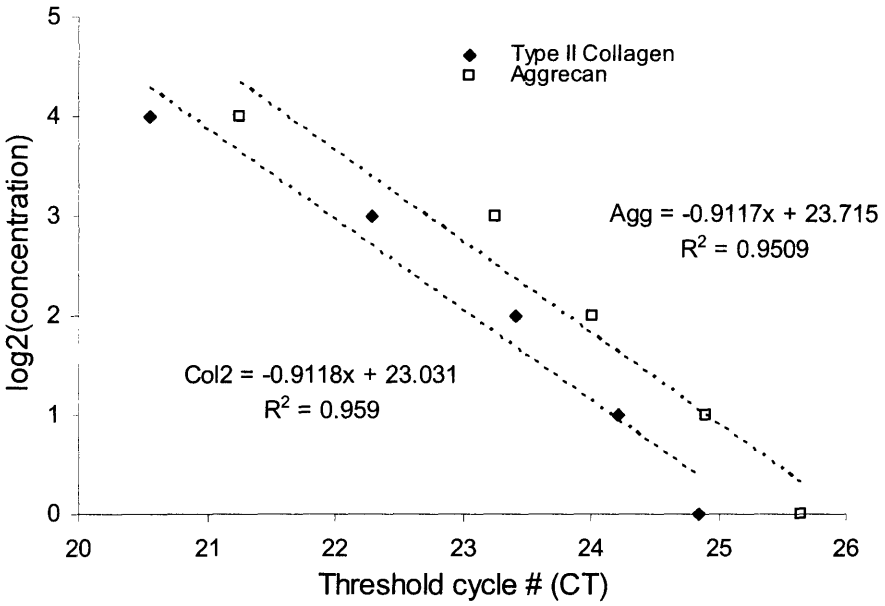

Figure B.3: Real-time PCR standard curves for type II collagen and aggrecan displaying proportional changes between fluorescence and starting copy number.

It was possible that the housekeeping genes were regulated by mechanical loading. Certain loading regimes (injury, or large-amplitude dynamic compression) have been shown to upregulate G3PDH and β-actin 5-6 fold. To determine if the housekeeping genes were affected by the milder mechanical loading applied in this study the following analysis was retrospectively performed. The relative copy numbers of 18S, and G3PDH were obtained from previous experiments, and loaded conditions were divided by unloaded controls. Experiments were averaged with loading type (static compression, dynamic compression, dynamic shear) and duration (short = 1-4 hrs, long = 24 hrs) compared separately. The average loaded/unloaded ratios for 18S and G3PDH were close to unity, with averages between 0.73 – 1.42 for individual loading types and durations, with a typical CoV of 60%. As total RNA measurements were not used during normalization the CoV includes RNA extraction efficiency variations which alone produces a CoV = 40%. Considering both the loaded and unloaded samples contain the RNA extraction variance, the loading induced CoV of ~60% suggests that mechanical loading does not affect the housekeeping genes, certainly not by 5-6 fold. In general 18S performed the best and the average of 18S and G3PDH was useful for minimizing the effects of outliers. β-actin was found to be upregulated 90% by 24 hours of dynamic shear and so was not used as a housekeeping gene.

B.2 RNA Extraction

Immediately following loading completion cartilage explants should be pooled, (usually 6 explants are combined for one sample), patted dry, and flash frozen in liquid nitrogen. Samples should then be stored at -80°C.

B.2.1 Material Preparation

- The pulverizer and homogenizer should be autoclaved after each use (Figure B.4)
- Label Eppendorf phase-gel heavy tubes (#955154045), pre-spin for 1min @ 10,000rpm
- Label QIAGEN silica-membrane tubes (pink, #74104)
- Label 5ml polypropylene tubes directly with tape
- In chemical hood: mix RLT buffer and 100X β-mercaptoethanol in specially marked bottle (require 350µl per sample)
- Add chloroform to a 50ml tube (polypropylene only), 60µl per sample
- Add 100% ethanol to a 50ml tube (create a stock tube)
- In hood: add 20mls of DNase/RNase-free water to two 50ml tubes
- Fill liquid nitrogen container (wear goggles)
- Fill ice bucket
- Get Trizol reagent and keep on ice
- Make DNase (QIAGEN, #79254) – see step 14 (experienced users can leave this until the 10 minute spin)

Base & Top of Pulverizer

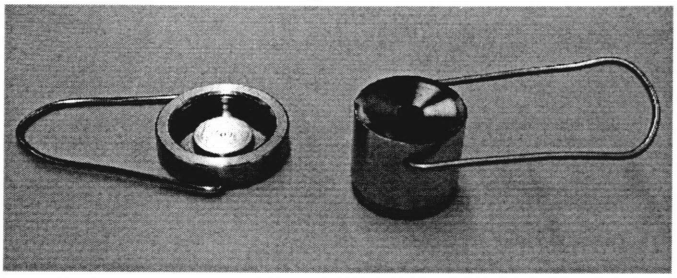

Stopper & Pole

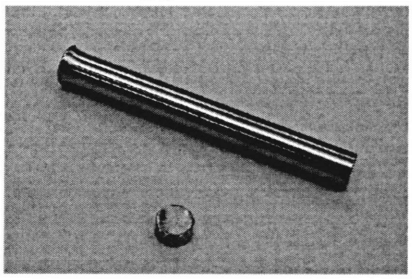

Pulverizer setup to be placed in freezing container

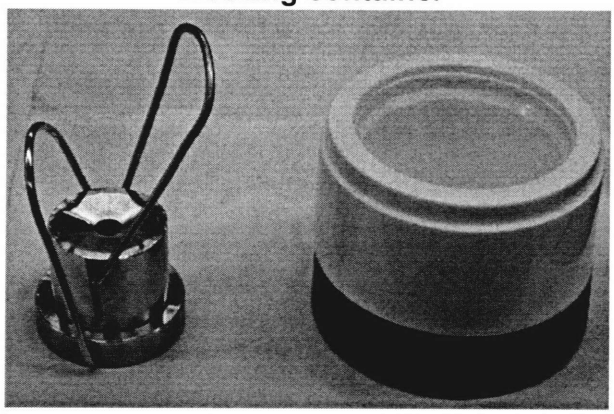

Pulverizer ready to pound

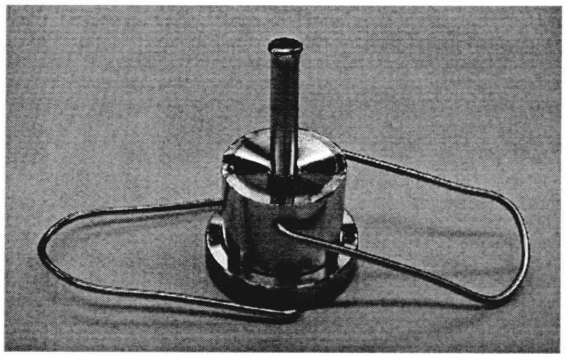

Tissue Tearor (Homogenizer)

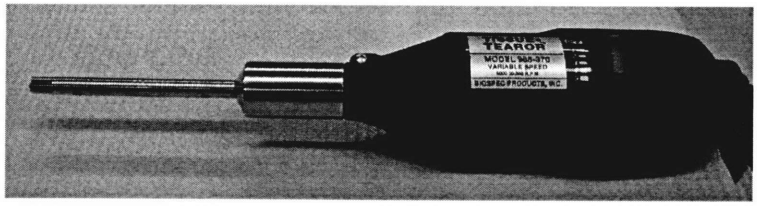

Sheath & Blade

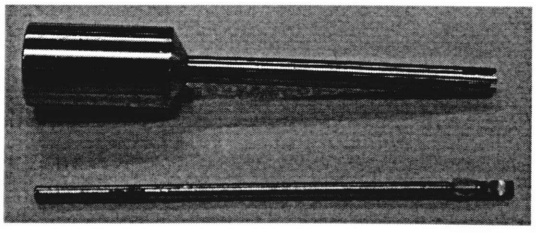

Blade flush within sheath

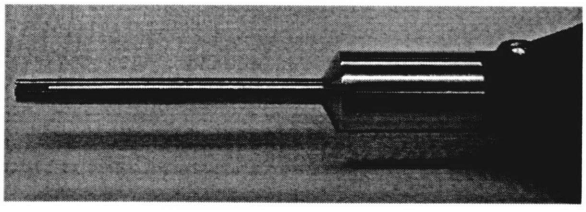

Figure B.4: RNA extraction tools.

B.2.2 Tissue Disruption

1) Place pulverizer and pole into the freezing container and bathe in liquid nitrogen four times. Remove two samples from the -80°C freezer and place in ice bath. Cool pulverizer again with liquid nitrogen.
2) Remove pulverizer and bend the arms downward (Figure B.4). Make sure the metal stopper is in place and add cartilage samples to top of pulverizer. Place pole into top base. Hit pole firmly 8-10 times with a hammer, while holding pole and top of pulverizer with a temperature-resistant glove.
3) Lift top of pulverizer and gently tap pole to release metal stopper. Place a 5ml polypropylene tube beneath pulverizer, turn pulverizer sideways and tap pole on side of bench to release the smashed cartilage into the tube. Place in ice bath.
4) Clean pulverizer with sterile gauss and if necessary re-cool with liquid nitrogen. Insert an autoclaved spatula through pulverizer top and wipe with gauss.
5) Repeat steps 2-4 for second sample. Return both samples to -80°C freezer and place into a separate tray.
6) Remove the next two samples from the -80°C freezer. Re-cool in liquid nitrogen (bathe twice). Repeat steps 2 to 6 until all samples are pulverized.
7) Clean and put aside pulverizer. Remove all samples from -80°C freezer. Add 540µl of Trizol to each sample, taking care to push any cartilage debris to the bottom of the tube. Keep samples on ice.
8) Set up the homogenizer by inserting the blade, pressing the button, and tightening with a spanner (wrench). Place sheath on top.
9) Place homogenizer in first 50ml water tube, turn to low speed (1 or 2) and rinse, turn off, remove, and shake dry. Repeat in second water tube. Washing between samples is performed to minimize sample carryover and the second water tube should still look clean at the end of protocol.
10) Place homogenizer into first sample, turn onto low speed (1 or 2), and slowly increase to speed setting 3. Sample should be homogenized in ~10 seconds (20 sec max). Place sample back in ice bath.
11) Repeat steps 9 and 10 for each sample.

12) Remove samples from ice bath and place onto a 96 well tray. Remove lids and add 60µl of chloroform (10% final concentration) to each tube. Mix (should turn cloudy pink) and transfer sample to pre-spun, labeled, phase-gel tubes.
13) Spin phase-gel tubes at maximum speed for 10 minutes in 4°C fridge. Change gloves. While tubes are spinning perform steps 14 and 15.
14) Make a mastermix of 10µl of DNase stock solution to 70µl of RDD Buffer per sample and store in ice bath. Thawed DNase aliquots should not be re-frozen, instead store in the 4°C fridge (choose aliquot size carefully). See pages 98-99 of the QIAGEN RNA extraction protocol for more details.
15) For each sample place a RNase/DNase-free, 1.5ml centrifuge tube into the 96 well tray. Add 250µl of 100% ethanol into each tube. Add 350µl of RLT+β-Me to each tube.

B.2.3 RNA Isolation

1) The following steps are taken from the QIAGEN RNeasy Mini Protocol, pages 54-55. Buffer RPE should have ethanol added to the bulk volume when the kit is first used. First time users should check with Han-Hwa regarding appropriate waste disposal.
2) After spinning, transfer the phase-gel tube supernatant to a centrifuge tube containing the ethanol and β-Me+RLT. Immediately mix the supernatant, ethanol and RLT buffer. Transfer half the solution to the pink RNA-easy spin-columns (less than 700µl). Repeat for each phase-gel tube.
3) Centrifuge the spin-columns for 30sec at 10,000 rpm. Discard flow through into a 50ml waste container. The RNA is now attached to the silica membrane in the pink tubes. Add the remaining sample from each centrifuge tube to the spin-columns and spin again at 10,000rpm. Discard flow through.
4) Pipette 350µl of Buffer RW1 into the spin-columns and centrifuge for 30sec at 10,000rpm. Discard flow-through.
5) Pipette 80µl aliquots of DNase mix directly onto the spin-column membrane of each sample. Tap gently to ensure the entire membrane is covered. Incubate at room temperature for 15 minutes.
6) During 15 minute incubation wash the pulverizer and homogenizer parts. Re-autoclave. Change gloves. Label 1.5ml collection tubes provided in QIAGEN kit.

7) After the 15 minute incubation, pipette 350µl of Buffer RW1 into the spin-columns and centrifuge for 30sec at 10,000rpm. Discard flow-through and collection tubes.
8) Place the spin-columns into new 2ml collection tubes, add 500µl of Buffer RPE (with ethanol previously added), centrifuge for 30sec at 10,000rpm. Discard flow-through.
9) Pipette 500µl of Buffer RPE (with ethanol added) into the spin-columns, centrifuge for 2 minutes at maximum speed. Remove the spin-columns from the collection tubes and wipe the outside gently with sterile gauze to remove any residual ethanol, which may interfere with subsequent reactions.
10) Place spin-columns into 1.5ml labeled collection tubes. Add 40µl of RNase/DNase-free dH_2O directly onto the membrane, changing tip between each sample (supplied in QIAGEN kit). Spin at 10,000rpm for 1 minute, which will elute the RNA, and then place immediately in ice bucket.
11) If proceeding directly with reverse transcription then keep tubes in an ice bucket. If not, freeze RNA in -80°C immediately to minimize degradation.

B.3 Reverse Transcription

Before commencing ethanol all surfaces, use alcohol wipes on pipettes, pens & trays.

This is done to avoid contamination with proteins, RNAs, RNase and DNase.

1) If proceeding straight from a RNA extraction ensure that RNA is kept cold (but not frozen) by placing vials in an ice bucket and then placing in the 4°C fridge. If RNA has been frozen and stored in the -80°C freezer only thaw it immediately before use.
2) Make a RT master mix using the following guide. Total reaction volume will be 60µl once RNA and H_2O have been added. Reagents are from Applied Biosystems.

RT Reagents	x1 (40µl)	x1 (60µl)
10x PCR buffer	4	6
$MgCl_2$	4	6
dNTP(10mM)	4	6
Random Hexamers	1	1.5
RNase Inhibitor	1	1.5
Multiscribe Reverse Transcriptase	1	1.5
dIH_20	5	17.5
Make mastermix of above reagents, step 3. Aliquot 20µl (40µl total) or 40µl (60µl total) for each sample		
Sample RNA	20	20

A total volume of 60µl was chosen as this produces forty 1.5µl cDNA aliquots to be used for PCR. Hence if you have less that 40 genes scale down the reagent volumes. However, keep the Sample RNA volume at 20µl, & adjust the water to compensate.

Keep cold, remove from freezer only when needed, mix thoroughly by pipetting, (do not vortex as enzymes are fragile).

3) Multiply all the above volumes by the number of cartilage samples to create a master mix (plus 10% to account for pipette errors).
4) After adding RNA to each sample place it in the ice bath. Once all samples are completed spin using the mini-centrifuge.

5) Load tubes into the thermocycler and follow these steps (GoldRT2 protocol):

25°C for 20 minutes	(hybridization)
42°C for 30 minutes	(reverse transcription)
Hold 4°C	(wait for removal)

6) Although cDNA is significantly more stable than RNA and doesn't degrade as fast, quantitative RT-PCR aims to avoid degradation as much as possible. Hence, move cDNA into the -20°C as soon as possible after the thermocycler reaches 4°C.

B.4 Real-time Polymerase Chain Reaction

B.4.1 Material Preparation

- It is important to run all housekeeping genes and control samples on the same plate for normalization purposes
- Keep all reagents as cool as possible
    - Thaw primers and cDNA immediately before use
    - Keep the SybrGreen Mastermix and water on ice
    - Setup the 96 well PCR plate on an ice tray
- Ethanol all surfaces, and pipettes before use
- Plates (#MLL-9651) and caps (#TCS-0803) are from BioRad
- Multi-pipette tips are from RANIN (#RT-L10F)

Each PCR plate well should contain 20µl consisting of:

10µl SybrGreen 2X Mastermix (Applied Biosystems, #4309155)

6.5µl H_20 (DNase/RNase-free)

2.0µl Diluted primer mix (final concentration 0.5µM each primer)*

1.5µl cDNA mix**

* Primers are shipped at a concentration of 100µM. To reduce the effects of contamination and avoid multiple freeze/thawing cycles, make a dilute mix of primers containing: 180µl of H_20 + 10µl forward primer + 10µl reverse primer. Use the diluted stock for the PCR. The primers will be in excess even for abundant genes such as 18S.

** Typical yield of RNA from 6-10 cartilage explants is 5µg in 40µl water. Typically 2.5µg of RNA are reverse transcribed in 40-60µl. 1.5µl of cDNA mix contains 41- 62ng of cDNA.

B.4.2 Plate Setup

- Aliquot reagents using a method that minimizes well to well variation. The following is a suggested protocol.
- Aliquoting multiple samples may result in insufficient volume remaining for the final sample. Increase the required volume by 10% to allow for this.

For a plate containing X conditions and Y genes:

1) Aliquot 10µl ×Y (+10%) of SybrGreen Mastermix into X tubes
2) Add 1.5µl × Y (+10%) of cDNA separately into the X tubes and mix thoroughly
3) Distribute 11.5µl of the SybrGreen/cDNA mix into each well. Using a multi-pipette aliquot all X conditions one gene at a time. The PCR plate should be on an ice tray.

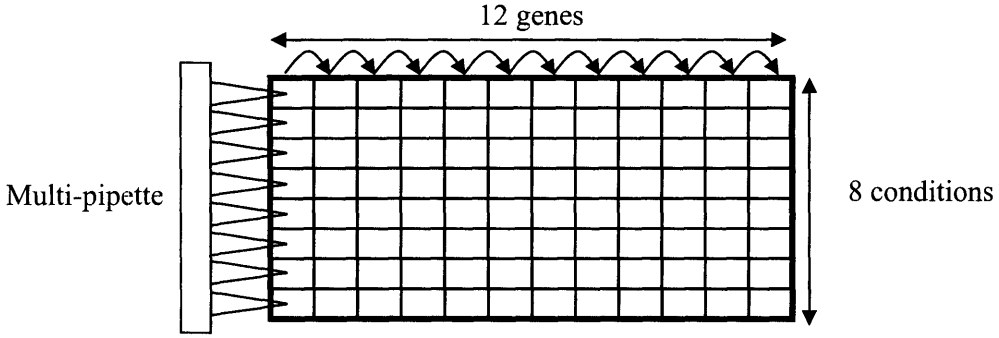

4) Aliquot 6.5µl × X (+10%) of H_20 into Y tubes
5) Add 2.0µl × X (+10%) of diluted primers separately into the Y tubes and mix thoroughly
6) Distribute 8.5µl of the H_20/primer mix into each well. Using a multi-pipette aliquot all the genes for a condition at once. Be sure to mix each well. Discard tips between each condition.

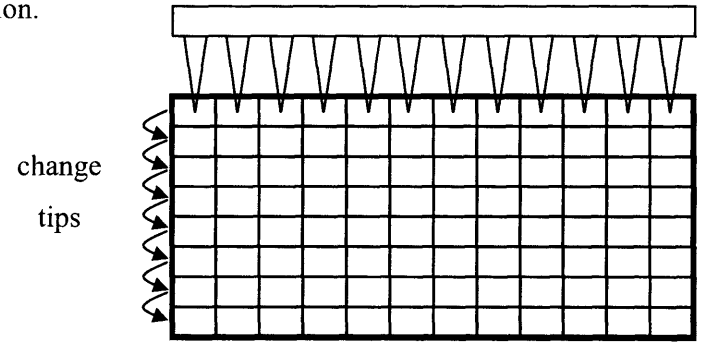

7) Cap and secure lids to wells.
8) To ensure reagents are kept cool, transport the PCR plate and two white 96 well trays to the real-time PCR machine in small box filled with ice and insulated with paper towels.

B.4.3 Real-time PCR Machine Operation

1) When at the BioMicro Center (68-316) spin the PCR plate in a plate centrifuge to ensure no liquid is attached to the lids. Place the PCR plate in a tray into the centrifuge and balance with another tray.
2) Place the PCR plate into the real-time PCR machine with well A1 in the back left corner. Close the door securely using the blue handle
3) The Opticon Monitor 2 uses a Master file which contains a Plate file and a Protocol file. When setting up a Plate file make sure that SybrGreen is selected for dye1 and dye2 and that Singleplex is selected. Select the White MJ Research plate option. *Ensure the correct volume is selected every time.*
4) The protocol consists of:
   I. Heat lid to 104°C to reduce evaporation
   II. 2 min at 50°C (enzyme digests RNA)
   III. 10 min at 95°C (activates Hot-start Taq polymerase)
   IV. 15 sec at 94°C (denatures double stranded DNA)
   V. 60 sec at 60°C (primer annealing and extension)
   VI. Take fluorescence measurement
   VII. Repeat steps IV to VI for 39 cycles (completes PCR)
   VIII. 60 sec at 60°C (extension for melting curve)
   IX. Step from 60°C to 92°C in 1°C increments. Record fluorescence at each temperature

   The entire protocol takes 2 hours to complete

5) Once the plate is setup press Run, and enter file name. The door light should turn blue to indicate a plate is running. At the bottom left of the screen *Door Closed* should be

highlighted in green. Wait 1 minute to be sure and restart if the screen indicates *Door Open* in red as the machine will not cycle.

B.4.4 Analysis

Once the run has finished and been saved it is necessary to covert the amplification plots into copy numbers.

1) Subtract the baseline values to set the zero point for the amplification plots. Do this by subtracting the average intensity of the first 3 cycles.
2) Set the threshold value at which C_T values will be calculated. The threshold should be high enough that it transects the amplification plots of all genes at the beginning of the linear region as shown in Figure B.5.

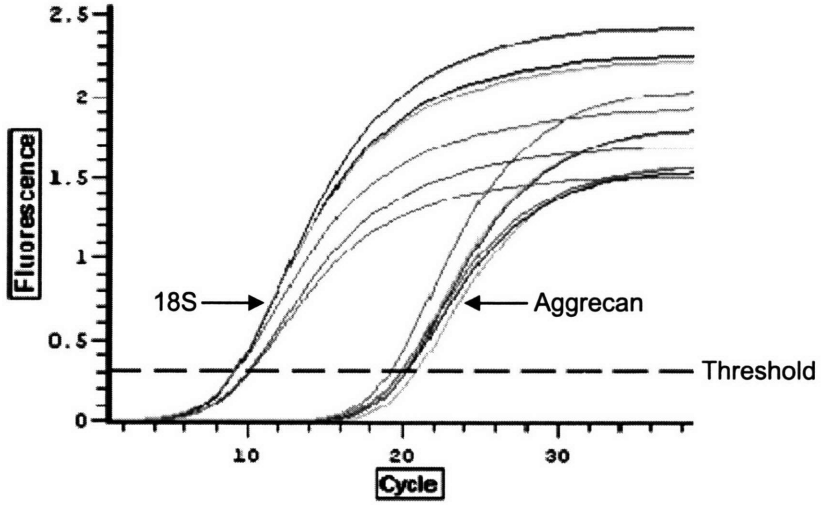

Figure B.5: Amplification plots of 6 samples for two genes (18S and aggrecan).

3) Export the C_T values into Excel using *Copy to Clipboard* under the *Quantity Calculations* tab, and arrange as appropriate.
4) Check the melting curves of each well by selecting the *Melting Curve* tab. The dI/dT curve should contain only one peak representing the PCR product, but may contain cooler primer dimer peaks (see Section B.5.1).

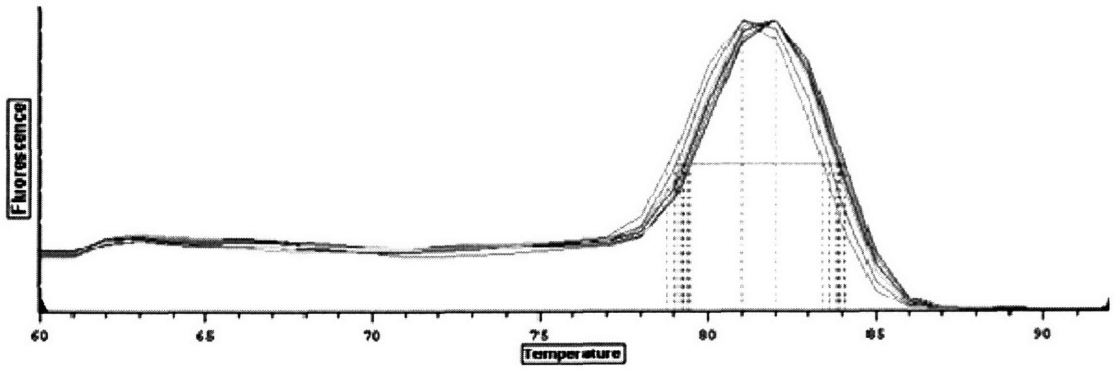

Figure B.6: Aggrecan dI/dT melting curve from 6 samples.

5) Convert C_T values to relative copy numbers using primer specific standard curves (see Section B.5.2)

$$\text{Relative copy number} = 2^{(\text{slope}*C_T+\text{offset})}$$

6) Normalize starting cDNA quantity by using the housekeeping genes 18S and G3PDH. As 18S is much more abundant than G3PDH, divide each housekeeping gene by its average copy number. Compare the scaled values of the housekeeping genes for each sample (there should be good agreement). Average the scaled values for each sample. Use the averaged values to normalize the remaining genes appropriately. As the housekeeping genes are vital it may be worthwhile repeating them on the plate to ensure highly accurate values.
7) To reduce variability a second normalization step may be required. Normalize to the untreated control samples which must be run on the same plate.

B.5 Primer Design

Primer design is limited by the availability of bovine mRNA sequences. To acquire a bovine sequence search the PubMed database at:

http://www.ncbi.nlm.nih.gov/entrez/query.fcgi?db=Nucleotide

Alternatively, the Entrez Gene database catalogues DNA, mRNA and protein sequence information and can be used to obtain all accession numbers listed for a particular bovine sequence.

http://www.ncbi.nlm.nih.gov/entrez/query.fcgi?CMD=search&DB=gene

Choose the coding sequence region (CDS) of the mRNA sequence for primer design.

B.5.1 Primer Selection

1) Copy a continuous part of the CDS into a primer design program. Primer3 works well.

   http://frodo.wi.mit.edu/cgi-bin/primer3/primer3_www.cgi

   - Product Size Range should be set to 80-120 (bp)
   - Primer Size Range should be set to 18-24 (bp)
   - Primer GC% should be set to 40-60 (%)

2) *Pick Primers* will choose the top five best primer pairs based on the selection criteria. The primer pairs should have a melting temperature close to 60°C, a GC content close to 50% and base pair length close to 100bp.

3) Chose a primer pair by examining the *any* and *3'* scores as well as the *pair any compl* and *pair 3' compl* scores for each primer pair. Minimizing these scores should decrease the likelihood of primer dimer formation or mispriming.

4) To determine the specificity of the primers *Blast* the forward primer against all other bovine sequences at:

http://www.ncbi.nlm.nih.gov/BLAST/Blast.cgi?CMD=Web&LAYOUT=TwoWindows&AUTO_FORMAT=Semiauto&ALIGNMENTS=50&ALIGNMENT_VIEW=Pairwise&CLIENT=web&DATABASE=nr&DESCRIPTIONS=100&ENTREZ_QUERY=%28none%29&EXPECT=10&FILTER=L&FORMAT_OBJECT=Alignment&FORMAT_TYPE=HTML&NCBI_GI=on&PAGE=Nucleotides&PROGRAM=blastn&SERVICE=plain&SET_DEFAULTS.x=34&SET_DEFAULTS.y=8&SHOW_OVERVIEW=on&END_OF_HTTPGET=Yes&SHOW_LINKOUT=yes&GET_SEQUENCE=yes

5) *Blast* results will produce a number of sequence similarity hits. Examine the bit-scores and the E-values. The bit-score sums the number of pairs of bases that match between the primer and the sequence that was found. The E-value is an inverse measure of the probability of this occurring. High bit-scores and low E-values indicate strong sequence similarity. A bit-score less than 75% of the maximum probably can be ignored. By examining the names of the sequences with high bit-scores the specificity of the primer can be determined.

6) Repeat steps 4 and 5 with the reverse primer, which must first be reversed and complimented before Blasting.

7) Primers are shipped dry-lyophilized and must be made up to a concentration of 100μM using DNase/RNase-free water. Primer validation using standard curves is described in the next section. It is also important to do a Melting Curve Analysis

8) Melting Curve Analysis is performed after real-time PCR. The plate temperature is increased from 60°C to 92°C in 1°C steps with a fluorescence reading performed at each temperature. As the temperature increases double-stranded DNA denatures and the fluorescence level (I) decreases. Denaturation temperature (T_m) is related to sequence length, hence, 100bp products have higher T_m's than primer dimer's.

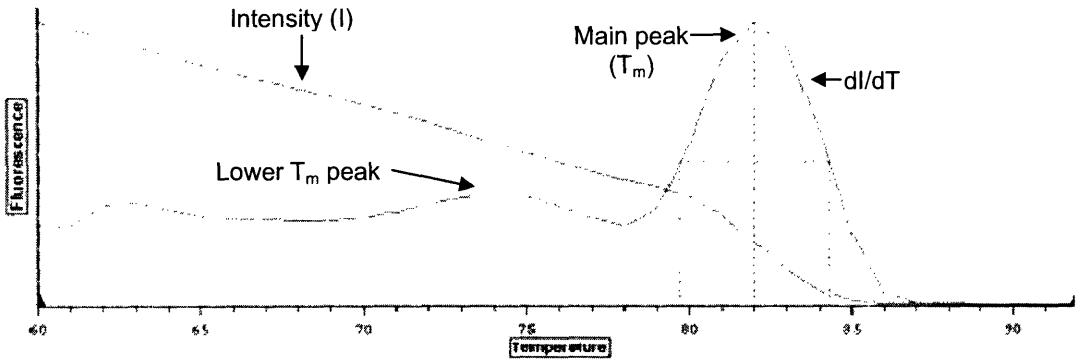

Figure B.7: Melting curve containing slight primer dimer interference.

9) The presence of a lower T_m peak indicates non-specific binding or primer dimers. As the fluorescence level is a relative measurement the larger the peak at the lower Tm the greater the amount of primer dimers compared to primer product. Hence, primer dimers for more abundant transcripts will be out-competed and not be a problem.

10) The presence of low T_m peaks indicates poor primer performance. To confirm the presence of primer dimers perform a real-time PCR on a non-template control (NTC) sample and normal sample. For NTC samples add SybrGreen Mastermix, primers, and water but no cDNA. Observe the amplification and melting curve plots. Most likely the melting curves for the NTC samples will have peaks at the lower Tm only (as no product exists). If the C_T values of the NTC are comparable to C_T values of normal samples (< 6 cycles apart) significant primer dimer formation is occurring and primers need to be redesigned.

11) Primer product lengths can be verified by performing a standard PCR and running the amplified product on an Ethidium bromide gel. This should be done to confirm the length is ~100bp and may highlight if primer dimering or non-specific binding is occurring.

B.5.2 Standard Curves

Once primers have been designed their performance should be tested. Although it is possible to optimize primer performance by adjusting $MgCl_2$ and primer concentrations, the Applied Biosystems SybrGreen Mastermix works sufficiently well.

1) To create standards a pure stock of the primer product must be obtained.

2) Amplify a stock of cDNA using a regular PCR machine with the real-time primers. Forty cycles should be sufficient. The amplified cDNA will contain the PCR product in high abundance, and also free primers, dNTPs, other cDNA, and perhaps primer dimers or artifacts.
3) Purify the primer product by running the amplified cDNA through Centri-Spin columns (or equivalent). Centri-Spin columns remove lower base-pair DNA molecules, in particular, primers, and primer dimers. Some primer product may also be removed.
4) For creating absolute standard curves quantify the amount of primer product by taking an absorbance reading at 260nm. Calculate the number of copies of the product by assuming approximately the same number of AGCTs.
5) In order to log-amplify with real-time PCR the primer product will need to be greatly diluted. First dilute the purified samples by a further 10^6 by performing 10:1 serial dilutions. It is important to change pipette tips after each dilution step.
6) Then serially dilute the primer product further in 2-fold increments (1, 0.5, 0.25, 0.125, 0.0625). Mix well and change pipette tips after each dilution step.
7) Use the 2 fold standard curve range as cDNA for performing a real-time PCR. SybrGreen Mastermix, primers and water will need to be added as in the standard protocol (see Section B.4.2). Also run a non-template control (NTC) which contains SybrGreen Mastermix, primers, and water, but no primer product. Any amplification in the NTC will indicate primer dimering.
8) Obtain threshold values, (C_T), from the amplification plots as described in Section B.4.4.
9) Create log-linear standard curves by plotting relative copy number (log to the base 2) on the Y-axis and the C_T value on the X-axis.

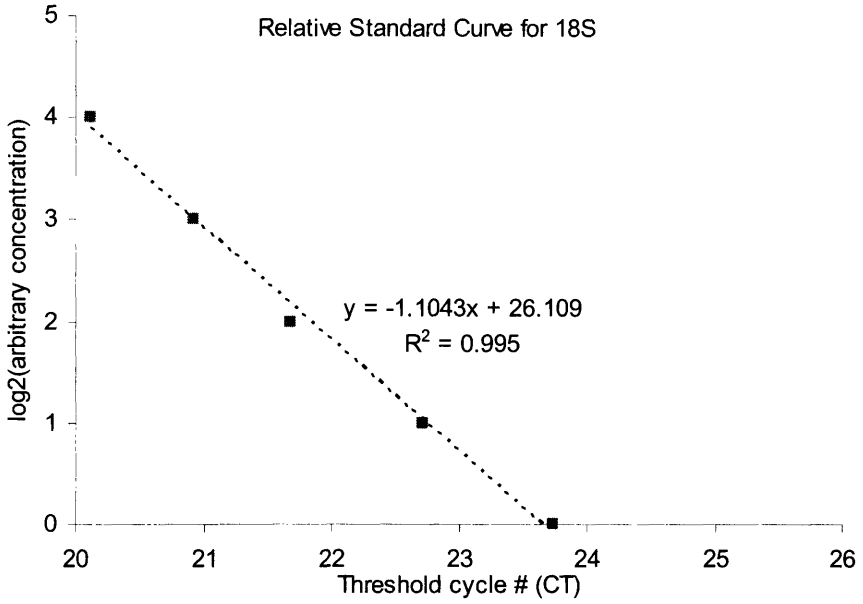

Figure B.8: Standard curve for 18S ribosomal protein.

10) Calculate the trendline. The slope of the trendline should be ~ -1 (-0.90 to -1.10). One source of non-linearity or divergence is if primer product is not mixed well or is carried over on the pipette tip (sometimes occurs for the most abundant sample).

11) C_T values can be converted to relative copy numbers using the following formula.

$$\text{Relative copy number} = 2^{y} = 2^{(ax+b)}$$

a is the trendline slope and should be negative, *b* specifies the C_T value for 1 starting copy of cDNA. For relative standard curves *b* is arbitrary and the trendline offset or a specified cycle number can be used.

12) If amplification occurs in the NTC then primer dimers exist. To determine the extent of primer dimering compare the C_T values from the NTC samples with C_T values from standard cDNA samples (not primer product samples). If the C_T values of NTC are 8 or more cycles greater than for cDNA samples the primer dimers can be ignored. However, if the C_T values of NTC and standard cDNA are close then redesign the primers. This step compliments the primer melting curve analysis described in the previous section.

Bibliography

[1] Grodzinsky, A. J., Levenston, M. E., Jin, M. and Frank, E. H. Cartilage tissue remodeling in response to mechanical forces. *Annual Review of Biomedical Engineering,* 2:691-713, 2000.

[2] Morgelin, M., Heinegard, D., Engel, J. and Paulsson, M. The cartilage proteoglycan aggregate: assembly through combined protein-carbohydrate and protein-protein interactions. *Biophysical Chemistry,* 50:113-128, 1994.

[3] Morgelin, M., Paulsson, M., Hardingham, T. E., Heinegard, D. and Engel, J. Cartilage proteoglycans. Assembly with hyaluronate and link protein as studied by electron microscopy. *Biochemical Journal,* 253:175-185, 1988.

[4] Albelda, S. M. and Buck, C. A. Integrins and other cell adhesion molecules. *Faseb Journal,* 4:2868-2880, 1990.

[5] Treppo, S., Koepp, H., Quan, E. C., Cole, A. A., Kuettner, K. E. and Grodzinsky, A. J. Comparison of biomechanical and biochemical properties of cartilage from human knee and ankle pairs. *Journal of Orthopaedic Research,* 18:739-748, 2000.

[6] Guilak, F., Jones, W. R., Ting-Beall, H. P. and Lee, G. M. The deformation behavior and mechanical properties of chondrocytes in articular cartilage. *Osteoarthritis and Cartilage,* 7:59-70, 1999.

[7] Jones, W. R., Ting-Beall, H. P., Lee, G. M., Kelley, S. S., Hochmuth, R. M. and Guilak, F. Alterations in the Young's modulus and volumetric properties of chondrocytes isolated from normal and osteoarthritic human cartilage. *Journal of Biomechanics,* 32:119-127, 1999.

[8] Nagase, H. and Woessner, J. F., Jr. Matrix metalloproteinases. *Journal of Biological Chemistry,* 274:21491-21494, 1999.

[9] Lohmander, L. S., Hoerrner, L. A. and Lark, M. W. Metalloproteinases, tissue inhibitor, and proteoglycan fragments in knee synovial fluid in human osteoarthritis. *Arthritis and Rheumatism,* 36:181-189, 1993.

[10] Lohmander, L. S., Hoerrner, L. A., Dahlberg, L., Roos, H., Bjornsson, S. and Lark, M. W. Stromelysin, Tissue Inhibitor of Metalloproteinases and Proteoglycan Fragments in Human Knee-Joint Fluid after Injury. *Journal of Rheumatology,* 20:1362-1368, 1993.

[11] Ng, L., Grodzinsky, A. J., Patwari, P., Sandy, J., Plaas, A. and Ortiz, C. Individual cartilage aggrecan macromolecules and their constituent glycosaminoglycans visualized via atomic force microscopy. *Journal of Structural Biology,* 143:242-257, 2003.

[12] Morales, T. I. and Roberts, A. B. Transforming growth factor beta regulates the metabolism of proteoglycans in bovine cartilage organ cultures. *Journal of Biological Chemistry,* 263:12828-12831, 1988.

[13] Luyten, F. P., Hascall, V. C., Nissley, S. P., Morales, T. I. and Reddi, A. H. Insulin-like growth factors maintain steady-state metabolism of proteoglycans in bovine articular cartilage explants. *Archives of Biochemistry and Biophysics,* 267:416-425, 1988.

[14] Hui, W., Rowan, A. D. and Cawston, T. Modulation of the expression of matrix metalloproteinase and tissue inhibitors of metalloproteinases by TGF-beta1 and IGF-1 in primary human articular and bovine nasal chondrocytes stimulated with TNF-alpha. *Cytokine,* 16:31-35, 2001.

[15] Irie, K., Uchiyama, E. and Iwaso, H. Intraarticular inflammatory cytokines in acute anterior cruciate ligament injured knee. *Knee,* 10:93-96, 2003.

[16] Liacini, A., Sylvester, J., Li, W. Q., Huang, W., Dehnade, F., Ahmad, M. and Zafarullah, M. Induction of matrix metalloproteinase-13 gene expression by TNF-alpha is mediated by MAP kinases, AP-1, and NF-kappaB transcription factors in articular chondrocytes. *Experimental Cell Research,* 288:208-217, 2003.

[17] Liacini, A., Sylvester, J., Li, W. Q. and Zafarullah, M. Inhibition of interleukin-1-stimulated MAP kinases, activating protein- 1 (AP-1) and nuclear factor kappa B (NF-kappa B) transcription factors down-regulates matrix metalloproteinase gene expression in articular chondrocytes. *Matrix Biology,* 21:251-262, 2002.

[18] Vincenti, M. P., Coon, C. I., Lee, O. and Brinckerhoff, C. E. Regulation of collagenase gene expression by IL-1 beta requires transcriptional and post-transcriptional mechanisms. *Nucleic Acids Research,* 22:4818-4827, 1994.

[19] Geng, Y., Blanco, F. J., Cornelisson, M. and Lotz, M. Regulation of cyclooxygenase-2 expression in normal human articular chondrocytes. *Journal of Immunology,* 155:796-801, 1995.

[20] Hui, A., Min, W. X., Tang, J. and Cruz, T. F. Inhibition of activator protein 1 activity by paclitaxel suppresses interleukin-1-induced collagenase and stromelysin expression by bovine chondrocytes. *Arthritis and Rheumatism,* 41:869-876, 1998.

[21] Gray, M. L., Pizzanelli, A. M., Lee, R. C., Grodzinsky, A. J. and Swann, D. A. Kinetics of the chondrocyte biosynthetic response to compressive load and release. *Biochimica et Biophysica Acta,* 991:415-425, 1989.

[22] Sah, R. L. Y., Kim, Y. J., Doong, J. Y. H., Grodzinsky, A. J., Plaas, A. H. K. and Sandy, J. D. Biosynthesis Response to Cartilage Explants to Dynamic Compression. *Journal of Orthopaedic Research,* 7:619-636, 1989.

[23] Herberhold, C., Faber, S., Stammberger, T., Steinlechner, M., Putz, R., Englmeier, K. H., Reiser, M. and Eckstein, F. In situ measurement of articular cartilage deformation in intact femoropatellar joints under static loading. *Journal of Biomechanics,* 32:1287-1295, 1999.

[24] Kurz, B., Jin, M., Patwari, P., Cheng, D. M., Lark, M. W. and Grodzinsky, A. J. Biosynthetic response and mechanical properties of articular cartilage after injurious compression. *Journal of Orthopaedic Research,* 19:1140-1146, 2001.

[25] Frank, E. H., Jin, M., Loening, A. M., Levenston, M. E. and Grodzinsky, A. J. A versatile shear and compression apparatus for mechanical stimulation of tissue culture explants. *Journal of Biomechanics,* 33:1523-1527, 2000.

[26] Guilak, F., Meyer, B. C., Ratcliffe, A. and Mow, V. C. The effects of matrix compression on proteoglycan metabolism in articular cartilage explants. *Osteoarthritis and Cartilage,* 2:91-101, 1994.

[27] Parkkinen, J. J., Lammi, M. J., Helminen, H. J. and Tammi, M. Local Stimulation of Proteoglycan Synthesis in Articular-Cartilage Explants by Dynamic Compression Invitro. *Journal of Orthopaedic Research,* 10:610-620, 1992.

[28] Parkkinen, J. J., Ikonen, J., Lammi, M. J., Laakkonen, J., Tammi, M. and Helminen, H. J. Effects of Cyclic Hydrostatic-Pressure on Proteoglycan Synthesis in Cultured Chondrocytes and Articular-Cartilage Explants. *Archives of Biochemistry and Biophysics,* 300:458-465, 1993.

[29] Wong, M., Siegrist, M. and Cao, X. Cyclic compression of articular cartilage explants is associated with progressive consolidation and altered expression pattern of extracellular matrix proteins. *Matrix Biology,* 18:391-399, 1999.

[30] Wong, M., Siegrist, M., Goodwin, K. and Park, Y. Hydrostatic pressure, tension and unconfined compression differentially regulate expression of cartilage matrix proteins. *Orthopaedic Research Society 48th Annual Meeting,* 0033, 2002.

[31] Bachrach, N. M., Valhmu, W. B., Stazzone, E., Ratcliffe, A., Lai, W. M. and Mow, V. C. Changes in proteoglycan synthesis of chondrocytes in articular cartilage are associated with the time-dependent changes in their mechanical environment. *Journal of Biomechanics,* 28:1561-1569, 1995.

[32] Blain, E. J., Gilbert, S. J., Wardale, R. J., Capper, S. J., Mason, D. J. and Duance, V. C. Up-regulation of matrix metalloproteinase expression and activation following cyclical compressive loading of articular cartilage in vitro. *Archives of Biochemistry and Biophysics,* 396:49-55, 2001.

[33] Kim, Y. J., Sah, R. L., Grodzinsky, A. J., Plaas, A. H. and Sandy, J. D. Mechanical regulation of cartilage biosynthetic behavior: physical stimuli. *Archives of Biochemistry and Biophysics,* 311:1-12, 1994.

[34] Buschmann, M. D., Kim, Y. J., Wong, M., Frank, E., Hunziker, E. B. and Grodzinsky, A. J. Stimulation of aggrecan synthesis in cartilage explants by cyclic loading is localized to regions of high interstitial fluid flow. *Archives of Biochemistry and Biophysics,* 366:1-7, 1999.

[35] Kim, Y. J., Bonassar, L. J. and Grodzinsky, A. J. The Role of Cartilage Streaming Potential, Fluid-Flow and Pressure in the Stimulation of Chondrocyte Biosynthesis During Dynamic Compression. *Journal of Biomechanics,* 28:1055-1066, 1995.

[36] Schnabel, M., Marlovits, S., Eckhoff, G., Fichtel, I., Gotzen, L., Vecsei, V. and Schlegel, J. Dedifferentiation-associated changes in morphology and gene expression in primary human articular chondrocytes in cell culture. *Osteoarthritis and Cartilage,* 10:62-70, 2002.

[37] Benya, P. D. and Shaffer, J. D. Dedifferentiated chondrocytes reexpress the differentiated collagen phenotype when cultured in agarose gels. *Cell,* 30:215-224, 1982.

[38] Millward-Sadler, S. J., Wright, M. O., Lee, H., Nishida, K., Caldwell, H., Nuki, G. and Salter, D. M. Integrin-regulated secretion of interleukin 4: A novel pathway of mechanotransduction in human articular chondrocytes. *Journal of Cell Biology,* 145:183-189, 1999.

[39] Salter, D. M., Hughes, D. E., Simpson, R. and Gardner, D. L. Integrin expression by human articular chondrocytes. *British Journal of Rheumatology,* 31:231-234, 1992.

[40] Yellowley, C. E., Jacobs, C. R., Li, Z. Y., Zhou, Z. Y. and Donahue, H. J. Effects of fluid flow on intracellular calcium in bovine articular chondrocytes. *American Journal of Physiology-Cell Physiology,* 42:C30-C36, 1997.

[41] Yellowley, C. E., Jacobs, C. R. and Donahue, H. J. Mechanisms contributing to fluid-flow-induced Ca2+ mobilization in articular chondrocytes. *Journal of Cellular Physiology,* 180:402-408, 1999.

[42] Jortikka, M. O., Parkkinen, J. J., Inkinen, R. I., Karner, J., Jarvelainen, H. T., Nelimarkka, L. O., Tammi, M. I. and Lammi, M. J. The role of microtubules in the regulation of

proteoglycan synthesis in chondrocytes under hydrostatic pressure. *Archives of Biochemistry and Biophysics,* 374:172-180, 2000.

[43] Ikenoue, T., Trindade, M. C., Lee, M. S., Lin, E. Y., Schurman, D. J., Goodman, S. B. and Smith, R. L. Mechanoregulation of human articular chondrocyte aggrecan and type II collagen expression by intermittent hydrostatic pressure in vitro. *Journal of Orthopaedic Research,* 21:110-116, 2003.

[44] Smith, R. L., Lin, J., Trindade, M. C. D., Shida, J., Kajiyama, G., Vu, T., Hoffman, A. R., van der Meulen, M. C. H., Goodman, S. B., Schurman, D. J. and Carter, D. R. Time-dependent effects of intermittent hydrostatic pressure on articular chondrocyte type II collagen and aggrecan mRNA expression. *Journal of Rehabilitation Research and Development,* 37:153-161, 2000.

[45] Sauerland, K., Raiss, R. X. and Steinmeyer, J. Proteoglycan metabolism and viability of articular cartilage explants as modulated by the frequency of intermittent loading. *Osteoarthritis and Cartilage,* 11:343-350, 2003.

[46] Edlich, M., Yellowley, C. E., Jacobs, C. R. and Donahue, H. J. Oscillating fluid flow regulates cytosolic calcium concentration in bovine articular chondrocytes. *Journal of Biomechanics,* 34:59-65, 2001.

[47] Muir, H. The chondrocyte, architect of cartilage. Biomechanics, structure, function and molecular biology of cartilage matrix macromolecules. *Bioessays,* 17:1039-1048, 1995.

[48] Parkkinen, J. J., Lammi, M. J., Pelttari, A., Helminen, H. J., Tammi, M. and Virtanen, I. Altered Golgi-Apparatus in Hydrostatically Loaded Articular-Cartilage Chondrocytes. *Annals of the Rheumatic Diseases,* 52:192-198, 1993.

[49] Szafranski, J. D., Grodzinsky, A. J., Burger, E., Gaschen, V., Hung, H. H. and Hunziker, E. B. Chondrocyte mechanotransduction: effects of compression on deformation of intracellular organelles and relevance to cellular biosynthesis. *Osteoarthritis and Cartilage,* 12:937-946, 2004.

[50] Jortikka, M. O., Inkinen, R. I., Tammi, M. I., Parkkinen, J. J., Haapala, J., Kiviranta, I., Helminen, H. J. and Lammi, M. J. Immobilisation causes longlasting matrix changes both in the immobilised and contralateral joint cartilage. *Annals of the Rheumatic Diseases,* 56:255-261, 1997.

[51] Behrens, F., Kraft, E. L. and Oegema, T. R., Jr. Biochemical changes in articular cartilage after joint immobilization by casting or external fixation. *Journal of Orthopaedic Research,* 7:335-343, 1989.

[52] Slowman, S. D. and Brandt, K. D. Composition and glycosaminoglycan metabolism of articular cartilage from habitually loaded and habitually unloaded sites. *Arthritis and Rheumatism,* 29:88-94, 1986.

[53] Hunter, C. J., Mouw, J. K. and Levenston, M. E. Dynamic compression of chondrocyte-seeded fibrin gels: effects on matrix accumulation and mechanical stiffness. *Osteoarthritis and Cartilage,* 12:117-130, 2004.

[54] Mauck, R. L., Soltz, M. A., Wang, C. C., Wong, D. D., Chao, P. H., Valhmu, W. B., Hung, C. T. and Ateshian, G. A. Functional tissue engineering of articular cartilage through dynamic loading of chondrocyte-seeded agarose gels. *Journal of Biomechanical Engineering,* 122:252-260, 2000.

[55] Jin, M., Frank, E. H., Quinn, T. M., Hunziker, E. B. and Grodzinsky, A. J. Tissue shear deformation stimulates proteoglycan and protein biosynthesis in bovine cartilage explants. *Archives of Biochemistry and Biophysics,* 395:41-48, 2001.

[56] Valhmu, W. B., Stazzone, E. J., Bachrach, N. M., Saed-Nejad, F., Fischer, S. G., Mow, V. C. and Ratcliffe, A. Load-Controlled Compression of Articular Cartilage induces a transient stimulation of Aggrecan gene expression. *Archives of Biochemistry and Biophysics,* 353:29-36, 1998.

[57] Ragan, P. M., Badger, A. M., Cook, M., Chin, V. I., Gowen, M., Grodzinsky, A. J. and Lark, M. W. Down-regulation of chondrocyte aggrecan and type-II collagen gene expression correlates with increases in static compression magnitude and duration. *Journal of Orthopaedic Research,* 17:836-842, 1999.

[58] Millward-Sadler, S. J., Wright, M. O., Davies, L. W., Nuki, G. and Salter, D. M. Mechanotransduction via Integrins and Interleukin-4 results in altered Aggrecan and Matrix Metalloproteinase 3 gene expression in Normal, but not Osteoarthritic, Human Articular Chondrocytes. *Arthritis and Rheumatism,* 43:2091-2099, 2000.

[59] Palmer, G. D., Chao, P. H. G., Raia, F., Mauck, R. L., Valhmu, W. B. and Hung, C. T. Time-dependent aggrecan gene expression of articular chondrocytes in response to hyperosmotic loading. *Osteoarthritis and Cartilage,* 9:761-770, 2001.

[60] Smith, R. L., Trindade, M. C. D., Ikenoue, T., Mohtai, M., Das, P., Carter, D. R., Goodman, S. B. and Schurman, D. J. Effects of shear stress on articular chondrocyte metabolism. *Biorheology,* 37:95-107, 2000.

[61] Smith, R. L., Donlon, B. S., Gupta, M. K., Mohtai, M., Das, P., Carter, D. R., Cooke, J., Gibbons, G., Hutchinson, N. and Schurman, D. J. Effects of fluid-induced shear on articular chondrocyte morphology and metabolism in vitro. *Journal of Orthopaedic Research,* 13:824-831, 1995.

[62] Yokota, H. and Sun, H. B. Mechanical shear downregulates matrix metalloproteinases in synovial and chondrocyte cells. *Orthopaedic Research Society 48th Annual Meeting,* 2002.

[63] Valhmu, W. B. and Raia, F. J. myo-Inositol 1,4,5-trisphosphate and Ca2+/calmodulin-dependent factors mediate transduction of compression-induced signals in bovine articular chondrocytes. *Biochemical Journal,* 361:689-696, 2002.

[64] Yang, S. H., Sharrocks, A. D. and Whitmarsh, A. J. Transcriptional regulation by the MAP kinase signaling cascades. *Gene,* 320:3-21, 2003.

[65] Fanning, P. J., Emkey, G., Smith, R. J., Grodzinsky, A. J., Szasz, N. and Trippel, S. B. Mechanical regulation of mitogen-activated protein kinase signaling in articular cartilge. *Journal of Biological Chemistry,* 278:50940-50948, 2003.

[66] Lee, H. S., Millward-Sadler, S. J., Wright, M. O., Nuki, G. and Salter, D. M. Integrin and mechanosensitive ion channel-dependent tyrosine phosphorylation of focal adhesion proteins and beta-catenin in human articular chondrocytes after mechanical stimulation. *Journal of Bone and Mineral Research,* 15:1501-1509, 2000.

[67] Hung, C. T., Henshaw, D. R., Wang, C. C. B., Mauck, R. L., Raia, F., Palmer, G., Chao, P. H. G., Mow, V. C., Ratcliffe, A. and Valhmu, W. B. Mitogen-activated protein kinase signaling in bovine articular chondrocytes in response to fluid flow does not require calcium mobilization. *Journal of Biomechanics,* 33:73-80, 2000.

[68] Watanabe, H., de Caestecker, M. P. and Yamada, Y. Transcriptional cross-talk between Smad, ERK1/2, and p38 mitogen-activated protein kinase pathways regulates transforming growth factor-beta-induced aggrecangene expression in chondrogenic ATDC5 cells. *Journal of Biological Chemistry,* 276:14466-14473, 2001.

[69] Starkman, B. G., Cravero, J. D., Delcarlo Jr, M. and Loeser, R. F. IGF-I stimulation of proteoglycan synthesis by chondrocytes requires activation of the PI3-kinase pathway but not ERK MAP kinase. *Biochemical Journal,* 2005.

[70] Studer, R. K., Bergman, R., Stubbs, T. and Decker, K. Chondrocyte response to growth factors is modulated by p38 mitogen-activated protein kinase inhibition. *Arthritis Research and Therapy,* 6:R56-R64, 2004.

[71] Studer, R. K. and Chu, C. R. p38 MAPK and COX2 inhibition modulate human chondrocyte response to TGF-beta. *Journal of Orthopaedic Research,* 23:454-461, 2005.

[72] Lawrence, R. C., Helmick, C. G., Arnett, F. C., Deyo, R. A., Felson, D. T., Giannini, E. H., Heyse, S. P., Hirsch, R., Hochberg, M. C., Hunder, G. G., Liang, M. H., Pillemer, S. R., Steen, V. D. and Wolfe, F. Estimates of the prevalence of arthritis and selected musculoskeletal disorders in the United States. *Arthritis and Rheumatism,* 41:778-799, 1998.

[73] Gelber, A. C., Hochberg, M. C., Mead, L. A., Wang, N. Y., Wigley, F. M. and Klag, M. J. Joint injury in young adults and risk for subsequent knee and hip osteoarthritis. *Annuals of Internal Medicine,* 133:321-328, 2000.

[74] Davis, M. A., Ettinger, W. H., Neuhaus, J. M., Cho, S. A. and Hauck, W. W. The association of knee injury and obesity with unilateral and bilateral osteoarthritis of the knee. *American Journal of Epidemiology,* 130:278-288, 1989.

[75] von Porat, A., Roos, E. M. and Roos, H. High prevalence of osteoarthritis 14 years after an anterior cruciate ligament tear in male soccer players: a study of radiographic and patient relevant outcomes. *Annals of the Rheumatic Diseases,* 63:269-273, 2004.

[76] Millward-Sadler, S. J., Wright, M. O., Lee, H., Caldwell, H., Nuki, G. and Salter, D. M. Altered electrophysiological responses to mechanical stimulation and abnormal signalling through alpha5beta1 integrin in chondrocytes from osteoarthritic cartilage. *Osteoarthritis and Cartilage,* 8:272-278, 2000.

[77] Fitzgerald, J. B., Jin, M., Dean, D., Wood, D. J., Zheng, M. H. and Grodzinsky, A. J. Mechanical compression of cartilage explants induces multiple time-dependent gene expression patterns and involves intracellular calcium and cyclic AMP. *Journal of Biological Chemistry,* 279:19502-19511, 2004.

[78] Hascall, V. C. and Kuettner, K. E. The Many Faces of Osteoarthritis. 495, 2002.

[79] Saamamen, A. M., Kiviranta, I., Jurvelin, J., Helminen, H. J. and Tammi, M. Proteoglycan and collagen alterations in canine knee articular cartilage following 20 km daily running exercise for 15 weeks. *Connective Tissue Research,* 30:191-201, 1994.

[80] Kim, Y. J., Grodzinsky, A. J. and Plaas, A. H. Compression of cartilage results in differential effects on biosynthetic pathways for aggrecan, link protein, and hyaluronan. *Archives of Biochemistry and Biophysics,* 328:331-340, 1996.

[81] Bonassar, L. J., Grodzinsky, A. J., Frank, E. H., Davila, S. G., Bhaktav, N. R. and Trippel, S. B. The effect of dynamic compression on the response of articular cartilage to insulin-like growth factor-1. *Journal of Orthopaedic Research,* 19:11-17, 2001.

[82] Thibault, M., Poole, A. R. and Buschmann, M. D. Cyclic compression of cartilage/bone explants in vitro leads to physical weakening, mechanical breakdown of collagen and release of matrix fragments. *Journal of Orthopaedic Research,* 20:1265-1273, 2002.

[83] Patwari, P., Cook, M. N., DiMicco, M. A., Blake, S. M., James, I. E., Kumar, S., Cole, A. A., Lark, M. W. and Grodzinsky, A. J. Proteoglycan degradation after injurious compression of bovine and human articular cartilage in vitro: Interaction with exogenous cytokines. *Arthritis and Rheumatism,* 48:1292-1301, 2003.

[84] Davisson, T., Kunig, S., Chen, A., Sah, R. and Ratcliffe, A. Static and dynamic compression modulate matrix metabolism in tissue engineered cartilage. *Journal of Orthopaedic Research,* 20:842-848, 2002.

[85] Hunter, C. J., Imler, S. M., Malaviya, P., Nerem, R. M. and Levenston, M. E. Mechanical compression alters gene expression and extracellular matrix synthesis by chondrocytes cultured in collagen I gels. *Biomaterials,* 23:1249-1259, 2002.

[86] Mizuno, S., Tateishi, T., Ushida, T. and Glowacki, J. Hydrostatic fluid pressure enhances matrix synthesis and accumulation by bovine chondrocytes in three-dimensional culture. *Journal of Cellular Physiology,* 193:319-327, 2002.

[87] Kisiday, J. D., Jin, M., DiMicco, M. A., Kurz, B. and Grodzinsky, A. J. Effects of dynamic compressive loading on chondrocyte biosynthesis in self-assembling peptide scaffolds. *Journal of Biomechanics,* 37:595-604, 2004.

[88] Sironen, R. K., Karjalainen, H. M., Torronen, K., Elo, M. A., Kaarniranta, K., Takigawa, M., Helminen, H. J. and Lammi, M. J. High pressure effects on cellular expression profile and mRNA stability. A cDNA array analysis. *Biorheology,* 39:111-117, 2002.

[89] Dougherty, E. R., Barrera, J., Brun, M., Kim, S., Cesar, R. M., Chen, Y. D., Bittner, M. and Trent, J. M. Inference from clustering with application to gene-expression microarrays. *Journal of Computational Biology,* 9:105-126, 2002.

[90] Eisen, M. B., Spellman, P. T., Brown, P. O. and Botstein, D. Cluster analysis and display of genome-wide expression patterns. *Proceedings of the National Academy of Sciences USA,* 95:14863-14868, 1998.

[91] Alter, O., Brown, P. O. and Botstein, D. Singular value decomposition for genome-wide expression data processing and modeling. *Proceedings of the National Academy of Sciences USA,* 97:10101-10106, 2000.

[92] Holter, N. S., Mitra, M., Maritan, A., Cieplak, M., Banavar, J. R. and Fedoroff, N. V. Fundamental patterns underlying gene expression profiles: Simplicity from complexity. *Proceedings of the National Academy of Sciences USA,* 97:8409-8414, 2000.

[93] Hodge, W. A., Fijan, R. S., Carlson, K. L., Burgess, R. G., Harris, W. H. and Mann, R. W. Contact Pressures in the Human Hip-Joint Measured Invivo. *Proceedings of the National Academy of Sciences USA,* 83:2879-2883, 1986.

[94] Bonassar, L. J., Grodzinsky, A. J., Srinivasan, A., Davila, S. G. and Trippel, S. B. Mechanical and physicochemical regulation of the action of insulin-like growth factor-I on articular cartilage. *Archives of Biochemistry and Biophysics,* 379:57-63, 2000.

[95] Li, K. W., Wang, A. S. and Sah, R. L. Microenvironment regulation of extracellular signal-regulated kinase activity in chondrocytes - Effects of culture configuration, interleukin-1, and compressive stress. *Arthritis and Rheumatism,* 48:689-699, 2003.

[96] Tsuzaki, M., Guyton, G., Garrett, W., Archambault, J. M., Herzog, W., Almekinders, L., Bynum, D., Yang, X. and Banes, A. J. IL-1 beta induces COX2, MMP-1, -3 and -13,

ADAMTS-4, IL-1 beta and IL-6 in human tendon cells. *Journal of Orthopaedic Research,* 21:256-264, 2003.

[97] Vincenti, M. P. and Brinckerhoff, C. E. Transcriptional regulation of collagenase (MMP-1, MMP-13) genes in arthritis: integration of complex signaling pathways for the recruitment of gene-specific transcription factors. *Arthritis Research,* 4:157-164, 2002.

[98] Murata, M., Bonassar, L. J., Wright, M., Mankin, H. J. and Towle, C. A. A role for the interleukin-1 receptor in the pathway linking static mechanical compression to decreased proteoglycan synthesis in surface articular cartilage. *Archives of Biochemistry and Biophysics,* 413:229-235, 2003.

[99] Vincenti, M. P. and Brinckerhoff, C. E. Early response genes induced in chondrocytes stimulated with the inflammatory cytokine interleukin-1beta. *Arthritis Research,* 3:381-388, 2001.

[100] Tsuji, M., Funahashi, S., Takigawa, M., Seiki, M., Fujii, K. and Yoshida, T. Expression of c-fos gene inhibits proteoglycan synthesis in transfected chondrocyte. *FEBS Letters,* 381:222-226, 1996.

[101] Fermor, B., Weinberg, J. B., Pisetsky, D. S., Misukonis, M. A., Fink, C. and Guilak, F. Induction of cyclooxygenase-2 by mechanical stress through a nitric oxide-regulated pathway. *Osteoarthritis and Cartilage,* 10:792-798, 2002.

[102] Hardy, M. M., Seibert, K., Manning, P. T., Currie, M. G., Woerner, B. M., Edwards, D., Koki, A. and Tripp, C. S. Cyclooxygenase 2-dependent prostaglandin E2 modulates cartilage proteoglycan degradation in human osteoarthritis explants. *Arthritis and Rheumatism,* 46:1789-1803, 2002.

[103] Lowe, G. N., Fu, Y. H., McDougall, S., Polendo, R., Williams, A., Benya, P. D. and Hahn, T. J. Effects of prostaglandins on deoxyribonucleic acid and aggrecan synthesis in the RCJ 3.1C5.18 chondrocyte cell line: role of second messengers. *Endocrinology,* 137:2208-2216, 1996.

[104] Kaarniranta, K., Holmberg, C. I., Lammi, M. J., Eriksson, J. E., Sistonen, L. and Helminen, H. J. Primary chondrocytes resist hydrostatic pressure-induced stress while primary synovial cells and fibroblasts show modified Hsp70 response. *Osteoarthritis and Cartilage,* 9:7-13, 2001.

[105] Armitage, P., Berry, G. and Matthews, J. N. S. *Statistical Methods in Medical Research, 4th Ed,* Blackwell Sciences Ltd., Oxford:455-463, 2002.

[106] Berrar, D. P., Dubitzky, W. and Granzow, M. *A Practical Approach to Microarray Data Analysis,* Kulwer Norwell:99-109, 2003.

[107] Yeung, K. Y. and Ruzzo, W. L. Principal component analysis for clustering gene expression data. *Bioinformatics,* 17:763-774, 2001.

[108] Misra, J., Schmitt, W., Hwang, D., Hsiao, L. L., Gullans, S. and Stephanopoulos, G. Interactive exploration of microarray gene expression patterns in a reduced dimensional space. *Genome Research,* 12:1112-1120, 2002.

[109] Mow, V. C., Wang, C. C. and Hung, C. T. The extracellular matrix, interstitial fluid and ions as a mechanical signal transducer in articular cartilage. *Osteoarthritis and Cartilage,* 7:41-58, 1999.

[110] Salter, D. M., Millward-Sadler, S. J., Nuki, G. and Wright, M. O. Integrin-interleukin-4 mechanotransduction pathways in human chondrocytes. *Clinical Orthopaedics and Related Research,* S49-S60, 2001.

[111] Wyrick, J. J. and Young, R. A. Deciphering gene expression regulatory networks. *Current Opinion in Genetics & Development,* 12:130-136, 2002.

[112] Zhu, J. and Zhang, M. Q. Cluster, function and promoter: analysis of yeast expression array. *Pacific Symposium on Biocomputing,* 479-490, 2000.

[113] Aerts, S., Thijs, G., Coessens, B., Staes, M., Moreau, Y. and Moor, B. D. Toucan: deciphering the cis-regulatory logic of coregulated genes. *Nucleic Acids Research,* 31:1753-1764, 2003.

[114] Hubbard, T., Barker, D., Birney, E., Cameron, G., Chen, Y., Clark, L., Cox, T., Cuff, J., Curwen, V., Down, T., Durbin, R., Eyras, E., Gilbert, J., Hammond, M., Huminiecki, L., Kasprzyk, A., Lehvaslaiho, H., Lijnzaad, P., Melsopp, C., Mongin, E., Pettett, R., Pocock, M., Potter, S., Rust, A., Schmidt, E., Searle, S., Slater, G., Smith, J., Spooner, W., Stabenau, A., Stalker, J., Stupka, E., Ureta-Vidal, A., Vastrik, I. and Clamp, M. The Ensembl genome database project. *Nucleic Acids Research,* 30:38-41, 2002.

[115] Wingender, E., Chen, X., Hehl, R., Karas, H., Liebich, I., Matys, V., Meinhardt, T., Pruss, M., Reuter, I. and Schacherer, F. TRANSFAC: an integrated system for gene expression regulation. *Nucleic Acids Research,* 28:316-319, 2000.

[116] Karin, M., Liu, Z. G. and Zandi, E. AP-1 function and regulation. *Current Opinion in Cell Biology,* 9:240-246, 1997.

[117] Eckstein, F., Tieschky, M., Faber, S., Englmeier, K. H. and Reiser, M. Functional analysis of articular cartilage deformation, recovery, and fluid flow following dynamic exercise in vivo. *Anatomy and Embryology,* 200:419-424, 1999.

[118] Fehrenbacher, A., Steck, E., Rickert, M., Roth, W. and Richter, W. Rapid regulation of collagen but not metalloproteinase 1, 3, 13, 14 and tissue inhibitor of metalloproteinase 1,

2, 3 expression in response to mechanical loading of cartilage explants in vitro. *Archives of Biochemistry and Biophysics,* 410:39-47, 2003.

[119] Lee, J. H. Chondrocyte response to in vitro mechanical injury and co-culture with joint capsule tissue. *Doctoral thesis in Biological Engineering, Massachussetts Institute of Technology,* 2005.

[120] Yang-Yen, H. F., Chambard, J. C., Sun, Y. L., Smeal, T., Schmidt, T. J., Drouin, J. and Karin, M. Transcriptional interference between c-Jun and the glucocorticoid receptor: mutual inhibition of DNA binding due to direct protein-protein interaction. *Cell,* 62:1205-1215, 1990.

[121] D'Andrea, P., Calabrese, A., Capozzi, I., Grandolfo, M., Tonon, R. and Vittur, F. Intercellular Ca2+ waves in mechanically stimulated articular chondrocytes. *Biorheology,* 37:75-83, 2000.

[122] Roberts, S. R., Knight, M. M., Lee, D. A. and Bader, D. L. Mechanical compression influences intracellular Ca2+ signaling in chondrocytes seeded in agarose constructs. *Journal of Applied Physiology,* 90:1385-1391, 2001.

[123] Parvizi, J., Parpura, V., Greenleaf, J. F. and Bolander, M. E. Calcium signaling is required for ultrasound-stimulated aggrecan synthesis by rat chondrocytes. *Journal of Orthopaedic Research,* 20:51-57, 2002.

[124] Alford, A. I., Yellowley, C. E., Jacobs, C. R. and Donahue, H. J. Increases in cytosolic calcium, but not fluid flow, affect aggrecan mRNA levels in articular chondrocytes. *Journal of Cellular Biochemistry,* 90:938-944, 2003.

[125] Veldhuijzen, J. P., Bourret, L. A. and Rodan, G. A. Invitro Studies of the Effect of Intermittent Compressive Forces on Cartilage Cell-Proliferation. *Journal of Cellular Physiology,* 98:299-306, 1979.

[126] Schaeffer, H. J. and Weber, M. J. Mitogen-activated protein kinases: specific messages from ubiquitous messengers. *Molecular and Cellular Biology,* 19:2435-2444, 1999.

[127] Grushko, G., Schneiderman, R. and Maroudas, A. Some biochemical and biophysical parameters for the study of the pathogenesis of osteoarthritis: a comparison between the processes of ageing and degeneration in human hip cartilage. *Connective Tissue Research,* 19:149-176, 1989.

[128] Verzijl, N., DeGroot, J., Ben, Z. C., Brau-Benjamin, O., Maroudas, A., Bank, R. A., Mizrahi, J., Schalkwijk, C. G., Thorpe, S. R., Baynes, J. W., Bijlsma, J. W., Lafeber, F. P. and TeKoppele, J. M. Crosslinking by advanced glycation end products increases the stiffness of the collagen network in human articular cartilage: a possible mechanism through which age is a risk factor for osteoarthritis. *Arthritis and Rheumatism,* 46:114-123, 2002.

[129] Sharma, P. K., Hota, D. and Pandhi, P. Biologics in rheumatoid arthritis. *Journal of Associated Physicians India,* 52:231-236, 2004.

[130] Dixon, W. G. and Symmons, D. P. Does early rheumatoid arthritis exist? *Best Practice Research and Clinical Rheumatology,* 19:37-53, 2005.

[131] Goldring, M. B. The role of the chondrocyte in osteoarthritis. *Arthritis and Rheumatism,* 43:1916-1926, 2000.

[132] Salter, D. M., Millward-Sadler, S. J., Nuki, G. and Wright, M. O. Differential responses of chondrocytes from normal and osteoarthritic human articular cartilage to mechanical stimulation. *Biorheology,* 39:97-108, 2002.

[133] Steinmeyer, J., Ackermann, B. and Raiss, R. X. Intermittent cyclic loading of cartilage explants modulates fibronectin metabolism. *Osteoarthritis and Cartilage,* 5:331-341, 1997.

[134] Berenbaum, F. Signaling transduction: target in osteoarthritis. *Current Opinion in Rheumatology,* 16:616-622, 2004.

[135] Fan, Z., Bau, B., Yang, H. and Aigner, T. IL-1beta induction of IL-6 and LIF in normal articular human chondrocytes involves the ERK, p38 and NFkappaB signaling pathways. *Cytokine,* 28:17-24, 2004.

[136] Scherle, P. A., Pratta, M. A., Feeser, W. S., Tancula, E. J. and Arner, E. C. The effects of IL-1 on mitogen-activated protein kinases in rabbit articular chondrocytes. *Biochemical and Biophysical Research Communications,* 230:573-577, 1997.

[137] Geng, Y., Valbracht, J. and Lotz, M. Selective activation of the mitogen-activated protein kinase subgroups c-Jun NH2 terminal kinase and p38 by IL-1 and TNF in human articular chondrocytes. *Journal of Clinical Investigation,* 98:2425-2430, 1996.

[138] Klooster, A. R. and Bernier, S. M. Tumor necrosis factor alpha and epidermal growth factor act additively to inhibit matrix gene expression by chondrocyte. *Arthritis Research and Therapy,* 7:R127-138, 2005.

[139] Borden, P., Solymar, D., Sucharczuk, A., Lindman, B., Cannon, P. and Heller, R. A. Cytokine control of interstitial collagenase and collagenase-3 gene expression in human chondrocytes (vol 271, pg 23577, 1996). *Journal of Biological Chemistry,* 271:33706-33706, 1996.

[140] Mengshol, J. A., Vincenti, M. P., Coon, C. I., Barchowsky, A. and Brinckerhoff, C. E. Interleukin-1 induction of collagenase 3 (matrix metalloproteinase 13) gene expression in chondrocytes requires p38, c-Jun N-terminal kinase, and nuclear factor kappaB:

differential regulation of collagenase 1 and collagenase 3. *Arthritis and Rheumatism,* 43:801-811, 2000.

[141] Murakami, S., Kan, M., McKeehan, W. L. and de Crombrugghe, B. Up-regulation of the chondrogenic Sox9 gene by fibroblast growth factors is mediated by the mitogen-activated protein kinase pathway. *Proceedings of the National Academy of Sciences USA,* 97:1113-1118, 2000.

[142] Ridley, S. H., Sarsfield, S. J., Lee, J. C., Bigg, H. F., Cawston, T. E., Taylor, D. J., DeWitt, D. L. and Saklatvala, J. Actions of IL-1 are selectively controlled by p38 mitogen-activated protein kinase: regulation of prostaglandin H synthase-2, metalloproteinases, and IL-6 at different levels. *Journal of Immunology,* 158:3165-3173, 1997.

[143] Badger, A. M., Cook, M. N., Lark, M. W., Newman-Tarr, T. M., Swift, B. A., Nelson, A. H., Barone, F. C. and Kumar, S. SB 203580 inhibits p38 mitogen-activated protein kinase, nitric oxide production, and inducible nitric oxide synthase in bovine cartilage-derived chondrocytes. *Journal of Immunology,* 161:467-473, 1998.

[144] Johnson, G. L. and Lapadat, R. Mitogen-activated protein kinase pathways mediated by ERK, JNK, and p38 protein kinases. *Science,* 298:1911-1912, 2002.

[145] Whitmarsh, A. J., Yang, S. H., Su, M. S., Sharrocks, A. D. and Davis, R. J. Role of p38 and JNK mitogen-activated protein kinases in the activation of ternary complex factors. *Molecular and Cellular Biology,* 17:2360-2371, 1997.

[146] Han, Z., Boyle, D. L., Aupperle, K. R., Bennett, B., Manning, A. M. and Firestein, G. S. Jun N-terminal kinase in rheumatoid arthritis. *Journal of Pharmacology and Experimental Therapeutics,* 291:124-130, 1999.

[147] Buschmann, M. D., Hunziker, E. B., Kim, Y. J. and Grodzinsky, A. J. Altered aggrecan synthesis correlates with cell and nucleus structure in statically compressed cartilage. *Journal of Cell Science,* 109:499-508, 1996.

[148] Quinn, T. M., Grodzinsky, A. J., Buschmann, M. D., Kim, Y. J. and Hunziker, E. B. Mechanical compression alters proteoglycan deposition and matrix deformation around individual cells in cartilage explants. *Journal of Cell Science,* 111:573-583, 1998.

[149] Park, S., Hung, C. T. and Ateshian, G. A. Mechanical response of bovine articular cartilage under dynamic unconfined compression loading at physiological stress levels. *Osteoarthritis and Cartilage,* 12:65-73, 2004.

[150] Jin, M., Emkey, G. R., Siparsky, P., Trippel, S. B. and Grodzinsky, A. J. Combined effects of dynamic tissue shear deformation and insulin-like growth factor I on chondrocyte biosynthesis in cartilage explants. *Archives of Biochemistry and Biophysics,* 414:223-231, 2003.

[151] Chen, C. T., Burton-Wurster, N., Lust, G., Bank, R. A. and Tekoppele, J. M. Compositional and metabolic changes in damaged cartilage are peak-stress, stress-rate, and loading-duration dependent. *Journal of Orthopaedic Research,* 17:870-879, 1999.

[152] Loening, A. M., James, I. E., Levenston, M. E., Badger, A. M., Frank, E. H., Kurz, B., Nuttall, M. E., Hung, H. H., Blake, S. M., Grodzinsky, A. J. and Lark, M. W. Injurious mechanical compression of bovine articular cartilage induces chondrocyte apoptosis. *Archives of Biochemistry and Biophysics,* 381:205-212, 2000.

[153] Ewers, B. J., Dvoracek-Driksna, D., Orth, M. W. and Haut, R. C. The extent of matrix damage and chondrocyte death in mechanically traumatized articular cartilage explants depends on rate of loading. *Journal of Orthopaedic Research,* 19:779-784, 2001.

[154] Quinn, T. M., Grodzinsky, A. J., Hunziker, E. B. and Sandy, J. D. Effects of injurious compression on matrix turnover around individual cells in calf articular cartilage explants. *Journal of Orthopaedic Research,* 16:490-499, 1998.

[155] D'Lima, D. D., Hashimoto, S., Chen, P. C., Colwell, C. W., Jr. and Lotz, M. K. Human chondrocyte apoptosis in response to mechanical injury. *Osteoarthritis and Cartilage,* 9:712-719, 2001.

[156] DiMicco, M. A., Patwari, P., Siparsky, P. N., Kumar, S., Pratta, M. A., Lark, M. W., Kim, Y. J. and Grodzinsky, A. J. Mechanisms and kinetics of glycosaminoglycan release following in vitro cartilage injury. *Arthritis and Rheumatism,* 50:840-848, 2004.

[157] Lohmander, L. S., Atley, L. M., Pietka, T. A. and Eyre, D. R. The release of crosslinked peptides from type II collagen into human synovial fluid is increased soon after joint injury and in osteoarthritis. *Arthritis and Rheumatism,* 48:3130-3139, 2003.

[158] Lohmander, L. S., Roos, H., Dahlberg, L., Hoerrner, L. A. and Lark, M. W. Temporal patterns of stromelysin-1, tissue inhibitor, and proteoglycan fragments in human knee joint fluid after injury to the cruciate ligament or meniscus. *Journal of Orthopaedic Research,* 12:21-28, 1994.

[159] Takahashi, K., Goomer, R. S., Harwood, F., Kubo, T., Hirasawa, Y. and Amiel, D. The effects of hyaluronan on matrix metalloproteinase-3 (MMP-3), interleukin-1beta(IL-1beta), and tissue inhibitor of metalloproteinase-1 (TIMP-1) gene expression during the development of osteoarthritis. *Osteoarthritis and Cartilage,* 7:182-190, 1999.

[160] Vankemmelbeke, M. N., Holen, I., Wilson, A. G., Ilic, M. Z., Handley, C. J., Kelner, G. S., Clark, M., Liu, C., Maki, R. A., Burnett, D. and Buttle, D. J. Expression and activity of ADAMTS-5 in synovium. *European Journal of Biochemistry,* 268:1259-1268, 2001.

[161] Jubb, R. W. and Fell, H. B. The effect of synovial tissue on the synthesis of proteoglycan by the articular cartilage of young pigs. *Arthritis and Rheumatism,* 23:545-555, 1980.

[162] Patwari, P., Fay, J., Cook, M. N., Badger, A. M., Kerin, A. J., Lark, M. W. and Grodzinsky, A. J. In vitro models for investigation of the effects of acute mechanical injury on cartilage. *Clinical Orthopaedics and Related Research,* S61-71, 2001.

[163] Jain, A. K., Murty, M. N. and Flynn, P. J. Data clustering: A review. *ACM Computing Surveys,* 31:264-323, 1999.

[164] Fell, H. B. and Jubb, R. W. The effect of synovial tissue on the breakdown of articular cartilage in organ culture. *Arthritis and Rheumatism,* 20:1359-1371, 1977.

[165] Le Graverand, M. P., Eggerer, J., Vignon, E., Otterness, I. G., Barclay, L. and Hart, D. A. Assessment of specific mRNA levels in cartilage regions in a lapine model of osteoarthritis. *Journal of Orthopaedic Research,* 20:535-544, 2002.

[166] Stanton, H., Rogerson, F. M., East, C. J., Golub, S. B., Lawlor, K. E., Meeker, C. T., Little, C. B., Last, K., Farmer, P. J., Campbell, I. K., Fourie, A. M. and Fosang, A. J. ADAMTS5 is the major aggrecanase in mouse cartilage in vivo and in vitro. *Nature,* 434:648-652, 2005.

[167] Bau, B., Gebhard, P. M., Haag, J., Knorr, T., Bartnik, E. and Aigner, T. Relative messenger RNA expression profiling of collagenases and aggrecanases in human articular chondrocytes in vivo and in vitro. *Arthritis and Rheumatism,* 46:2648-2657, 2002.